

INFORMATION TO USERS

While the most advanced technology has been used to photograph and reproduce this manuscript, the quality of the reproduction is heavily dependent upon the quality of the material submitted. For example:

- Manuscript pages may have indistinct print. In such cases, the best available copy has been filmed.
- Manuscripts may not always be complete. In such cases, a note will indicate that it is not possible to obtain missing pages.
- Copyrighted material may have been removed from the manuscript. In such cases, a note will indicate the deletion.

Oversize materials (e.g., maps, drawings, and charts) are photographed by sectioning the original, beginning at the upper left-hand corner and continuing from left to right in equal sections with small overlaps. Each oversize page is also filmed as one exposure and is available, for an additional charge, as a standard 35mm slide or as a 17"x 23" black and white photographic print.

Most photographs reproduce acceptably on positive microfilm or microfiche but lack the clarity on xerographic copies made from the microfilm. For an additional charge, 35mm slides of 6"x 9" black and white photographic prints are available for any photographs or illustrations that cannot be reproduced satisfactorily by xerography.



8629747

Strauss, Rosalyn Silbermintz

OROTATE PHOSPHORIBOSYLTRANSFERASE FROM BAKER'S YEAST: I.
KINETIC ANALYSIS, CHEMICAL MODIFICATION, AND PROTON NMR
SPECTROSCOPY OF THE ENZYME-SUBSTRATE COMPLEX. II. AMINO
ACID ANALYSIS AND NMR SPECTROSCOPY OF THE PROTEIN

City University of New York

PH.D. 1986

University
Microfilms
International

300 N. Zeeb Road, Ann Arbor, MI 48106

Copyright 1986

by

Strauss, Rosalyn Silbermintz

All Rights Reserved



PLEASE NOTE:

In all cases this material has been filmed in the best possible way from the available copy. Problems encountered with this document have been identified here with a check mark .

1. Glossy photographs or pages _____
 2. Colored illustrations, paper or print _____
 3. Photographs with dark background _____
 4. Illustrations are poor copy _____
 5. Pages with black marks, not original copy _____
 6. Print shows through as there is text on both sides of page _____
 7. Indistinct, broken or small print on several pages
 8. Print exceeds margin requirements _____
 9. Tightly bound copy with print lost in spine _____
 10. Computer printout pages with indistinct print
 11. Page(s) _____ lacking when material received, and not available from school or author.
 12. Page(s) _____ seem to be missing in numbering only as text follows.
 13. Two pages numbered _____. Text follows.
 14. Curling and wrinkled pages _____
 15. Dissertation contains pages with print at a slant, filmed as received _____
 16. Other Pages 145-152, 167-173 contain indistinct print.
-
-

University
Microfilms
International

OROTATE PHOSPHORIBOSYLTRANSFERASE FROM BAKER'S YEAST:

I. KINETIC ANALYSIS, CHEMICAL MODIFICATION, AND PROTON

NMR SPECTROSCOPY OF THE ENZYME-SUBSTRATE COMPLEX

II. AMINO ACID ANALYSIS AND NMR SPECTROSCOPY OF THE PROTEIN

BY

ROSALYN SILBERMINTZ STRAUSS

**A dissertation submitted to the Graduate Faculty
in Biochemistry in partial fulfillment of the
requirements for the degree of Doctor of
Philosophy, The City University of New York**

1986

COPYRIGHT BY
ROSALYN SILBERMINTZ STRAUSS
1986

This manuscript has been read and accepted for the Graduate Faculty in Biochemistry in satisfaction of the dissertation requirement for the degree of Doctor of Philosophy.

6/27/86
Date


Chair of Examining Committee

9/11/86
Date

Horace Schultz
Executive Officer

Thomas W. Guine
William Sweeney
Donald D. Bird
Supervisory Committee

The City University of New York

This thesis is dedicated to the memory of Dr. Arthur Spier, my high school science and calculus teacher, whose unique outlook on the interplay of science and philosophy inspired me to pursue science as part of my life's avocation.

I would like to acknowledge my parents who gave me the freedom to begin this endeavor, my children Kalman, Blima, and Rochel who gave me the inspiration to go on, (as Kalman told his kindergarten teacher: "I know what a scientist is. My mother is one!"). my family, in-laws and babysitters, for supporting me and most of all my husband, Sidney, for standing by me, constantly encouraging me, putting up with my anxieties and frustrations, and helping me to reach for this goal.

I would like to thank Jake for introducing me to the word 'Biochemistry' and to Dr. Sloan, Dr. Charlotte Russell for being a role-model and a friend, Dr. M. Fishman for free reign of his Apple computer to develop and run my computer programs, and my thesis committee, Dr. T. Haines, Dr. R. Rockwell, Dr. R. Birke, and Dr. W. Sweeney for their patience.

Most of all, I want to thank, Dr. Donald Sloan, my mentor, for his years of encouragement and advice, for never giving up on me, even through all the delays and leaves-of-absence and for all his guidance throughout every aspect of my research and graduate work.

"How overwhelmingly great are Thy works, O Lord!
In wisdom hast Thou made them all; the earth is full
of Thy property."

Psalms 104:24

Table of Contents

	<u>Page</u>
TITLE PAGE.....	i
COPYRIGHT PAGE.....	ii
APPROVAL PAGE.....	iii
ACKNOWLEDGEMENTS.....	iv
PREFACE.....	v
TABLE OF CONTENTS.....	vi,vii
LIST OF TABLES.....	viii
LIST OF FIGURES.....	ix-xi
I. INTRODUCTION.....	1-4
II. RATIONALE.....	5-6
III. MATERIALS.....	7
IV. METHODS.....	8-22
Purification of OPRTase.....	8
Spectroscopic Assays.....	12
PH-Stability Studies.....	13
PH-Activity Studies.....	13
Chemical Modification Studies.....	13
Amino Acid Analysis.....	15
Computation of ¹ H-NMR Spectrum of OPRTase.....	16
¹ H-NMR Spectra of OPRTase.....	19
³² P-NMR Spectra.....	20
Relaxation Studies.....	20
V. RESULTS.....	23-135
Purification of OPRTase.....	23
PH-Stability Studies.....	23
PH-Activity Studies.....	26
Chemical Modification Studies.....	50
Amino Acid Analysis.....	78
Computed ¹ H-NMR Spectrum of OPRTase.....	85
¹ H-NMR Spectra of OPRTase.....	85
³² P-NMR Spectra.....	110
Conformation of PRPP on and off OPRTase.....	114

VI. DISCUSSION	136-143
VII. APPENDICES	144-174
Appendix 1: Listing of HYPER.....	145
Appendix 2: Listing of PHBELL.....	147
Appendix 3: Listing of HABELL.....	149
Appendix 4: Listing of MANIP DATA.....	150
Appendix 5: Listing of NMRSPEC.....	152
Appendix 6: Data Entry and Interactive Manipulations.....	153
Appendix 7: Sample Printouts.....	160
Appendix 8: Printout of NMRSPEC.....	166
Appendix 9: ¹ H-NMR Spectra of OPRTase.....	174
VIII. BIBLIOGRAPHY	175-177
CURRICULUM VITAE	178-180

List of Tables

<u>Table</u>	<u>Page</u>
IV.1 Input for NMRSPEC.....	18
V.1 Theoretical curves for the forward reaction of OPRTase.....	41
V.2 Theoretical curves for the reverse reaction of OPRTase.....	45
V.3 Inactivation of OPRTase by NH ₂ OH and its partial reactivation.....	77
V.4 Amino acid analysis of OPRTase in picomoles per sample.....	79
V.5 Amino acid analysis of OPRTase in number of residues per subunit.....	81
V.6 Amino acid analysis of OPRTase in number of residues per subunit (rounded off to the nearest whole number).....	82
V.7 Amino acid analysis of OPRTase in weight of each amino acid contributing to the total M.W.....	83
V.8 Central positions and heights of composite triangles of computed ¹ H-NMR spectrum of OPRTase	86
V.9 Sample data for the generation of T ₁ values.....	122
V.10 (fT _{1p}) ⁻¹ values for the protons of PRPP in the presence of OPRTase and Mn ²⁺	126
V.11 Distances to Mn ²⁺ from the proton of PRPP in the presence and absence of OPRTase.....	130
V.1.1 Amino acid distributions of: PRTases, proteins, OPRTase.....	137

List of Figures

<u>Figure</u>	<u>Page</u>
V.1 Stability of OPRTase between pH 5-9.....	25
V.2 Initial Velocity patterns for the formation of OMP over a pH range of 4.3-9.5.....	28
V.3 Logarithmic plots of kinetic constants for the forward reaction versus pH.....	31
V.4 Logarithmic plots of kinetic constants for the reverse reaction versus pH.....	33
V.5 Curve of Vmax versus pH for the forward reaction as generated by HABELL.....	36
V.6 Curve of Vmax versus pH for the reverse reaction as generated by PHBELL.....	38
V.7 Apriori generated curves of Vmax versus pH for the forward reaction: assuming one or two pka's.....	43
V.8 Apriori generated curves of Vmax versus pH for the reverse reaction: assuming bell-shaped curve or levelling off at high pH.....	47
V.9 Best theoretical Vmax curves of the forward and reverse reactions: assuming equal quantity of enzyme used for each assay.....	49
V.10 The breakdown of DEPC in the presence of potassium phosphate buffer at various pH's between pH 4.5 and pH 9.1	52
V.11 The breakdown of DEPC in the presence and absence of substrates.....	54
V.12 The inactivation of OPRTase by DEPC between pH 4.6 and pH 9.1.....	56
V.13 Rates of breakdown of DEPC and inactivation of OPRTase in the presence of DEPC in potassium phosphate buffer between pH 4.6 and pH 9.1	59
V.14 Concentration dependence of the inactivation of OPRTase by DEPC.....	61

V.15	Substrate protection studies for the inactivation of OPRTase by DEPC.....	63
V.16	Time and concentration dependence of the inactivation of OPRTase by pBPB.....	66
V.17	Substrate protection studies for the inactivation of OPRTase with pBPB.....	68
V.18	Inactivation of OPRTase at pH 7.5 in the presence of NH ₂ OH.....	71
V.19	Comparison of inactivation of OPRTase at pH 6.5 and pH 8.5.....	73
V.20	Comparison of inactivation of OPRTase by NH ₂ OH in the presence and absence of orotate.....	75
V.21	Predicted ¹ H-NMR spectrum of OPRTase.....	88
V.22	¹ H-NMR spectrum of OPRTase in D ₂ O at pH 8.0.....	90
V.23	¹ H-NMR spectrum of OPRTase in D ₂ O at pH 7.7.....	92
V.24	¹ H-NMR spectrum of OPRTase in D ₂ O at pH 7.0.....	94
V.25	¹ H-NMR spectrum of OPRTase in D ₂ O at pH 7.0 (more acquisitions).....	96
V.26	¹ H-NMR spectrum of OPRTase in D ₂ O at pH 6.0.....	99
V.27	¹ H-NMR spectrum of OPRTase in D ₂ O at pH 5.0.....	101
V.28	¹ H-NMR spectrum of PRPP.....	103
V.29	¹ H-NMR spectra of lysozyme.....	108
V.30	³² P-NMR spectra of OPRTase in search of a phosphoribosylated intermediate.....	113
V.31	Sample relaxation of the ¹ H-NMR spectrum of PRPP in the presence of Mn ²⁺	116

V.32	Sample relaxation of the $^1\text{H-NMR}$ spectrum of PRPP in the presence of Mn^{2+} and OPRTase.....	118
V.33	$^1\text{H-NMR}$ spectrum of Mn^{2+} -PRPP.....	121
V.34	Sample plots for the generation of T_1 's.....	124
V.35	Extrapolation of T_{1p}/T_{2p} to infinite enzyme	128
V.36	Graphical representation to the PRPP- Mn^{2+} complex in solution.....	133
V.37	Graphical representation to the PRPP- Mn^{2+} complex on OPRTase.....	135
V1.1	Proposed mechanism of OPRTase in the presence of excess Mg^{2+}	141

Section I: INTRODUCTION

Orotate phosphoribosyltransferase (OPRTase, E. C. 2.4.2.10) catalyzes the formation of a beta-glycosidic bond between the ribose-5'-phosphate moiety of 5'-formation of a beta-glycosidic bond between the ribose-5'-phosphate moiety of 5'-phosphoribosyl-alpha-1'-pyrophosphate (PRPP) and orotate to form orotidine 5'-phosphate (OMP) and pyrophosphate (PP_i). In organisms which have been studied so far, the OMP thus formed is decarboxylated by orotidine-5'-phosphate decarboxylase (ODCase, E. C. 4.1.1.23) to produce UMP.

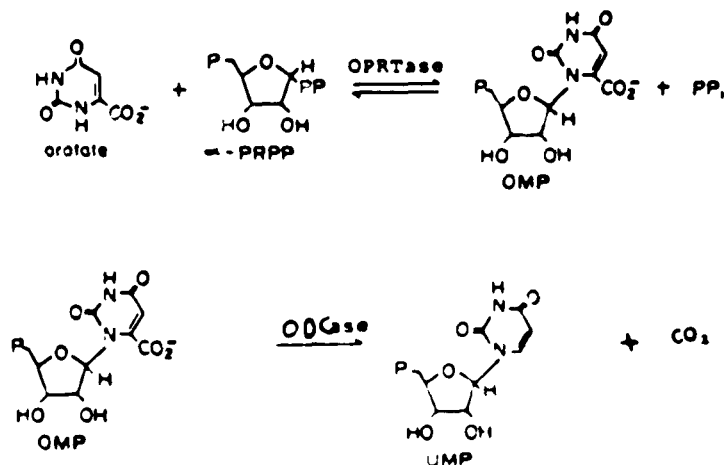


Figure 1.1

It is now generally believed that OPRTase and ODCase exist as a bifunctional enzyme complex (also referred to as UMP Synthase) in mammalian

tissues such as human erythrocytes and diploid cell strains (Foster et al.,1973) , other mammalian erythrocytes (Tax et al.,1976), bovine brain (Appel,1968), calf thymus (Kasbekar et al.,1964), Erlich ascites carcinoma (Kavipurapu and Jones,1964), rat (Sweeney et al.,1974), and mouse liver and heart (Reyes and Intress, 1978). Evidence that a single polypeptide catalyzes the two step conversion of orotate to UMP has also been found in tomato cells in culture (Walther et al.,1984). The complex of these two activities allows for the efficient channelling of OMP to UMP without its release into the cytoplasm where it can be attacked by nucleotidases. While the separation of the two activities (OPRTase and ODCase) has been observed in extracts of Erlich ascites carcinoma cells (Brown and O'Sullivan, 1977), these studies were done after prolonged storage of impure protein and proteases could have been involved (McClard et al., 1980). When the two activities are separated, there is rapid inactivation of both activities, with OPRTase activity the more labile (Jones, 1972). More recently, UMP synthase from Erlich ascites cells has been purified to homogeneity and it has been shown that both activities are present on the same polypeptide (McClard et al., 1980). Two isomers exist of the same molecular weight but with different isoelectric points. Both however, contain both the OPRTase and ODCase activities (ibid.).

Deficiencies of OPRTase and ODCase activities in humans produce the hereditary abnormality, orotic aciduria. Those suffering from the Type I form of the disease exhibit deficiency of both OPRTase and ODCase activities while those having the Type II form are deficient in only ODCase activity and are found to have normal or elevated OPRTase levels (Worthy et al., 1974). Individuals with orotic aciduria are pyrimidine-starved and are affected with severe anemia.

mental retardation, and excretion of excessive orotic acid in their urine (Smith et al., 1972).

In malignant tissue, the rate of nucleotide synthesis is higher and the PRPP pool size larger (Sperling et al., 1979) than in normal tissue. For instance, OPRTase levels are significantly higher in fast-growing colon tumors (Weber, 1981). Therefore, the phosphoribosyltransferase enzymes are the logical targets of chemotherapeutic reagents. 5-fluorouracil effectively inhibits tumor growth (Ardalan et al., 1982) but is highly toxic. Allopurinol, an inhibitor of purine nucleotide synthesis, reduces the toxicity of 5-fluorouracil (Schwartz et al., 1980). Thus it has been suggested that a combination chemotherapy of inhibition of both purine and pyrimidine nucleotide synthesis may provide effective treatment against certain tumors provided nucleotide transport can be accomplished (Plagemann et al., 1981).

In Saccharomyces cerevisiae (Baker's yeast), OPRTase is found not to exist in a complex with ODCase, but rather usually exists as a dimer of 2 identical subunits with a molecular weight of $20,000 \pm 2,000$ per subunit (Victor et al., 1979). Yeast cells lack nucleotidase activity (Traut, 1980) and therefore there is no need for channelling. OMP has been observed to accumulate in yeast cells while UMP is being synthesized (Reyes, 1977). The human malarial parasite Plasmodium falciparum also contains OPRTase and ODCase activities that can be resolved (Rathod and Reyes, 1983) and its OPRTase is more sensitive to mercurial reagents than are red blood cells. This difference might offer a possible point of action for an anti-malarial agent.

The kinetic mechanism of CPRTase from Saccharomyces cerevisiae was unknown before 1978 (Goitein et al.). It has been shown by Victor et al. (1979 a & b) that in the presence of excess Mg^{+2} , the reaction catalyzed by OPRTase

proceeds according to a Bi Bi Ping Pong kinetic mechanism with PRPP as the first binder in the forward direction, followed by the release of PP_i , followed by the addition of orotate, and finally the release of OMP. This mechanism was revealed using standard initial velocity measurements and isotope exchange of ^{32}P - PP_i and ^{32}P -PRPP and of ^{14}C -Orotate and ^{14}C -OMP. Mn^{+2} can replace Mg^{+2} in the reaction and 5-flouro-orotate can be substituted for orotate. It is not yet known what form of complex the enzyme forms with the phosphoribosyl (PR) moiety of PRPP. Attempts to isolate the E-PR complex by gel filtration or to visualize it in ^{31}P -NMR have been unsuccessful as of this writing. Experiments have been accomplished which point to the presence of at least one lysine residue at or near the active sight (Ashton and Sloan, 1986). A nucleophilic amino acid residue at the OPRTase active site could stabilize or be interactive with the charged ribosyl group (Jencks,1975). It has been theorized that the reaction mechanism of OPRTase, proceeds by the formation of a carbocation (Goitein et al., 1978).

Section II: RATIONALE

The purpose of this thesis research was to examine the structural entities of OPRTase and its first substrate, PRPP. This was the first attempt in this laboratory to study a PRPP utilizing enzyme in this way and it is hoped that similar studies may be done eventually on the other PRTases so that comparisons can be made among them. The structure of OPRTase was considered from two perspectives: its amino acid composition and its interface with substrate its active site. Similarly, the structure of the substrate was to be studied free in solution and bound to OPRTase.

For the substrate, we have chosen to study PRPP, since it is the common substrate of all of the PRTases. By utilizing $^1\text{H-NMR}$ spectroscopy to determine the distances between the C-protons of the sugar and the metal attached to it, it is possible to compare the structure of PRPP- Mn^{2+} both on and off the enzyme, thereby gaining insight into possible changes in structure which are introduced as the enzyme-substrate interaction takes place.

To begin to understand the structure of the enzyme and already knowing something of its subunit composition and monomer molecular weight, our next step is to determine its amino acid distribution. This gives us a basis to speculate on the meaning of the results of other experiments which implicate various essential and strategically located amino acids. The second method used to study the structure of OPRTase was through the $^1\text{H-NMR}$ spectroscopy of the enzyme. If the $^1\text{H-NMR}$ spectrum of an enzyme is resolved enough so that individual peaks can be discerned, then it is possible to determine whether the enzyme is undergoing any gross conformational changes over conditions such

as pH change, by examining the native spectra, the affected spectra, and the predicted random coil spectra.

On a different level is the enzyme active site, the juxtaposition of amino acids which sets the stage for catalysis. The amino acids of the active site were studied by two methods: 1) change in enzymatic activity with pH over a range in which the enzyme and substrate are stable and 2) reaction of OPRTase with group specific modifying reagents with concomitant loss of enzymatic activity and the protection from inactivation afforded by substrates.

All of the experiments mentioned above can be used to better understand the events taking place at the active site of OPRTase during catalysis.

Section III: MATERIALS

Pressed Baker's yeast (Budweiser Brand) was obtained from Valenti Yeast, Inc. (Flushling, N. Y.). Sephadex G-10, -25, and -100, and Blue Sepharose CL 6B were purchased from Pharmacia Fine Chemicals (Piscataway, N. J.). Cellex-D (DEAE Cellulose) and Biogel HTP (hydroxylapatite) were purchased from Bio-Rad Laboratories (Richmond, Ca.). Sigma Chemical Co. supplied PRPP (sodium salt), OMP (sodium salt), diethylpyrocarbonate, orotic acid, p-bromo-phenacyl-bromide, and hydroxylamine-HCl. Absolute ethanol was supplied by U.S. Industrial Chemical Co. All other chemicals were reagent grade.

Section IV: METHODS

PURIFICATION OF OPRTASE

All steps were performed at 4 ° C unless otherwise indicated. The purification procedure was basically that of Victor et al (1979), with a few alterations.

Autolysis: Baker's Yeast (Budweiser Brand, St. Louis, Mo. distributed by Valente Yeast Co., Flushing, N. Y.) was suspended in a mixture of 0.3 M potassium phosphate buffer at pH 8 and toluene. Three liters of buffer and 500 ml toluene were used for each 10 lbs. of yeast. The mixture was stirred gently for 4 hours, kept at a constant temperature of 30° C in a water bath, and adjusted periodically to pH 8 by adding small portions of 5 N KOH. The autolysate was then centrifuged in a Sorvall RC-2B refrigerated centrifuge for 20 minutes at 8,000 rpm (approximately 10,000 x g). Alternatively, it was filtered through Whatman fluted filter paper. The supernatant from the centrifugation was filtered through a few layers of cheesecloth to remove fluffy lipid materials.

Ammonium Sulfate Fractionation: The partially clarified autolysate was adjusted to pH 5 with 8 N acetic acid with gentle stirring in the presence of 1% ethanol to prevent foaming. Solid ammonium sulfate was added to the acidified autolysate to obtain 50% saturation (313 grams ammonium sulfate per liter of autolysate). This addition was carried out over several hours with gentle stirring, and the solution was then allowed to stand overnight to allow complete precipitation. The precipitate was collected by centrifugation (9,000 rpm, approximately 12,500 x g for 20 minutes) and then redissolved in a minimum volume of 25 mM Tris-HCl at pH 8 (about 1 liter per 10 lbs. yeast). This produced

a cloudy suspension. The preparation was then adjusted to pH 8 with 1 N KOH and dialyzed against 16 liters of 10 mM Tris-HCl pH 8 overnight. It was then centrifuged at 8,500 rpm for 20 minutes to remove undissolved material.

Removal of Nucleic Acids: 1M $MnCl_2$ was added to the clarified ammonium sulfate fraction to a final concentration of 50 mM with respect to $MnCl_2$. The solution was stirred gently for 30 minutes and then centrifuged (8,500 rpm, 20 minutes) to remove nucleic acids.

Ethanol Fractionation: To each 250 ml of the above supernatant, 100 ml of acetate buffer (2 M, pH 6) and solid orotate to a final concentration of 1mM, were added. The solution was cooled to below 0° C in an ice-ethanol-dry ice bath. 95% ethanol (chilled in dry ice-acetone to below -20° C) was added to the acidified protein preparation, with swirling, to a concentration of 15% (v/v, 180 ml EtOH/1,000 ml solution). Temperature of the mixture was checked after each addition of ethanol, and the mixture was cooled to between 0° C to -2° C before more was added. The precipitate was quickly removed by centrifugation (8,500 rpm, 10 minutes) at -15° C, in metal centrifuge cups which had been precooled. At any given time, only enough solution was treated as could be centrifuged in one run. The supernatant was then treated with additional ethanol to increase the concentration to 50% (820 ml EtOH/1,000 ml original solution). The precipitate was collected by centrifugation at -15° C and dissolved in a minimum volume of Tris-HCl (25mM, pH 8, 200ml). After stirring for 30 minutes, the suspension was centrifuged and the precipitate re-extracted with a small volume of the same buffer. The combined extracts were then dialyzed overnight against 16 liters of 25 mM Tris at pH 8.

Heat Treatment: The dialyzed ethanol fraction was made to 2 mM in $MgCl_2$ and 1mM in orotate. Aliquots of 250-300 ml each were heated rapidly in metal

centrifuge cups by placing them in a constant temperature bath at 53° C for 5 minutes. They were then transferred immediately to an ice-salt mixture at 2° C. The preparation was then centrifuged at 8,500 rpm for 20 minutes to sediment denatured protein. A small amount of pink-tinged precipitate was removed by this procedure.

Note: Throughout the rest of the purification procedure, all buffers, both for chromatography and dialysis, were at pH 8 and contained 1mM orotate, unless otherwise specified.

Sephadex G-100 Gel Chromatography: The supernatant from the previous step was concentrated by an Amicon ultrafiltration unit (400 ml capacity) using a PM-10 membrane. (Two attempts were made to concentrate the protein solution at this stage of purification by adhesion and elution of OPRTase from DEAE Cellulose, but the OPRTase failed to bind to the DEAE matrix until it had been eluted from Sephadex.) A nitrogen pressure of 70 psi was employed until a volume of less than 100 ml/10 lbs. of yeast was obtained. The retentate was divided into portions of approximately 40 ml and carefully applied to a column of Sephadex G-100 equilibrated with 10mM Tris-Hcl and 40mM NaCl (2.5 x 60 cm). Fractions of 10 ml each were collected and an elution profile of one peak of activity following a huge peak of protein and unprecipitated debris was produced. Those fractions containing over 20% of the activity found in the most active portion were pooled. The protein cleared the column in four hours, allowing for at least 2 runs a day.

Cellex-D (DEAE Cellulose) Chromatography: The pooled G-100 fraction was dialyzed twice against 10 liters of 10 mM potassium phosphate buffer for 4 hours. The dialysate was then applied to a column (2.5 cm x 37 cm) of DEAE-cellulose

equilibrated with the same buffer. The enzyme was then eluted with a linear gradient between 750 ml each of 10 mM and 200 mM potassium phosphate buffer. Fractions of 6.6 ml were collected. The elution profile of the enzyme from DEAE-cellulose was composed of one minor peak followed by one major peak, followed by a plateau of activity. As the DEAE-cellulose was re-used, the resolution of the peaks became less distinct. The two peaks have been studied by other researchers (Yoshimoto et al, 1978) and found to have molecular weights of 32,000 and 39,000 respectively, as determined by calibrated Sephadex G-100. These two forms do not seem to interconvert.

It was found by this researcher and Lewis Hanna that OPRTase and NPRTase copurify through the ethanol fractionation step. In later preparations, Phosho-Cellulose column chromatography was run after that stage of the purification. NPRTase binds to the Phosho-Cellulose column at low buffer concentration while most of the OPRTase passes through the column. When this procedure is performed during the purification of OPRTase, it is observed that only one significant peak of activity appears in the elution profile of DEAE. This peak elutes at the same ionic strength as the major peak mentioned above.

Bio-Gel HTP (Hydroxylapatite) Chromatography: The fractions of the major active peak from the DEAE-cellulose were pooled and then dialyzed against 10 liters of 10 mM potassium phosphate buffer. The dialysate was then applied to a column (2 x 37 cm) of Biogel HTP hydroxylapatite, previously equilibrated with the same buffer. The enzyme was eluted with a linear gradient between 500 ml each of 10 mM and 200 mM potassium phosphate buffer. (If this procedure is omitted, the enzyme eluting from Blue Sepharose gives two bands on disc gel electrophoresis.) Fractions of 6.6 ml were collected. The enzyme activity eluted

from the hydroxylapatite column in one peak, unless the DEAE Cellulose column was omitted.

Blue Sepharosa Affinity Adsorbent: Twenty grams of Blue Sepharose CL-6B was washed in a sintered glass funnel with cold distilled water (200 ml per gram dry weight). The gel was then suspended in 10 mM Tris-HCl (without orotate) and poured into a column (2.5 x 25 cm) and equilibrated with the same buffer. The hydroxylapatite fraction was dialyzed against 10 mM Tris (without orotate) for four hours and then applied to the column. The column was then washed with 10 mM Tris-HCl buffer (without orotate) until no more protein eluted. OPRTase was then eluted by washing the column with a solution of 0.1 mM OMP in 10 mM Tris-HCl buffer (pH 8). The enzyme eluted in a very sharp band. The column was then washed with high salt to remove all protein. This eluent contained little or no OPRTase activity.

SPECTROSCOPIC ASSAYS

Initial velocity measurements were carried out spectrophotometrically at 25°C, using a Cary 15 recording spectrophotometer by the method of Umezū et al. (1971). The final saturating substrate concentrations of reactants in 1 ml of assay solution for the phosphonobosyltransferase (forward) reaction were 100 μM PRPP, 300 μM orotate, and 1 mM MgCl₂ in 50 mM Tris-HCl buffer at pH 8.0. The final saturating reactant concentrations in 1 ml of assay solution for the pyrophosphorylase (reverse) reaction were 125 μM OMP, 2.5 mM pyrophosphate, and 2 mM MgCl₂ in 50 mM Tris-HCl at pH 8.0. The reaction was initiated by the addition of an aliquot of enzyme (2.5x10⁻⁴ mg purified OPRTase) to 1 ml assay solution. Initial velocities were determined as the slope of the tangent to the beginning of the trace of absorbance versus time at 295 nm, and then converted to units of μmoles of OMP synthesized or degraded per minute.

A drop in absorbance is seen during the phosphoribosyl transfer reaction and an increase in absorbance is seen in the pyrophosphorylase reaction. The difference in the molar extinction coefficient for orotate and OMP at 295 nm is 3950.

PH-STABILITY STUDIES

The stability of OPRTase over the pH range studied was determined by incubating aliquots of the enzyme at each pH and removing catalytic amounts at various times and assaying them for the phosphoribosyl transferase activity in Tris-HCl at pH 8.

PH-ACTIVITY PROFILES

Assays were performed over a pH range of 4.5 through 9.5. Various buffers with optimal buffering capacity at a range of pH's were used so that the entire range of 4.5 through 9.5 could be covered. These included: Sodium acetate (pKa=4.75), Tris-HCl (pKa=8.15), glycylglycine (pKa=8.2), potassium phosphate (pKa=6.6), and triethanolamine. The pH of the mixture was recorded before and after the reaction to check if any change occurred during the reaction. The pH of the mixture, not the added buffer, was recorded as the pH studied in kinetic work. For the phosphoribosyltransferase (forward) reaction, the assay mixture contained 300 μ M orotate, 1mM $MgCl_2$, and a range of 10-200 μ M PRPP in 50 mM Buffer at the pH indicated. For the pyrophosphorylase (reverse) reaction, the assay mixture contained 2.5 mM pyrophosphate, 2 mM $MgCl_2$ and a range of 3.75 -25 μ M OMP in 50 mM buffer at the pH indicated.

CHEMICAL MODIFICATION

Purified OPRTase was passed through a PD-10 Sephadex column equilibrated with 10 mM potassium phosphate buffer (pH 8) to remove OMP added during the last step of purification.

General Incubation Procedure for Chemical Modification

Each incubation mixture contained 0.2 ml of 15 mM buffer 0.05 ml of H₂O, 0.05 ml of OPRTase stock solution (enough for six assays). A 0.050 ml aliquot (or 1/6 the volume) was removed and assayed for phosphoribosyltransferase activity as described under "Spectroscopic Assays," to give a before or zero-time activity. This left enough enzyme for five assays. As is detailed under each experiment, concentrated reagent solution, H₂O, PRPP and/or Mg⁺² to make a total volume of 0.050 ml, were then added to the remaining 0.25 ml of incubation mixture and the clock was started. At various intervals, usually 1/2 min., 5 min., 15 min., and 30 min., 0.060 ml (or 1/5 the volume) aliquots were removed and assayed for phosphoribosyltransferase activity.

Breakdown of Diethyl Pyrocarbonate under Controlled Conditions

Diethyl Pyrocarbonate (DEPC) is unstable in aqueous solution, rapidly breaking down to CO₂ and ethanol. Therefore, the concentration of DEPC in the incubation mixture does not remain constant with time. Since the rate of breakdown of DEPC is also influenced by pH, a study was performed to determine a rate of breakdown of DEPC over a pH range of 4.5 thru 9 in potassium phosphate buffer. DEPC in ethanol was added to 0.1 mM potassium phosphate buffer at the indicated pH. At various times, 1ml aliquots were removed and placed in disposable culture tubes containing 2 ml of 10 mM imidazole. Since imadazole reacts with DEPC to form a compound which has an extinction coefficient of $3 \times 10^3 \text{ M}^{-1} \text{ cm}^{-1}$ at 240 nm, this property can be utilized to determine the concentration of DEPC in solution.

Inhibition with Diethyl Pyrocarbonate

DEPC was placed in absolute ethanol and diluted to various concentrations just prior to use. The DEPC concentration of these solutions was determined

spectroscopically using published procedures (Miles, 1977). The buffer used was potassium phosphate since DEPC has a very short half-life in Tris-HCl. After removing an aliquot and assaying for zero-time activity (see "General Incubation Procedures" above), 0.03 ml of distilled water and 0.02 ml of one of a range of concentrations of DEPC in ethanol were added. Control samples contained 0.02 ml of ethanol in place of DEPC solution.

Inhibition with p-Bromo Phenacyl Bromide

Stock solutions of p-bromo-phenacyl bromide (pBPB) were made up in acetone. Incubations were run in 10 mM potassium phosphate buffer. After the removal of an aliquot for zero-time assay, 0.02 ml of distilled water (or a Mg^{+2} -PRPP solution) was added to the 0.25 ml incubation mixture remaining and 0.03 ml of pBPB stock solution added to initiate the reaction. Control samples contained 0.03 ml acetone in place of pBPB solution.

Inhibition with Hydroxylamine Hydrochloride

Hydroxylamine hydrochloride ($NH_2OH \cdot HCl$) was adjusted to pH 8 with NaOH and made up to a concentration of 1 M for the stock solution which was then diluted as necessary. Incubations were performed in Tris-HCl according to the procedure described under "General Incubation Procedures" above.

AMINO ACID ANALYSIS

Samples of OPRTase, purified to homogeneity, were subjected to amino acid analysis. Some were analyzed as is and others were first incubated with DEPC or NH_2OH . The samples were dialyzed against double distilled water. All handling of dialysis tubing was done wearing rubber gloves, to reduce the possibility of contamination of samples with amino acids from skin and sweat. An equal volume of dialysate was removed and saved for baseline comparison and then each sample was frozen and lyophilized. The samples were then given to

Larry Brink in the laboratory of Stanley Stein (Roche Institute for Molecular Biology) for analysis by his published procedure (Stein et al, 1973). In short, this method involves the acid hydrolysis of the protein to its constituent amino acids, separation of the amino acids by HPLC, reaction of HPLC effluent with fluorescamine to produce fluorescent complexes and quantification by passing through a fluorescent detector. This method can detect amino acids in the picomole range and therefore protein in the microgram range, which amounts to catalytic amounts of enzyme. Proline, tryptophan, and cysteine content were determined separately. Proline is degraded by the acid hydrolysis and tryptophan and cysteine complexed with fluorescamine are internally quenched (Chen et al., 1978 and Stein and Brink, 1981).

COMPUTATION OF NMR SPECTRUM

McDonald and Phillips (1969) have designed a procedure which can predict the ^1H -NMR spectrum of a protein, using the amino acid analysis of the protein and triangles to represent the resonance of individual residues. This procedure was developed for random coil proteins, where the residue side chains are in an aqueous environment. However, since the native protein contains residues, many of which are in the internal protein environment, this procedure cannot be expected to produce an accurate picture of the native enzyme. It can, however, be used to preliminarily identify the peaks of the actual NMR spectrum.

McDonald and Phillips' basic procedure involves the assignment of a triangle for each proton species. Each triangle is of equal area, but the base is determined by the expected amount of splitting by adjacent protons (i.e. the more splitting, the wider the base, and thereby the shorter the altitude.) The altitude of the triangle is then multiplied by the number of equivalent protons per amino acid.

To predict the NMR spectrum of OPRTase, the values for base and altitude determined by McDonald and Phillips and the amino acid analysis performed on purified enzyme were utilized. The altitude of each triangle was multiplied by the distribution of amino acids residues of each type determined in the amino acid analysis experiment.

A computer program, NMRSPEC (Appendix 5), was written to determine the total altitude value for each constituent proton species triangle and to perform the summation of these triangles. This involved the determination of the composite height of all the contributing triangles.

For each proton species, the height of the triangle was determined at positions 5 Hz apart (based on a 220 M Hz instrument), for a maximum of 360 positions for the entire spectrum. This value was added to a master file of those positions and the name of the proton species recorded. These positions were then converted to chemical shifts in parts per million so that the generated spectrum could be comparable to the actual spectrum (taken with a 300 MHz instrument). The data for NMRSPEC (Appendix 5) are listed in Table IV.1 All values are from a published article (McDonald & Phillips, 1969) except for that listed under "Number." For each proton species, the central position and base are listed in Hz (for a 220 M Hz instrument). Heights are the altitudes of the constituent triangles. Number represents the quantity of each amino acid present in OPRTase as determined by amino acid analysis (see "Results"). The printout for NMRSPEC (Appendix 5) is listed in Appendix 8. Graphical representation of the composite spectrum as well as a comparison of it to the experimentally derived spectrum can be found in "Results."

PH DEPENDENCE OF ^1H NMR SPECTRUM OF OPRTASE

TABLE IV.1
Input for NMRSPEC

Residue-Protons	Position	Base	Altitude	Number
LEU CH3	195	30	40	16
LEU B-CH2+G-CH	360	40	15	16
ILEU CH3	183	40	30	14
ILEU CH2	250	60	3.3	14
ILEU CH2	310	60	3.3	14
ILEU B-CH2	425	50	4	14
VAL GH3	205	34	35.2	9
VAL B-CH2	495	50	4	9
ALA CH3	310	36	16.7	16
THR CH3	270	32	18.7	8
LYS G-CH2	315	60	6.7	12
LYS D-CH2+B-CH2	370	60	13.3	12
LYS E-CH2	665	44	9.1	12
ARG G-CH2	365	56	7.2	7
ARG B-CH2	405	48	8.4	7
ARG D-CH2	705	28	14.3	7
PRO G-CH2	445	42	9.5	7
PRO B-CH2	465	50	8	7
PRO D-CH2	725	60	6.7	7
GLU B-CH2	435	40	10	11
GLU G-CH2	500	40	10	11
GLN B-CH2	455	40	10	11
GLN G-CH2	510	40	10	11
ASP B-CH2	590	110	3.6	8
ASN B-CH2	615	60	3.3	8
ASN B-CH2	635	60	3.2	8
MET CH3	455	20	30	2
MET B-CH2	455	44	9.1	2
MET G-CH2	565	32	12.5	2
CYS B-CH2	665	24	16.6	2
HIS B-CH2	700	56	7.15	6
HIS IM-C4	1555	20	10	6
HIS IM-C2	1740	20	10	6
TYR CH2	655	60	6.7	7
TYR O TO OH	1500	34	11.8	7
TYR M TO OH	1560	34	11.8	7
PHE B-CH2	650	60	3.3	8
PHE B-CH2	700	60	3.3	8
PHE AROM	1600	60	16.7	8
TRP B-CH2	745	54	7.4	2
TRP IN C2	1585	20	10	2
TRP IN C5,C6	1550,1565	30,30	6.7,6.7	2.2
TRP IN C4,C7	1640,1660	36,36	5.6,5.6	2.2

The $^1\text{H-NMR}$ spectra of OPRTase, purified to homogeneity, was taken on a 300 MHz Nicolet FT-NMR spectrometer with temperature controls set at 19°C . I wish to acknowledge the Rockefeller NMR Consortium for allowing me this instrument time.

The enzyme had been dialyzed extensively against phosphate at pH 8.0. It was then lyophilized, dissolved in 95% D_2O , re-lyophilized, and dissolved in 99.9% D_2O . The first spectrum was run on this sample of OPRTase.

Concentrated DCl was then added to the sample to adjust its pH successively to pH 7.7, then pH 7.0 then pH 6.0 and finally pH 5.0. At each pH, the spectrum was printed out after all the acquisitions were completed. The one exception was pH 7.0 at which the spectrum was first printed out after 936 acquisitions and then after 3072 acquisitions.

In an effort to conserve the enzyme and reduce the time it spent unfrozen and at low pH, the number of acquisitions was restricted to just enough to discern individual peaks. Therefore, a comparison of heights of one spectrum versus the other cannot be done.

After the sample was analyzed at pH 5.0, it was quickly brought up to pH 7 with NaOD, PRPP and Mg^{+2} were added as stabilizers, and it was quickly frozen at -76°C .

USE OF ^{32}P -NMR SPECTROSCOPY IN SEARCH OF
A P-RIB-OPRTASE INTERMEDIATE

The ^{32}P -NMR spectra were performed on a JEOL 400 M Hz FT-NMR. I wish to acknowledge the CUNY NMR Consortium for this instrument time.

The enzyme used in the NMR study above, remained frozen for 2 years. When it was thawed, it still retained catalytic activity. To test whether a P-Rib-OPRTase had formed, three spectra were taken. First, the ^{32}P -NMR spectrum of this solution was performed. The OPRTase solution was then dialyzed extensively and its ^{32}P -NMR spectrum taken again. Following that, orotate was then added to the solution and its ^{32}P -NMR spectrum taken again. The spectra and analysis thereof are found in "Results."

DETERMINATION OF METAL-PROTON DISTANCES OF THE Mn^{2+} -PRPP
COMPLEX IN THE PRESENCE AND ABSENCE OF OPRTASE

Preparation of PRPP and OPRTase solutions

All glassware was washed with distilled water, soaked for at least 5 hours in HNO_3 , rinsed again with double distilled water and then re-rinsed with water which had been passed thru a Chelex-100 column. PRPP was dissolved in 5 mM Tris-HCl buffer at pH 8.0 and the solution pressure squeezed through a mini-column of Chelex-100, previously equilibrated with metal-free 5mM, pH 8.0 buffer. The column was then washed with three-1 ml aliquots of Chelexed water, to insure removal of residual PRPP from the column. The PRPP solution was then lyophilized and the residue dissolved in 95% D_2O followed by re-lyophilization and dissolving in 99.9% D_2O to a final PRPP concentration of 100 mM PRPP. A second solution was made up with 10 μM Mn^{2+} .

A 17 mg sample of homogeneous OPRTase, (showing 1 band on disc-gel electrophoresis both with and without SDS) was used for this experiment. This represented the yield from nearly 150 pounds of yeast. All handling of the sample in preparation for the NMR experiments was performed at 4° C, with storage at -76° C. The sample was dialyzed extensively against 1 mM Tris-HCl buffer, at pH 8.0. Metal ion traces were removed from the enzyme sample by pressure squeezing through a mini-column of Chelex-100. The H₂O was then replaced with D₂O as follows: The enzyme solution was lyophilized, and the residue dissolved in 95% D₂O. The sample was then rehydrated and stored frozen in a desiccator until time of experiment. The residue was then dissolved in 99.9% D₂O and PRPP prepared in D₂O added to a final volume of 0.4 ml. The 5mm NMR tubes used in this experiment were obtained from Wilmad Glass Company. Chronologically, this was the first NMR experiment performed. The sample was then used for the pH-dependence and E-RP intermediate studies.

The samples containing enzyme were run sequentially, (as listed in "Results") and were prepared from the initial PRPP-OPRTase sample in the following manner: Additions of Mn²⁺ were done by the addition of 5 µl aliquots of a 0.4 mM solution of Mn²⁺. Dilutions of OPRTase were done by the addition of a equal volume of solution containing amounts of Mn²⁺ and PRPP, without OPRTase. This solution was divided and half used as the next sample.

Relaxation Measurements

Magnetic relaxation measurements of the longitudinal relaxation rates of the proton resonances of PRPP were measured, at 19° C, by employing an inversion recovery method at 220 MHz using a Varian HF-200 FT-NMR Spectrophotometer at Rockefeller University. For PRPP alone, readings were taken at $T = 0.1, 0.2, 0.3, 0.4, 0.5, 0.6, 0.7, 0.8, 0.9, 1.0, 2.0, 3.0, 5.0,$ and 10.0 seconds. For the

PRPP-Mn²⁺ complex, readings were taken at $T = 0.01, 0.05, 0.07, 0.1, 0.2, 0.3, 0.4, 0.5, 0.6, 0.7, 0.8, 0.9,$ and 1.0 seconds. In the presence of OPRTase, spectra were collected at $T = 0.01, 0.05, 0.1, 0.2, 0.3, 1.0,$ and 5.0 seconds. The spectra, thus produced, were based on 256 acquisitions under each T listed.

Assignment of Proton Resonances

The different proton resonance signals of PRPP were assigned by comparing different peak heights and by comparison with previously established resonances of protons of sugar rings in nucleosides and nucleotides (Altona and Sundaralingam, 1973, and Davies and Danyluk, 1974).

Section V: RESULTS

PURIFICATION OF OPRTASE FROM BAKER'S YEAST

Orotate phosphoribosyltransferase was purified from Baker's yeast according to the procedure described in "Methods." The procedure was performed in several batches, over the course of four years, on a total of approximately 200 pounds of yeast. The total yield was approximately 25 mg. The bulk of the enzyme was needed for the NMR work. Some of it could be conserved between NMR experiments. The enzyme used for pH studies, chemical modification, and amino acid analysis was not recyclable.

If all steps were followed, a single protein band was obtained on polyacrylamide gel electrophoresis run at pH 8.9 in the presence and absence of sodium dodecyl sulfate. Any protein used for amino acid analysis or NMR work gave one band, while some of the enzyme used for the kinetic studies contained a small amount of a single impurity.

PH-STABILITY PROFILE OF OPRTASE

The stability of the OPRTase over the pH range studied is represented in Fig. V.1. Depicted in Fig.V.1a is the activity remaining at various times during the incubation of OPRTase at pH's 5 thru 8. Fig. V.1b depicts the activity remaining after 15 minutes of incubation at various pH's from 4.5 thru 9.5. As can be seen from these figures, OPRTase is stable for 15 minutes thru pH 9.5, with over 80% of the activity remaining at pH 5.5 and 73% of the activity remaining after that length of time at pH values as low as 4.5.

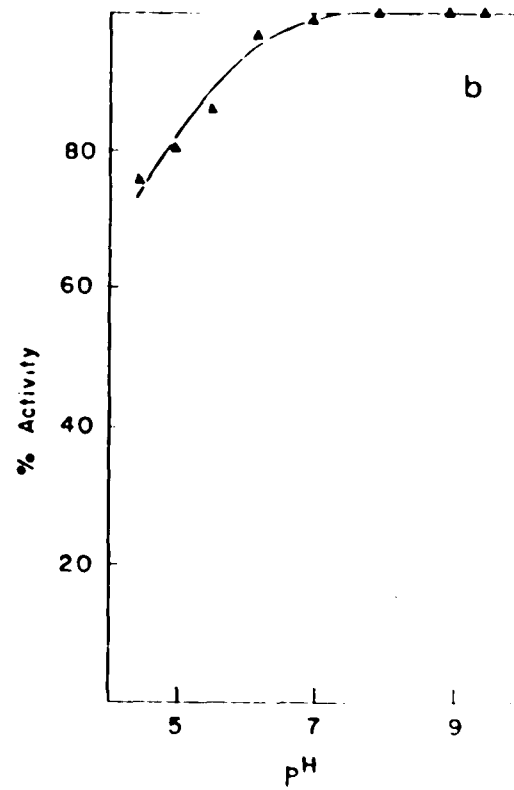
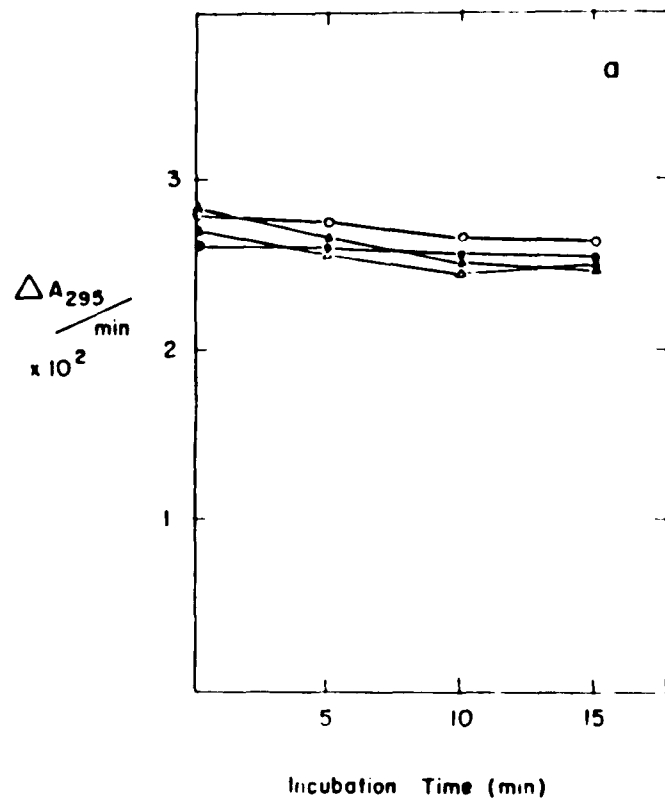
Since the velocities derived for the kinetic studies utilized, at most, only the first 2 to 3 minutes of each trace, any denaturation of the enzyme at the pH's studied should only account for up to a 5% drop in activity even at pH 4.5.

Figure V.1

Stability of OPRTase:

a) Activity remaining at various times with incubation at: pH 5 (open triangles), pH 6 (open circles), pH 7 (closed triangles), pH 8 (closed circles)

b) Activity remaining after 15 minutes of incubation versus pH of incubation mixture.



Therefore, the change in velocity of the enzyme catalyzed reaction (in the pH range of 4.5 to 9.5) cannot be attributed to the denaturation of the enzyme.

PH-ACTIVITY PROFILES

Determination of Vmax's and Km's

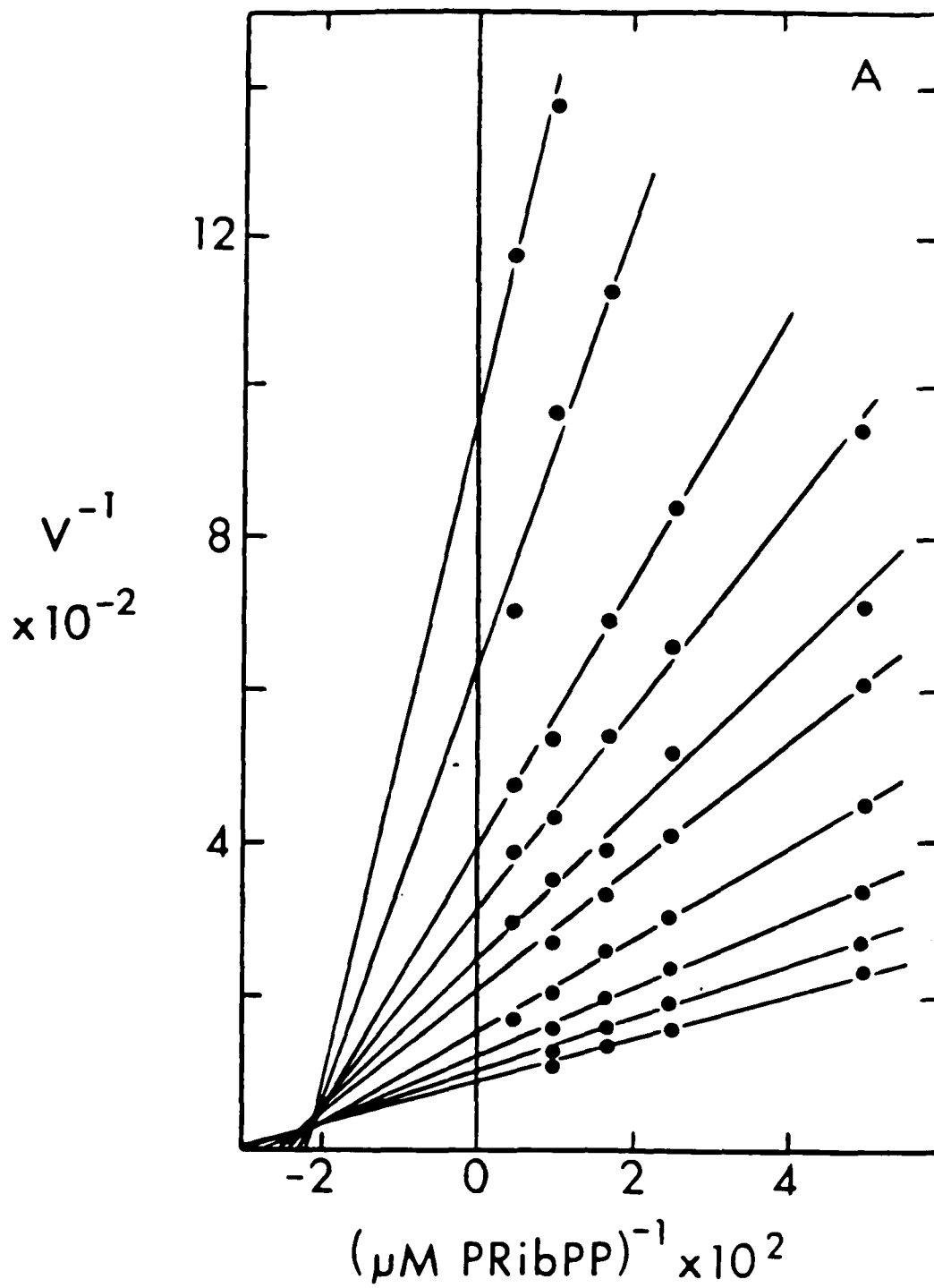
As described in "Methods," OPRTase activity was assayed in both directions over a range of pH values. The kinetic data gathered under these conditions were then analyzed graphically and with the aid of four computer programs. Three programs (i.e. HYPER, PHBELL, and HABELL) were adaptations of those written by Cleland in Fortran and published in *Methods of Enzymology* (1979). They were converted to Basic and adapted for use on the Apple II minicomputer with Epson printer. Listings of HYPER, PHBELL, and HABELL can be found in Appendix 1, Appendix 2, and Appendix 3, respectively. Descriptions of data entry for all three programs can be found in Appendix 6 and sample printouts in Appendix 7. Descriptions and applications of these programs, and a fourth, MANIP DATA, can be found in the Appendix and the text below.

Phosphoribosyltransferase (Forward) Reaction: To study the forward reaction, the concentrations of orotate and Mg^{+2} were held fixed while the concentration of PRPP was varied over a range of 10-100 μM . The data for the forward reaction were then analyzed graphically by plotting mean values of $1/v$ vs $1/[PRPP]$ for each pH tried. This is illustrated in Fig. V.2. Each point represents at least three assays. Apparent V_{max} and K_m values were determined from the inverse of the y-intercept and the negative inverse of the x-intercept respectively. Logarithmic plots of these values are found in Fig V.3. The data was also subjected to the program HYPER (see below) and this gave similar results.

Figure V.2

Double reciprocal plots for the determination of apparent V_{max} 's of the forward reaction and the apparent K_m 's for PRPP over a pH range of 4.3-9.5:

The lines starting from the bottom and going counterclockwise represent the following pH values: 9.5, 8.0, 7.5, 7.0, 6.5, 6.0, 5.5, 5.0, 4.7, and 4.3.



Within the range of pH's for which the enzyme is stable, the K_m for PRPP varies only slightly compared to the change observed for V_{max} , so the change in activity with pH is probably not due to ionization state of PRPP (Fig. V.3).

Pyrophosphorylase (Reverse) Reaction: To study the reverse reaction, the concentrations of PP_i and Mg^{+2} were held fixed while the concentration of OMP was varied over a range of 1-30 μM . The data for the reverse reaction, however, were much more scattered than that for the forward direction due to the lower K_m of OMP vs PRPP and the nature of the assay. It was, therefore, more difficult to analyze this data graphically in an unbiased way, and so it was subjected to the program HYPER. This program was converted from Fortran to Basic by me and made interactive and able to store data. (This Basic adaption of HYPER has also been utilized by Hanna et al. (1983) and Gabrielle et al. (1985)) For each pH, the raw data was used, instead of averages of points, so that there could be some weighting of concentrations of substrate for which more assays were done. HYPER fits the velocity data directly to the equation:

$$V = V_{max} \times A / (K_m + A) \quad (\text{Eq. V.1})$$

with:

A = the substrate concentration

V = the velocity at substrate concentration A

V_{max} = the projected velocity at infinite substrate concentration

K_m = concentration of substrate at half-maximal velocity

It combines least square analysis with iteration to derive best fit values for V_{max} and K_m .

Graphically determined constants were plotted to show that within the range of pH's for which the enzyme is stable, the K_m for OMP varies only slightly compared to the change in V_{max} so that the change in activity observed is probably not due to ionization state of the substrates (Fig. V 4).

Determination of pK's By Cleland Programs

Figure V.3

Kinetic constants for the forward reaction:

Logarithmic plots of apparent K_m (closed circles),
apparent V_{max} (open circles), and apparent V_{max}/K_m
(half closed circles).

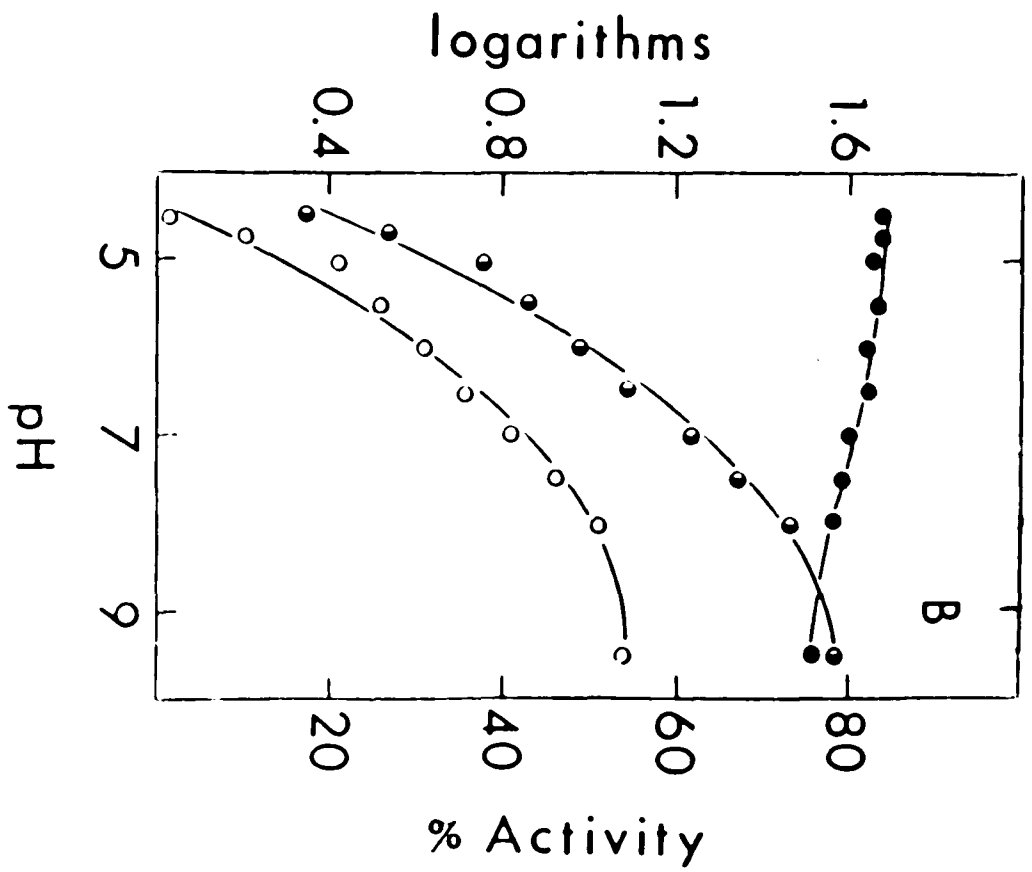
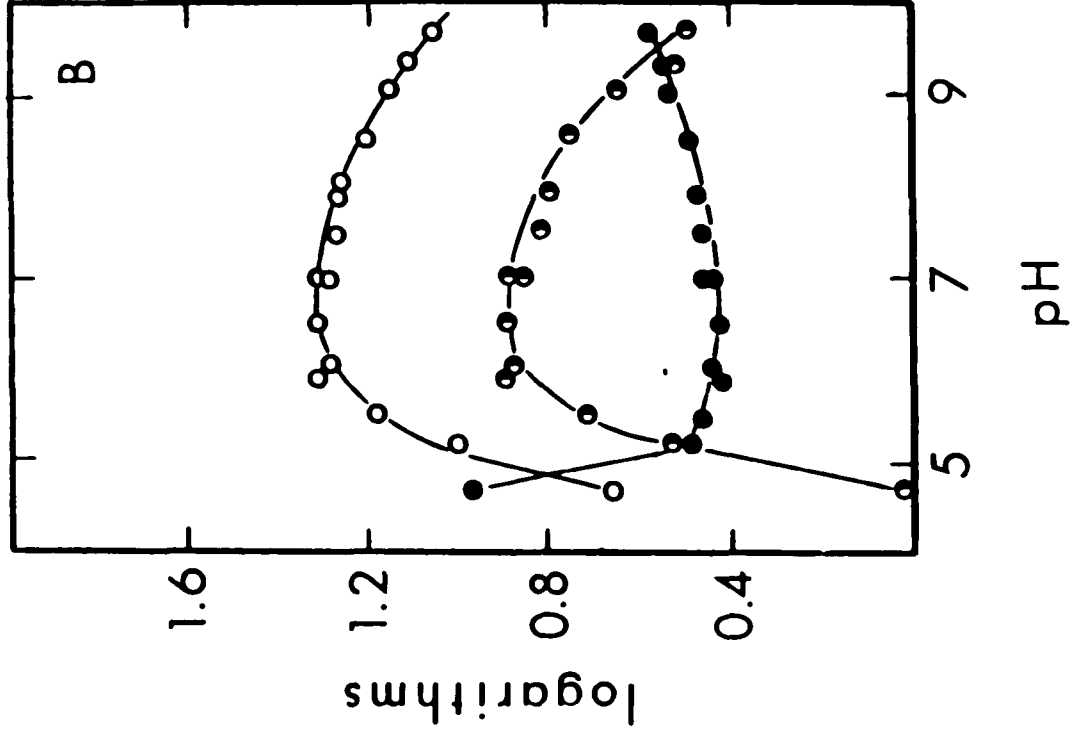


Figure V.4

Kinetic constants for the reverse reaction:

Logarithmic plots of apparent K_m (closed circles),
apparent V_{max} (open circles) and apparent V_{max}/K_m
(half closed circles).



General Considerations: Visually, the plot of Vmax's vs pH for the back reaction approximated that of a bell-shaped curve and that for the forward reaction approximated the left half of such a curve (individual points on Figs. V.6 and V.5, respectively).

To determine the pK's of the curves, the generated Vmax values for the forward and back reactions were then fitted to the following equations respectively:

$$\log Y = \log (C/(1 + [H^+]/K_a)) \quad (\text{Eq. V.2})$$

$$\log Y = \log(C/(1+[H^+]/K_a + K_b/[H^+])) \quad (\text{Eq. V.3})$$

with :

Y = Vmax at a given [H⁺]

C = a constant which is approximately the maximum Vmax

The computer programs HABELL and PHBELL were used for the forward and reverse data respectively. These programs were also originally written in Fortran by Cleland (1979) and converted to Basic by me and adapted for use on the Apple II. The latter program assumes that the data fits a bell-shaped curve and generates the best fitting theoretical curve and the pK's on either side. The former fits the data to the left half of such a curve.

The theoretical curves generated by these programs did not seem to approximate the data well (Fig. V.5, Fig. V.6). The generated K and C values were used, however, as starting points for later computer manipulation of data. For the forward reaction, HABELL generated the values of pK_a = 5.225 and C = 0.0292. For the reverse reaction, PHBELL generated the values of pK_a = 5.12, pK_b = 9.36, and C = 0.0207.

Determination of pK's by A priori Generation of Theoretical Curves

A computer program was developed in Basic for the Apple II computer and Epson printer which could be multi-purpose and in addition generate and compare the fit of theoretical curves to experimental data. This program, MANIP

Figure V.5

Points: Apparent Vmax's for forward reaction
Curve: Generated by HABELL.

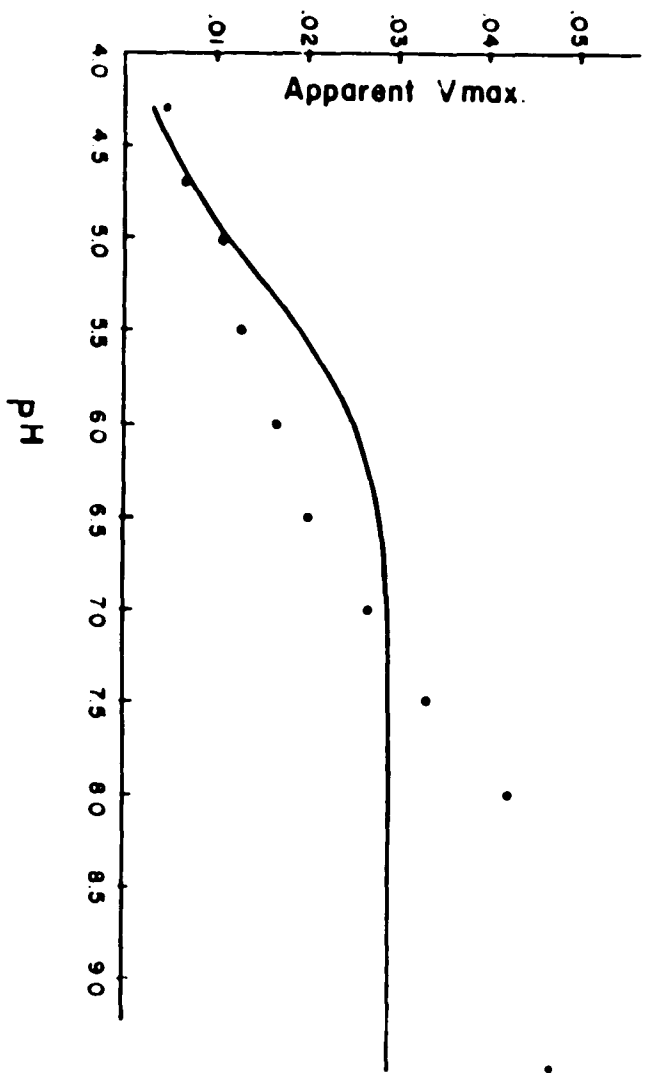
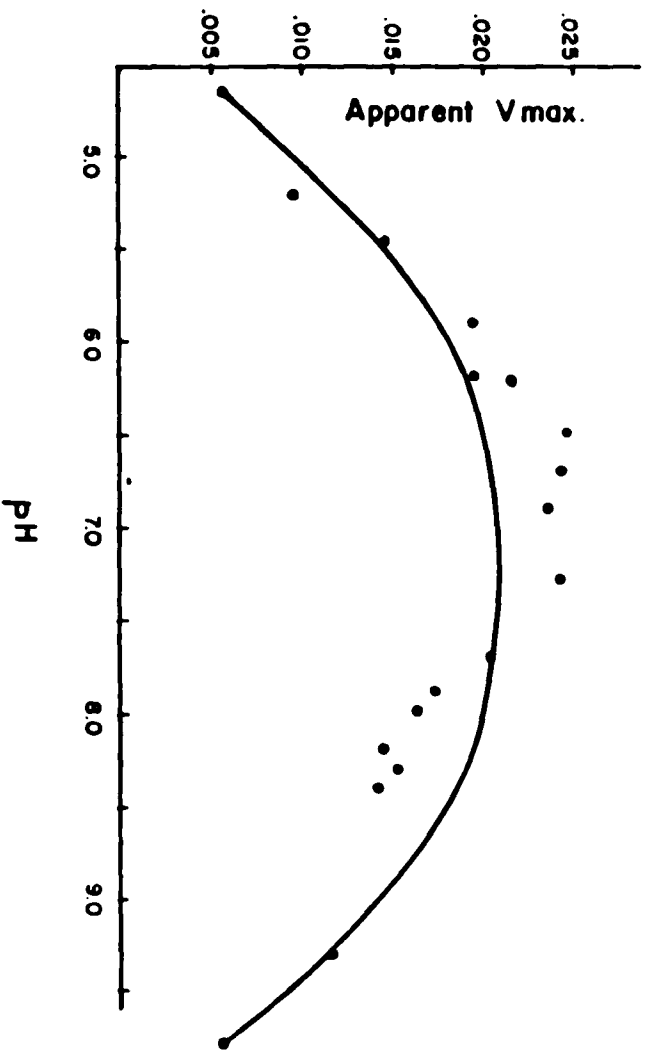


Figure V.6

Points: Apparent V_{max} 's for reverse reaction as
determined by HYPER
Curve: Generated by PHBELL.



DATA, can perform functions on columns of data . It yields a printed output format of up to eight columns and up to 150 points per column. The data entered can be retained for future use, but any generated values are erased when the run is ended. The general functions MANIP DATA performs are on one or two columns but the program can be easily amended to include any equation, no matter how many variables or constants.

Appendix 4 contains a listing of MANIP DATA. A description of data entry and interactive manipulations for MANIP DATA is contained in Appendix 6. Sample printouts are contained in Appendix 7.

Forward Reaction: The equation:

$$V_{max} = C/(1 + [H^+]/K_a) \quad (\text{Eq. V.4})$$

was used for the forward reaction since the data approximates only the left half of a bell-shaped curve. The pH values were stored in Col#1 and corresponding Vmax values in Col #2. $[H^+]$ values were then generated from the pH values and placed in Col #3. Then five combinations of C and Ka were entered and the series of Vmax's generated were placed in Cols #4-8 and printed.

These theoretical curves were then compared to the experimental data as follows: A function was performed which subtracted the corresponding value in Col #4-8 from that in #2 and squared the difference. This value was substituted for that in Cols #4-8. The sum of each column from 4 thru 8 then gave the sum of the squares of the difference between the experimental and theoretical for each of the five theoretical curves generated. The procedure was then repeated for other combinations of C and K.

The sum of the squares of the difference between the theoretical and experimental, the residual sum of squares (RSS) is an indication of the closeness

of fit. The lower the RSS the closer the fit. The RSS for the HABELL generated curve was 0.673×10^{-3} .

The closest apriori generated fit to also visually approximate the data was that with a $pK_a = 6.5$ and $C = 0.0420$ with an $RSS = 0.339 \times 10^{-3}$. Even this curve, however, did not seem to fit the shape of the data (Fig. V.7a). Therefore, a second series was generated which assumes two ionizable species. This gave a very close curve ($RSS = 0.0273 \times 10^{-3}$). It employed Equation V.4 for the first part of the data to the plateau and the following equation from the plateau to the peak.

$$Y = (Y_L + Y_H \times K/[H^+]) / (1 + K/[H^+]) \quad (\text{Eq. V.5})$$

with:

Y_L = the value of Y at low pH (in this case, the plateau $Y=0.0120$)

Y_H = the value of Y at high pH (in this case, the peak $Y=0.0470$)

This method generated a curve with pK 's of 4.6 and 7.1 respectively (Fig. V.7b).

A summary of the theoretical curves generated by the procedures outlined above is given in Table V.1.

Reverse Reaction: For the reverse reaction data, the curve generated by PHBELL (Fig. V.6) gave a closer fit than the curve generated by HABELL (Fig. V.5) for the forward reaction data. The RSS was only 1.802×10^{-4} for 20 points. The MANIP DATA program was used, however, to refine the fit.

The equation:

$$V_{max} = C / (1 + [H^+]/K_a + K_b/[H^+]) \quad (\text{Eq. V.6})$$

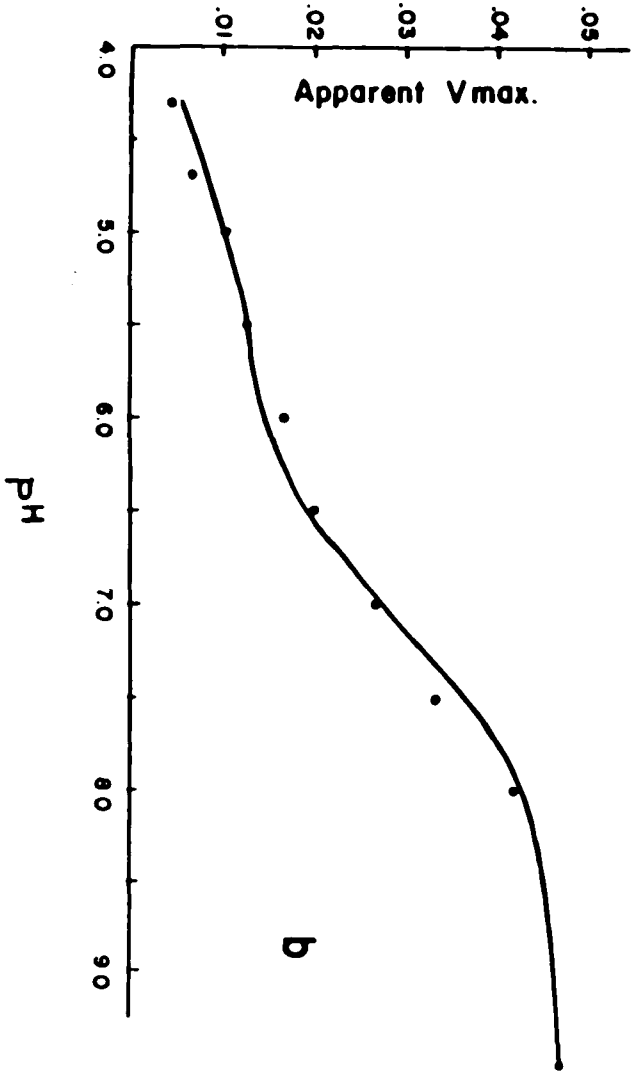
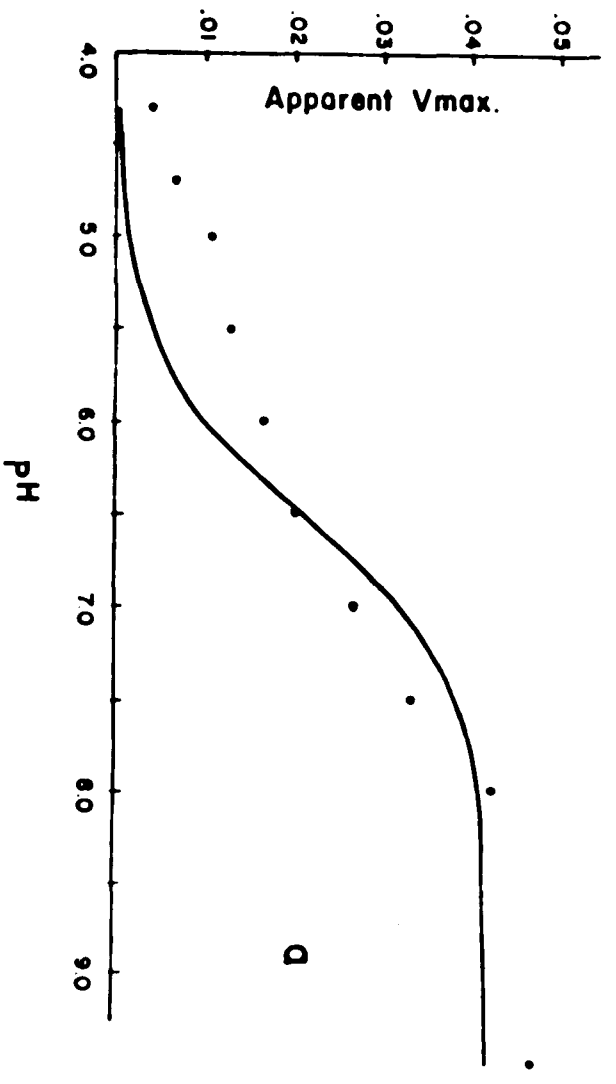
was used for the reverse reaction since the data approximates a bell-shaped curve. As with the forward reaction data, the pH values were stored in Col#1 and corresponding V_{max} values in Col #2. $[H^+]$ values were then generated from the pH values and placed in Col #3. Combinations of C, K_a , and K_b were then entered and the series of V_{max} 's generated were placed in Cols #4-8 and

TABLE V.1
Theoretical Curves for the Forward Reaction of OPRTase

pH	Exp. Data	HABELL	One pK_a	Two pK_a's
4.3	0.0042	0.0031	0.0003	0.0054
4.7	0.0064	0.0067	0.0007	0.0086
5.0	0.0105	0.0109	0.0013	0.0106
5.5	0.0129	0.0191	0.0038	0.0128
6.0	0.0167	0.0250	0.0101	0.0146
6.5	0.0200	0.0277	0.0210	0.0190
7.0	0.0267	0.0287	0.0319	0.0275
7.5	0.0333	0.0291	0.0382	0.0370
8.0	0.0421	0.0292	0.0407	0.0431
9.5	0.0470	0.0292	0.0420	0.0469
C		0.0292	0.0420	0.0120
Y_L				0.0120
Y_H				0.0470
pK_a		5.225	6.5	
pK_{a1}				4.6
pK_{a2}				7.1
RSS x 10⁴		6.73	3.39	0.273
RSS x 10⁵/pts		6.73	3.39	0.273

Figure V.7

Apriori generated curves for the pH dependence of
apparent V_{max} for the forward reaction:
Points: Apparent V_{max} 's for the forward reaction
Curves: a) assuming one pK_a
b) assuming two pK_a 's.



printed. This was repeated for other combinations of the constants. RSS values for these curves were generated as described above. The closest fit that visually approximated the data was with $C = 0.0240$, $pK_a = 5.3$ and $pK_b = 8.55$, with an RSS of 1.287×10^{-4} (Fig V.8a).

Since the last points at high pH deviate from the bell shape, theoretical curves were then generated without the data gathered at the 4 highest pH values (and the two replicates) and the closest fit for equation V.6 generated was with $C = 0.0260$, $pK_a = 5.4$, and $pK_b = 8.3$. Since the right side of the curve linking experimental data points shows leveling out at high pH, the right side of the curve was further investigated using equation V.5 using the values of 0.0255 and 0.0115 for Y_L and Y_H respectively. The best fit for pK_b was found to be 7.9. If this curve is combined with the left half of the previous curve, the curve generated closely approximates the data with $RSS/\#pts. = 0.01256 \times 10^{-4}$ (Fig. V.8b).

A summary of the theoretical curves generated by the procedures outlined above is given in Table V.2.

Comparison of the Forward and Reverse Reactions

If OPRase is assayed at pH 8, the V_{max} for both the forward and reverse reactions closely agree. Studies to determine the ping-pong kinetics of the enzyme had been done at this pH by Victor et al. (1979). The V_{max} vs pH profiles in the two directions are quite dissimilar however. Fig V.9 depicts the two preferred profiles, the 'two pk's' in the forward reaction (Table V.1) and 'Curve V' for the reverse reaction (Table V.2). Note that the forward reaction reaches a maximum near pH 8 and stop there, while reverse reaction reaches a maximum below pH 7.

Table V.2
Theoretical Curves for the Reverse Reaction of OPRTase

pH	Data	Theoretical curves				
		I	II	III	IV	V
4.65	0.00533	0.00521	0.00439	0.00393	----->	0.00393
5.2	0.00953	0.01126	0.01062	0.01006	----->	0.01006
5.45	0.01472	0.01406	0.01405	0.01374	----->	0.01374
5.9	0.01945	0.01773	0.01915	0.01969	----->	0.01969
6.2	0.01928	0.01909	0.02123	0.02229	----->	0.02229
6.2	0.02155	0.01909	0.02123	0.02229	----->	0.02229
6.5	0.02494	0.01983	0.02239	0.02374	----->	0.02374
6.7	0.02435	0.02012	0.02277	0.02418	0.02467-->	0.02467
6.7	0.02435	0.02012	0.02277			
6.9	0.02375	0.02029	0.02291	0.02427--	0.02423-->	0.02423,7
7.3	0.02451	0.02039	0.02251	0.02337	0.02269-->	0.02269
7.7	0.02050	0.02020	0.02100	0.02070	0.02008-->	0.02008
7.9	0.01729	0.01997	0.01957	0.01855	0.01850-->	0.01850
8.0	0.01665	0.01981	0.01869	0.01729	0.01770-->	0.01770
8.0	0.01665	0.01981	0.01869			
8.2	0.01485	0.01934	0.01658	0.01448	0.01617-->	0.01617
8.3	0.01554	0.01903	0.01535		0.01549-->	0.01549
8.4	0.01455	0.01864	0.01405		0.01487-->	0.01487
9.3	0.01189	0.01105	0.00362		0.01204-->	0.01204
9.8	0.00582	0.00551	0.00128			
C		0.0207	0.0240	0.0260		
YL					0.0255	
YH					0.0115	
pKa		5.12	5.3--	5.4		5.4
pKb		9.36	8.55	8.3	7.9	7.9
# pts		20	20	14	10	18
RSS x10⁴		1.802	1.287	0.18114	0.0855	0.2322
RSSx10⁵/# pts		0.901	0.644	0.1295	0.0855	0.1290

Figure V.8

Apriori generated curves for the pH dependence of
apparent V_{max} for the reverse reaction:

Points: Apparent V_{max} 's for reverse reaction

Curves: a) assuming Bell-shaped curve
b) assuming levelling off at high pH.

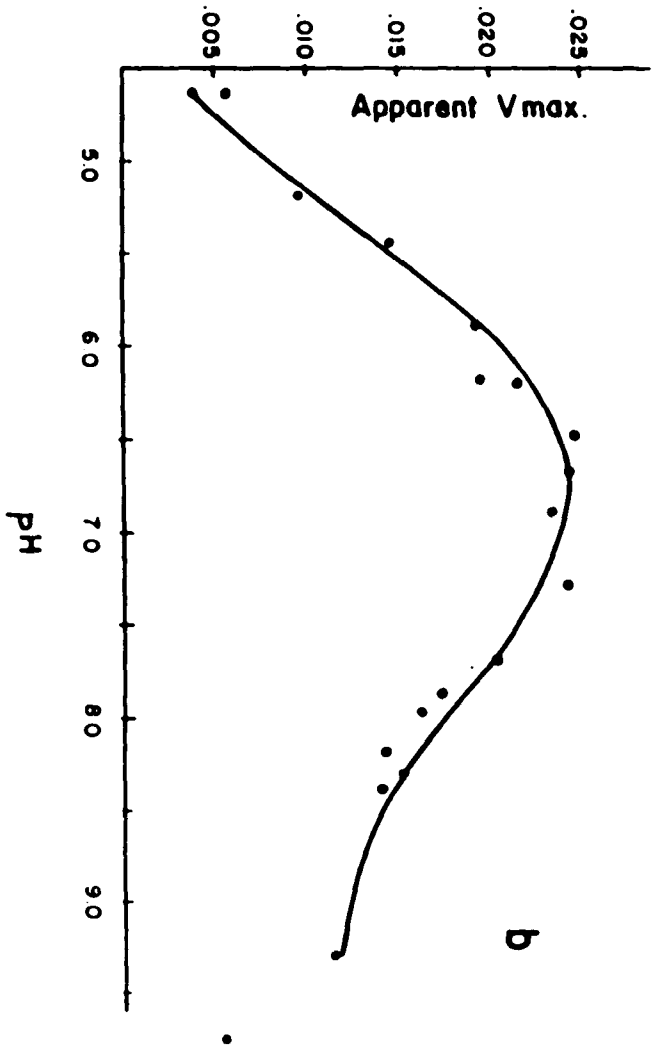
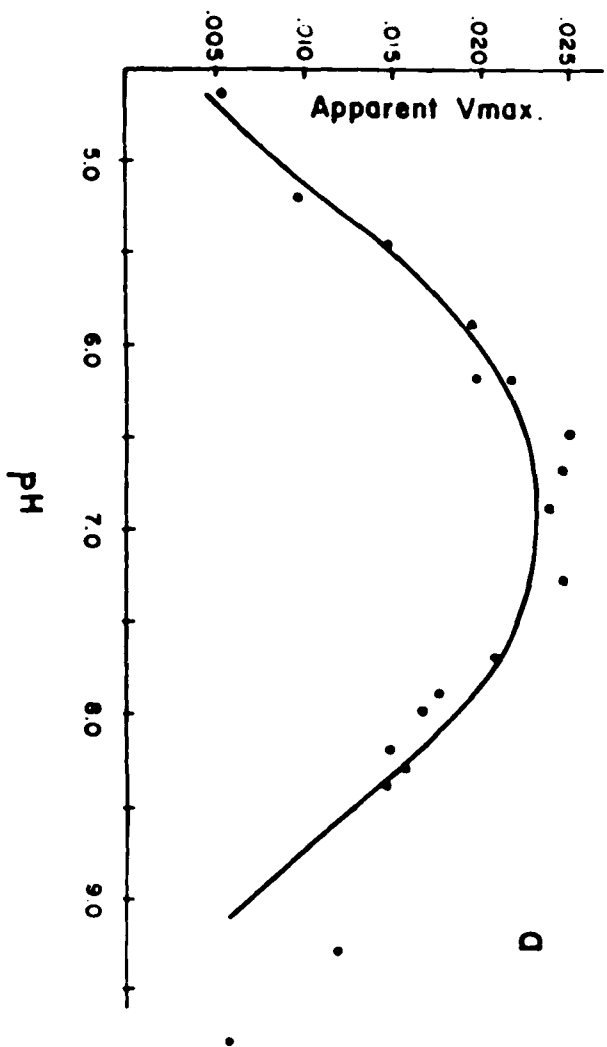
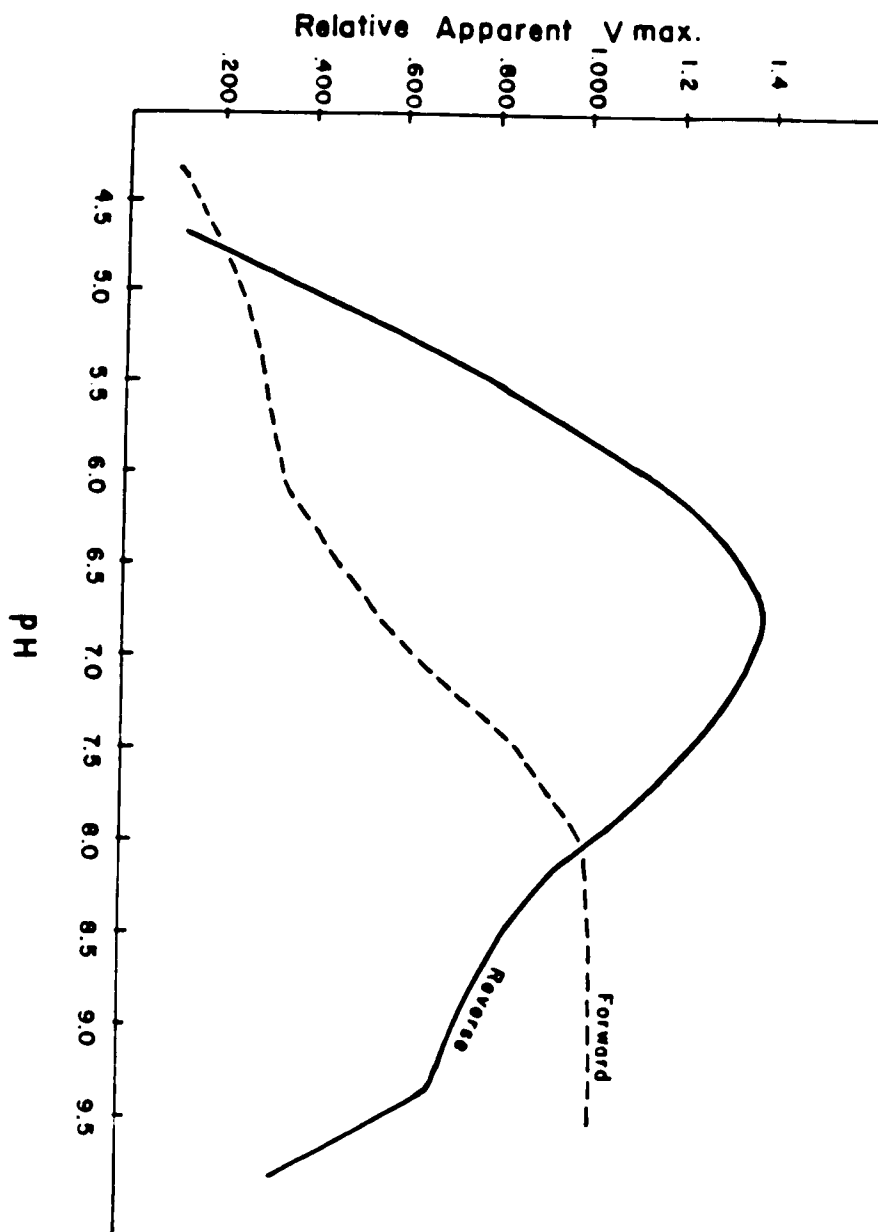


Figure V.9

Best theoretical V_{max} curves of the forward and reverse reactions assuming equal amount of enzyme is used for each assay.



CHEMICAL MODIFICATION

Breakdown of DEPC in Solution

To characterize the stability of DEPC in solution DEPC at a concentration of 1mM was incubated in potassium phosphate buffer at various pH's as described in "Methods." Aliquots were removed at various times, reacted with imidazole, and the absorbance of the solution at 240 nm was determined. The results of this experiment are depicted in Fig. V.10. As the pH of the incubation mixture is increased, the half-life of DEPC in solution decreases. For example, at pH 4.6, over 50% of the DEPC remained intact after 30 minutes while at pH 9.1, over 50% of the DEPC was degraded in less than 10 minutes.

As will be seen later, PRPP and Mg^{+2} offer protection to OPRTase from inactivation with DEPC. To determine if this effect can be explained by the enhanced breakdown of the reagent in the presence of substrates, the experiment depicted in Fig V.11 was performed. The top graph represents the breakdown of DEPC in phosphate buffer at pH 6.5. The bottom graph represents the breakdown of DEPC with 1mM PRPP and 20 mM $MgCl_2$ present in the solution. Note that the breakdown follows the same pattern for the two conditions.

Inactivation of OPRTase with Diethylpyrocarbonate

OPRTase was then incubated with 1mM DEPC at various pH's and its activity taken at 0.5, 5, and 10 minutes as described in "Methods." The results of this experiment are depicted Fig. V.12. The insert is a close-up of the first half minute. As can be seen, the rate of inactivation of OPRTase with DEPC increases with increasing pH. The rates of breakdown of DEPC and inactivation of OPRTase were determined using initial slopes and the slopes were plotted

Figure V.10

Semilog plot of the breakdown of DEPC in the presence of potassium phosphate buffer at various pH values between 4.5 and 9.1.

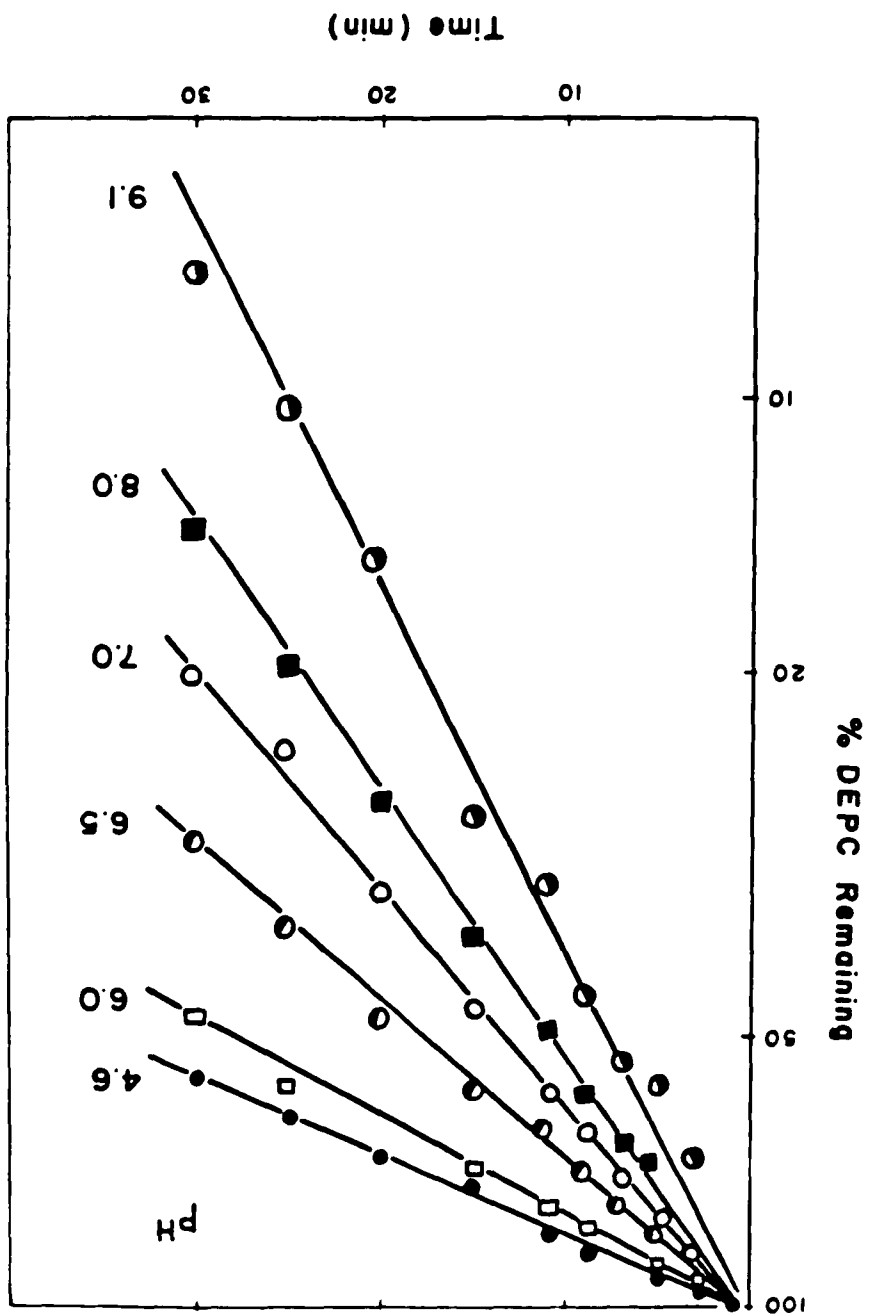


Figure V.11

Breakdown of DEPC in the presence and absence of substrates:

- A) DEPC in 0.1 M potassium phosphate (pH 6.5)
- B) DEPC in 0.1 M potassium phosphate (pH 6.5)
with 1 mM PRPP and 20 mM MgCl₂.

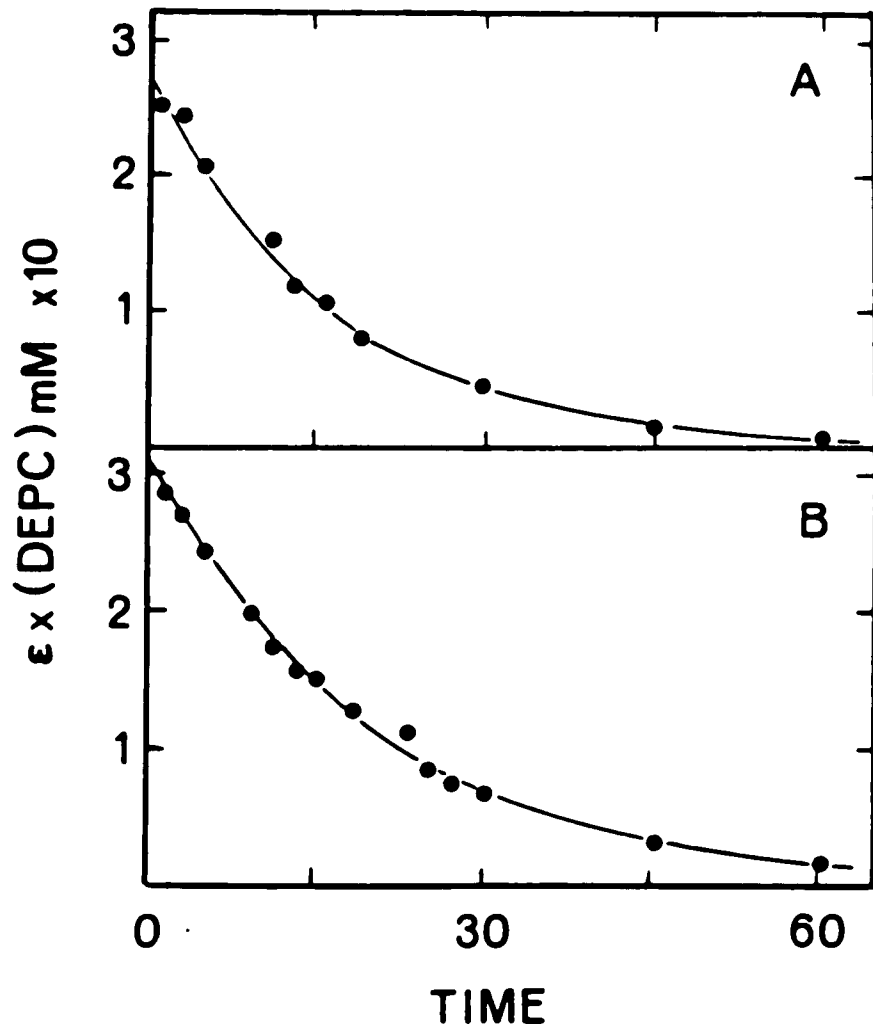
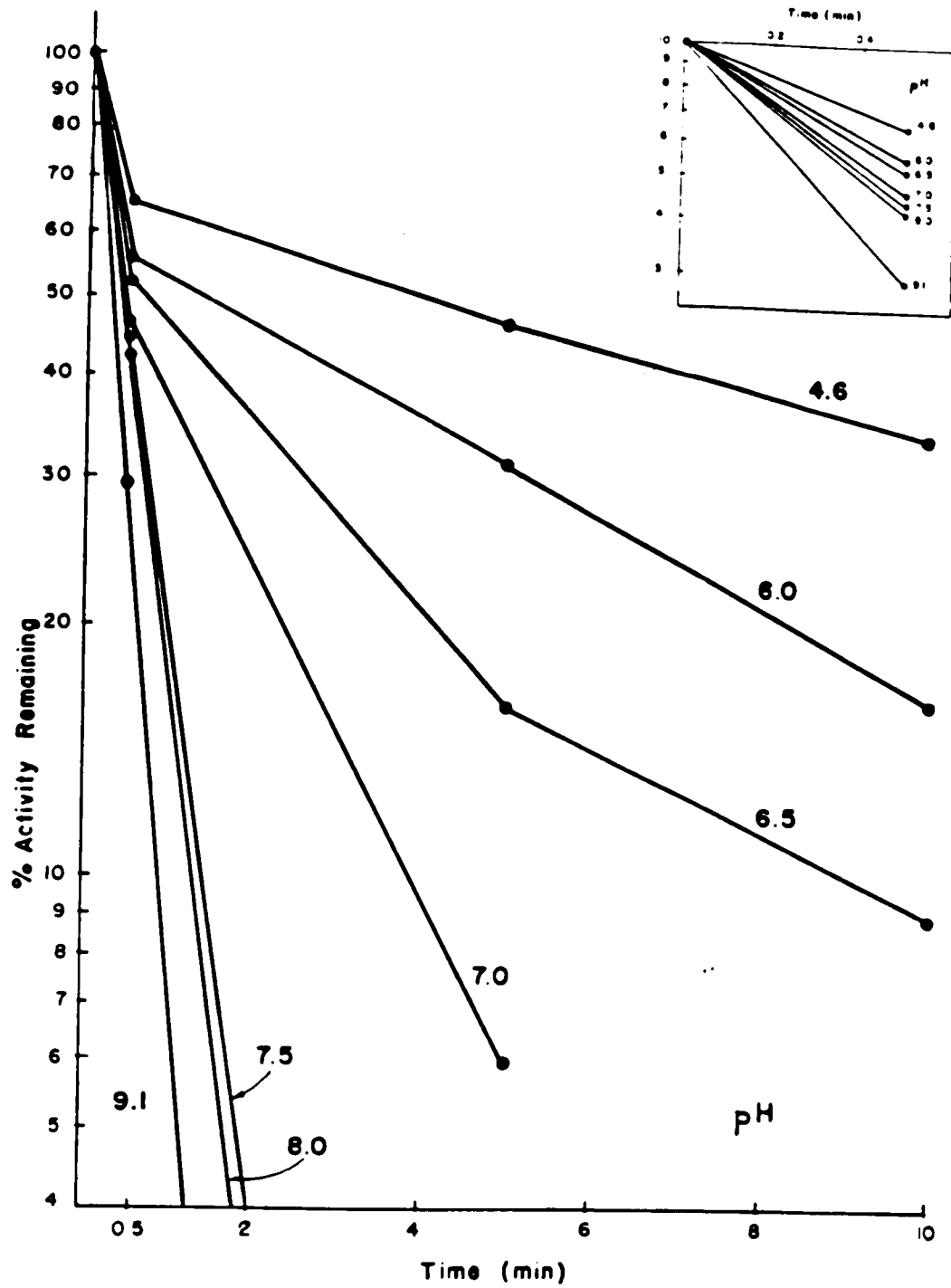


Figure V.12

The inactivation of OPRTase in the presence of 1.8 mM DEPC in potassium phosphate between pH 4.6 and 9.1.



versus pH (Fig. V.13). Notice that the rate of breakdown of DEPC in phosphate buffer is faster at high pH, thereby leading to less DEPC remaining in solution at high pH. Even so, the rate of inactivation of the enzyme is greater at high pH, thereby demonstrating that the pH dependence of the inactivation is not just due to the concentration of reagent remaining.

The pH 6.5 condition was chosen for the remainder of the studies. OPRTase was incubated at various concentrations of DEPC (0.17-11.5 mM) and time dependent inactivation at various concentrations of reagent was demonstrated (Fig. V.14). Notice that the initial rate and extent of inactivation were both affected.

Fig. V.15 contains several graphs demonstrating substrate protection of OPRTase from inactivation by DEPC. In all 3 graphs, curves b-d depict the fraction of the initial activity remaining when DEPC is added to the incubation mixture and aliquots are removed at various times to be carried through the assay procedure. Curves a and d represent the ethanol control and unprotected inactivation respectively. Protection from inactivation by DEPC was observed in all cases in which PRPP and /or Mg^{+2} were present, with more protection seen with both PRPP and Mg^{+2} present. Each curve is the result of several experiments. Graph A demonstrates that PRPP and Mg^{+2} offer greater protection from inactivation than Mg^{+2} alone. Graph B demonstrates that PRPP and Mg^{+2} offer more protection from inactivation than PRPP alone. Graph C demonstrates that higher concentrations of PRPP and Mg^{+2} (at the same ratio) provides greater protection.

In order to show that the inactivation of the enzyme by DEPC was due to the reaction with a histidine group, reactivation of the enzyme with NH_2OH was attempted. Following incubation of DEPC-inactivated enzyme with NH_2OH , it

Figure V.13

Rate of breakdown of DEPC and inactivation of OPRTase
in the presence of DEPC in potassium phosphate buffer
between pH 4.6 and pH 9.1.

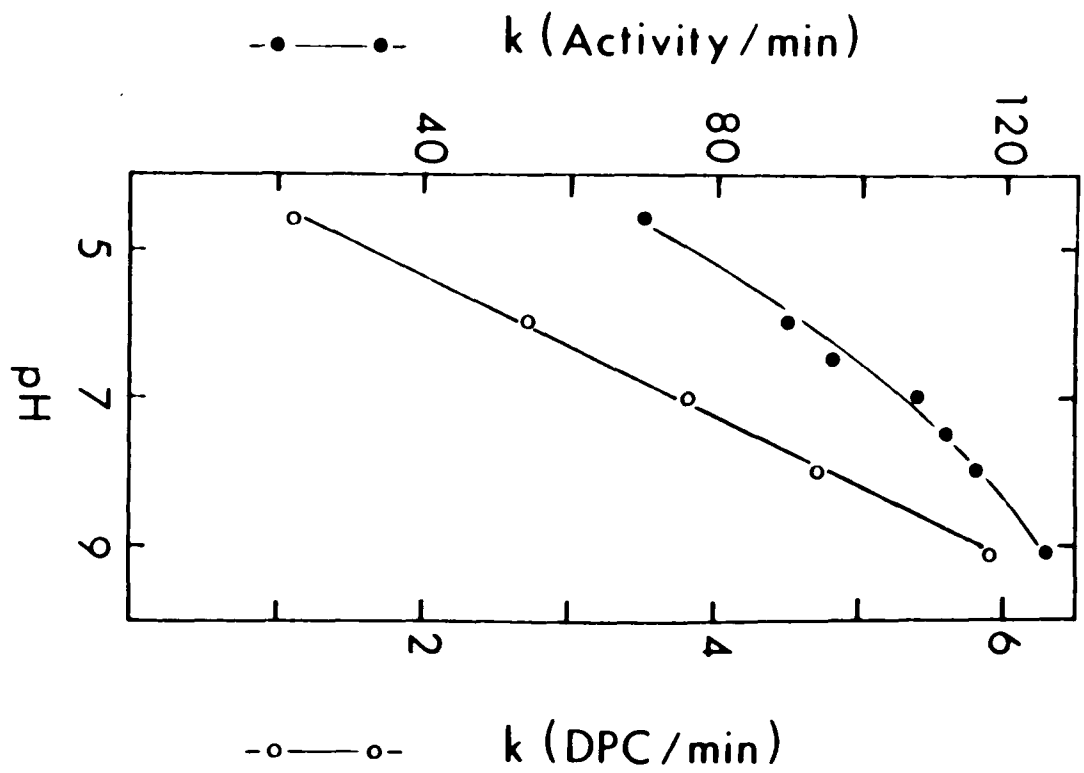


Figure V.14
Concentration dependence of the inactivation of OPRTase
by DEPC in potassium phosphate buffer at pH 6.5.

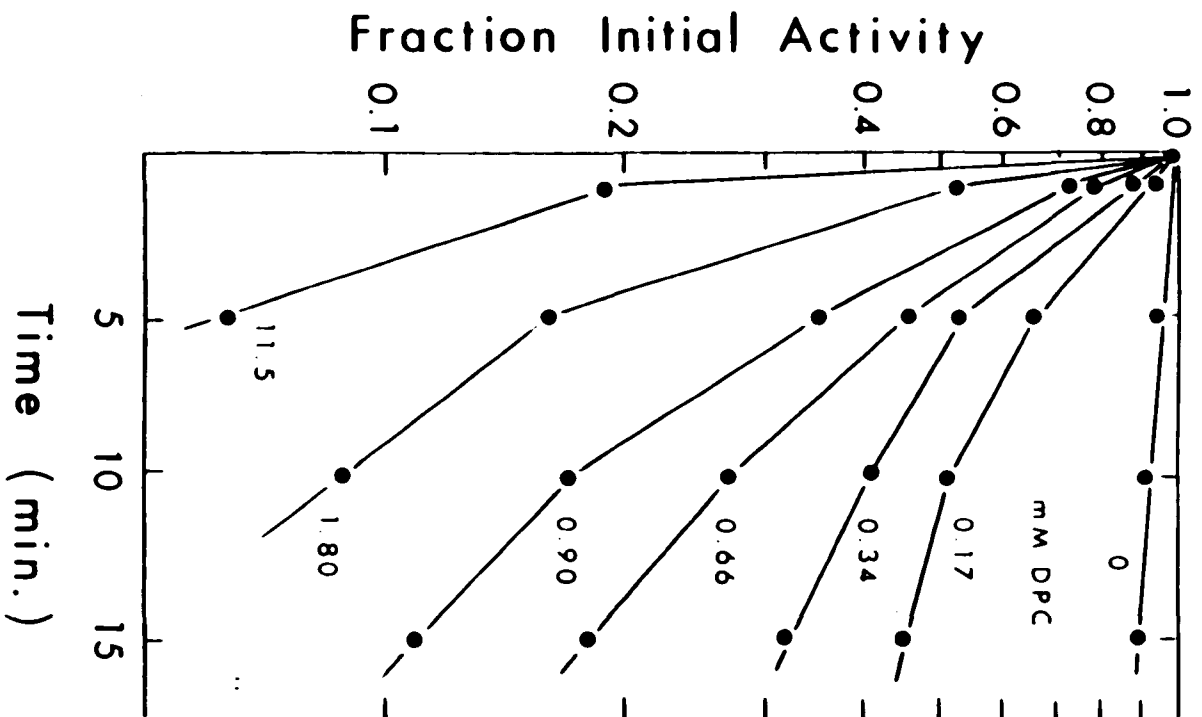


Figure V.15

Substrate protection studies for the inactivation of OPRTase with DEPC:

Graph A is the result of incubation of OPRTase with 0.4 mM DEPC.

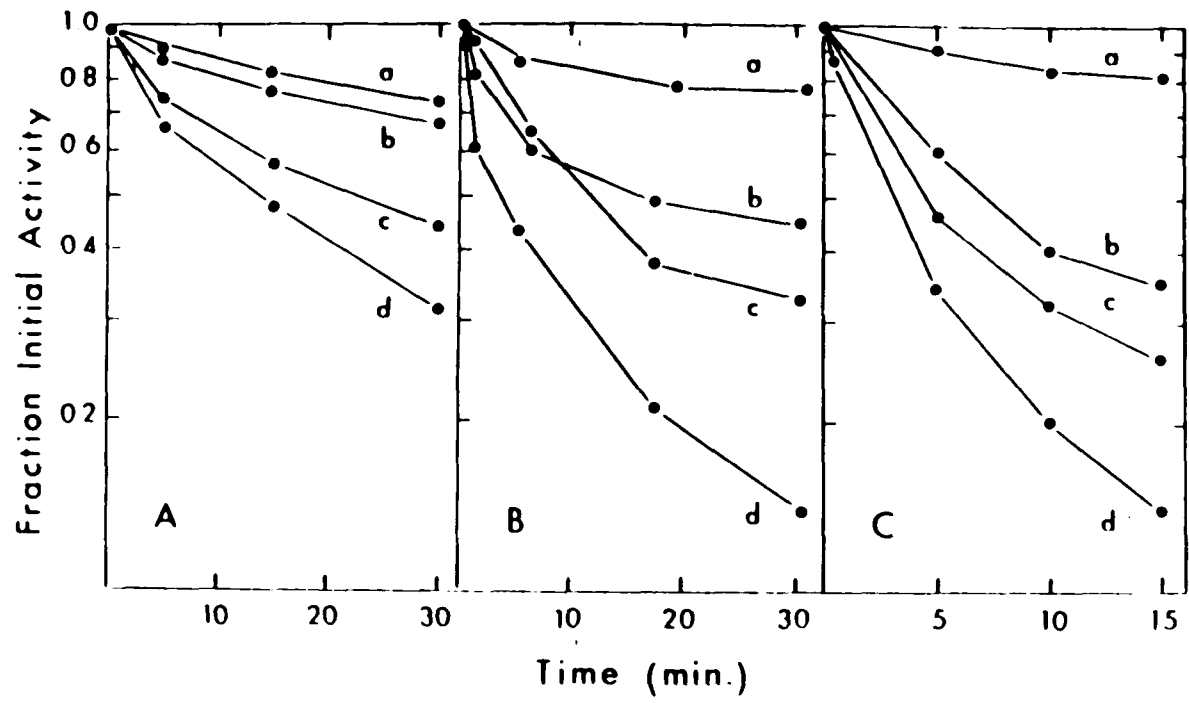
- a) control without DEPC or substrate
- b) incubation mixture containing 1mM PRPP and 10 mM Mg⁺²
- c) incubation mixture containing 10 mM Mg⁺²
- d) without substrate

Graph B is the result of incubation with 0.6 mM DEPC.

- a) control without DEPC or substrate
- b) incubation mixture containing 1mM PRPP and 10 mM Mg⁺²
- c) incubation mixture containing 1 mM PRPP
- d) without substrate

Graph C is the result of incubation with 0.8 mM DEPC.

- a) control without DEPC or substrate
- b) incubation mixture containing 10 mM PRPP and 100 mM Mg⁺²
- c) incubation mixture containing 1 mM PRPP and 10 mM Mg⁺²
- d) without substrates.



was found that even after extensive dialysis the enzyme activity did not return. It was later found that NH_2OH itself inactivates the enzyme. This will be discussed in a later section.

Inactivation of OPRTase with pBPB

A second histidine-specific reagent, para-Bromo-phenacyl Bromide (pBPB) was used to support the theory that there is a histidine at the active site of OPRTase. Ting Wong, an undergraduate student at C.C.N.Y., assisted in performing experiments with pBPB. As seen in Fig. V.16, pBPB inactivates OPRTase in a time-dependent manner. This inactivation is also concentration dependent. Each point represents an average of 3-6 measurements. Experiments were also performed to determine if substrates can protect the enzyme from inactivation. The results of these experiments are depicted in Fig. V.17. Curve a is the control with acetone in place of pBPB solution. Curves b-e represent inactivation in the presence of 1 mM pBPB.

PRPP and Mg^{+2} offer more protection from inactivation than Mg^{+2} alone, and higher concentrations of PRPP and Mg^{+2} offer better protection than lower concentrations at the same ratio of PRPP to Mg^{+2} . This is similar to the protection afforded by substrates to inactivation with DEPC.

Inactivation of OPRTase with NH_2OH

Hydroxylamine (NH_2OH) has been used by several researchers to reactivate enzymes which have been inactivated by DEPC (Miles, 1977). This was attempted in our case but it was found that NH_2OH itself inactivates OPRTase. This occurs at concentrations as low as 2 mM and the concentration needed for re-activation from DEPC is in the Molar range. When experiments were performed as described in "Methods," the individual experiments showed a

Figure V.16

Semilogarithmic plot of the time and concentration dependence of the inactivation of OPRTase with pBPB.

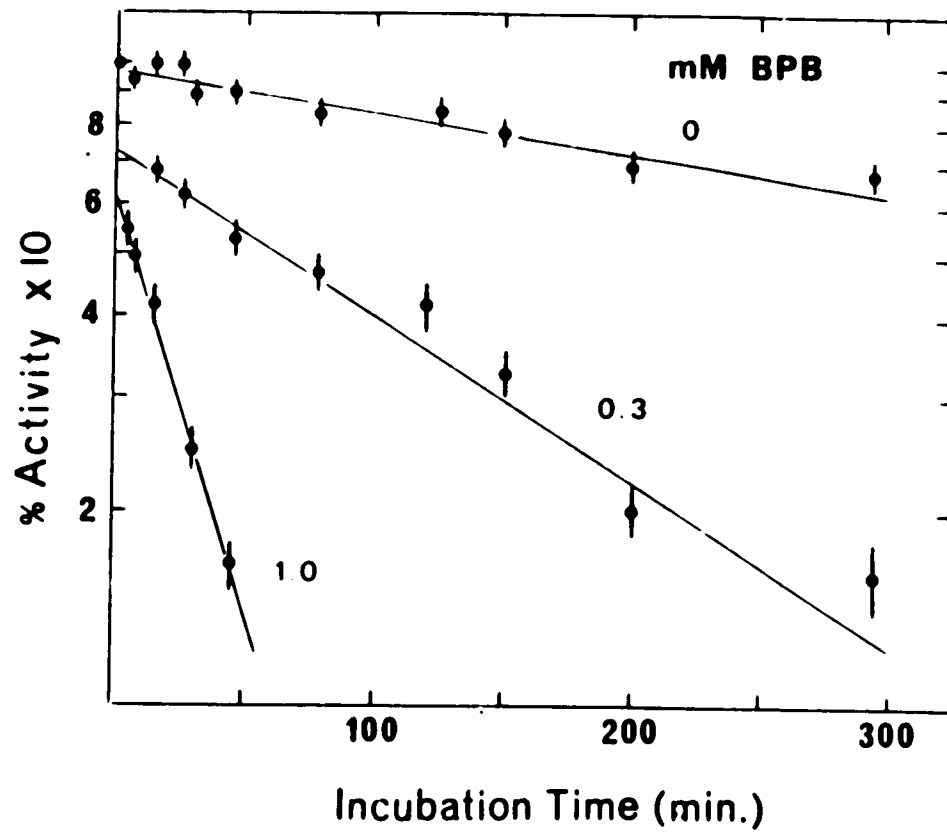
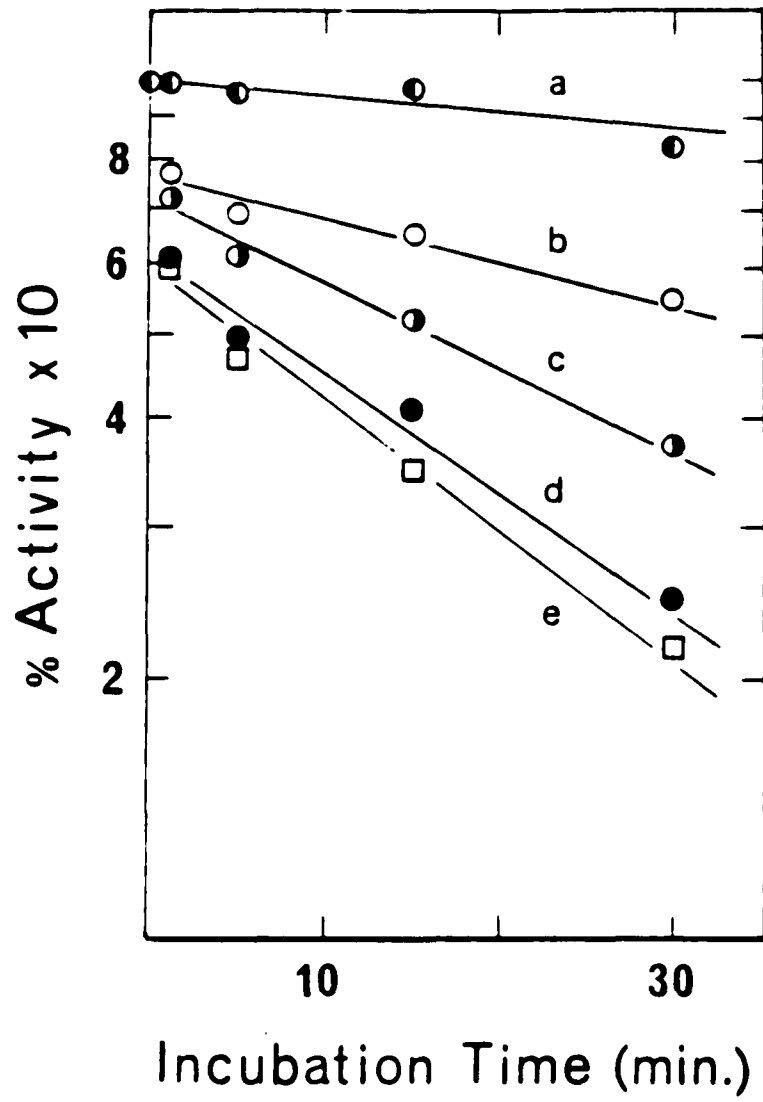


Figure V.17

Substrate protection studies for the inactivation of
OPRTase with 1 mM pBPB:

- a) Control without pBPB or substrates
- b) incubation mixture containing 10 mM PRPP and
100mM Mg⁺²
- c) incubation mixture containing containing 1 mM
PRPP and 10 mM Mg⁺²
- d) incubation mixture containing 10 mM Mg⁺²
- e) without substrates.



lot of scatter, but patterns did emerge if several replicates were performed and their mean values at various stages plotted.

The inactivation by NH_2OH is time dependent. This has been shown at each pH, concentration, and condition used. Therefore, the inactivation is not just due to the competition of NH_2OH with assay components for a sight on the enzyme. That the observed inactivation is not just an artifact of interference with the assay system was further displayed by the inability of pre-incubation of the assay mixture with NH_2OH to result in a drop in initial velocity.

Catalytic quantities of OPRTase were incubated with NH_2OH for up to 20 minutes at concentrations of 1-10 mM. Each point is the result of 2-4 samples. The inactivation of the enzyme by NH_2OH is concentration dependent, with higher concentrations of NH_2OH resulting in faster inactivation (Fig V.18). At 10 mM NH_2OH , OPRTase is totally inactivated in under 10 minutes. The inactivation of the enzyme is also pH dependent (Fig V.19) with 50% activity lost after 20 minutes at pH 6.5 (mean of 3) and 100% lost after only 15 minutes at pH 8.5 (mean of 4). Inactivation at pH 7.5 (not pictured) was nearly indistinguishable from that performed at pH 8.5. Orotate does not afford any protection against inactivation. In fact, as illustrated in Fig. V.20, in the presence of 3mM orotate (mean of 6) OPRTase was inactivated by faster 5mM NH_2OH than without orotate (mean of 3). When solutions were prepared for amino acid analysis, we attempted to regenerate OPRTase from NH_2OH inactivation by extensive dialysis. The enzyme remained inactivated after several attempts. Later, using successive dilution and concentration with a Centricon (Amicon) concentrator, there was some regeneration of activity. The inactivation of OPRTase with NH_2OH was done, however, at much milder conditions than is necessary for reactivation of the enzyme from DEPC inactivation and therefore this reactivation

Figure V.18

Inactivation of OPRTase at pH 7.5 in the presence of:
1 mM NH_2OH (closed circles), 2 mM NH_2OH
(triangles), 5 mM NH_2OH (dotted circles), 10 mM
 NH_2OH (open circles).

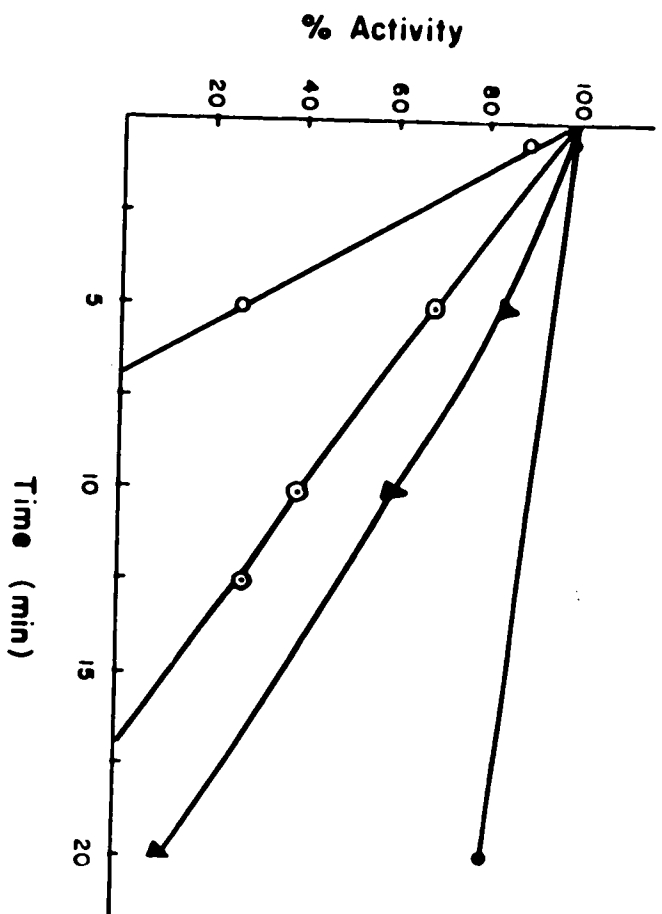


Figure V.19

Comparison of inactivation of OPRTase with 5 mM NH_2OH at pH 6.5 (closed circles) and pH 8.5 (open circles).

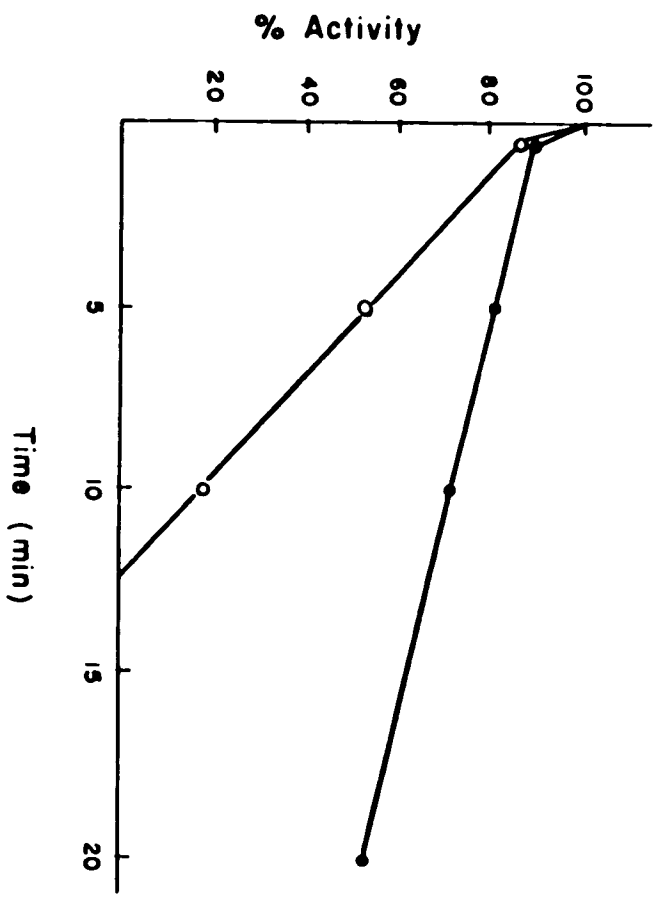
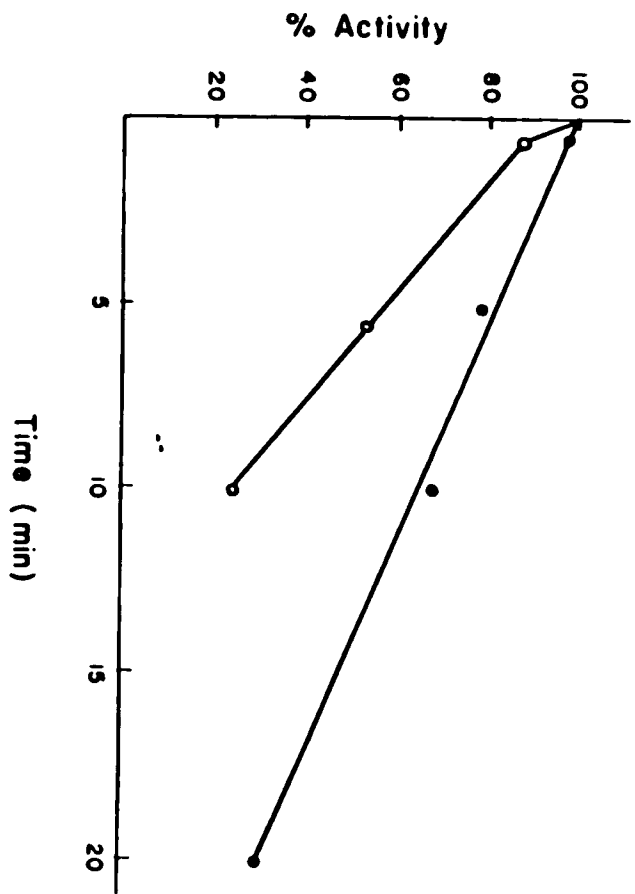


Figure V.20

Comparison of inactivation of OPRTase by 5 mM NH_2OH at pH 7.5 with (open circles) and without (closed circles) 3mM orotate.



does not necessarily imply that we could get reactivation from DEPC. Table V.3 details this experiment. Two incubation mixtures were made up and both were assayed for initial activity. Then water was added to the control, NH_2OH added to the other, and the clock started. The solution, to which NH_2OH had been added, was assayed at several intervals, the last time being 50 minutes. Its activity had dropped to 38% of the initial value. The control retained over 85% of its initial activity after this time. A 150 μl aliquot of each was then diluted with 800 μl of Tris-HCl (pH 8), concentrated by centrifugation for 1 hour, diluted again, concentrated by centrifugation, and then assayed three times each. The activity of the control was essentially that of the OPRTase before successive dilution, but that of the NH_2OH -inactivated now had 80% of its initial activity, up from 38% prior to successive dilution and concentration.

TABLE V.3
Inactivation of OPRTase by NH₂OH and Its Reactivation

	Control		NH ₂ OH	
	Volumes	Activity	Volumes	Activity
Incubation mixture:				
Tris	200 μl		400 μl	
H ₂ O	+50 μl		+100 μl	
OPRTase	+50 μl		+100 μl	

Total	300 μl		600 μl	
Assay(Before)-50 μl		0.0214	-50 μl(x2)	0.0170
H ₂ O	+50 μl		+20 μl	
0.25 M NH ₂ OH			+80 μl	

Total	300 μl		600 μl	
<i>Assayed at intervals</i>				
Assay(50 min)-60 μl(x2)		0.0182	-60 μl	0.0065
Final Vol.	180 μl		200 μl	
Vol. Diluted	150 μl		150 μl	
Tris	+800 μl		+800 μl	

Total	950 μl		950 μl	
<i>Centrifuged in Centricon for 1 Hour</i>				
Final Vol.	300 μl		300 μl	
Tris	+800 μl		+800 μl	

Total	1100 μl		1100 μl	
<i>Centrifuged in Centricon for 1.5 Hour</i>				
Final Vol.	350 μl		350 μl	
Assays	100 μl(x3)	0.0136	100 μl(x3)	0.0097
Adjusted Activities		0.0190		0.0136

AMINO ACID ANALYSIS

The amino acid compositions of various samples of purified OPRTase (homogeneous on disc electrophoresis) were determined, as described in "Methods." Values were provided to us in terms of picomoles of each amino acid residue in each sample. Below is a discussion of the calculation of the amino acids in the native enzyme and protein modified under three conditions: 0.5 mM DEPC, 1 mM DEPC, and 30 mM NH₂OH.

Analysis of Control OPRTase

Three separate analyses were run on each of three samples of purified OPRTase. An equal volume of dialysate from the final dialysis of each sample was also analyzed. The results of the three samples were averaged and the mean of the three dialysates were subtracted from that of the enzyme samples. This gave the average number of picomoles of each amino acid residue in the sample. These values are listed in the 'control' column of Table V.4.

The number of picomoles of cysteine, tryptophan and proline were each, determined separately. Their relative amounts in the protein were determined by subtracting out the dialysate and then multiplying by the ratio of the total number of picomoles of amino acid in the original mean of three samples to that in this particular sample.

In order to convert these values to number of residues per subunit (with a M.W. of 21,000 ± 1000 grams per mole), the following calculation was done:

$$NR = \frac{AA \times 22,000}{TA \times 114} \quad (\text{Eq. V.7})$$

with:

NR = number of residues of a given amino acid in OPRTase
AA = picomoles of a given amino acid in the sample
TA = total picomoles of amino acids in the entire sample
114 = median amino acid molecular weight(minus 18 for condensed H₂O)

TABLE V.4
A. A. Analysis of OPRTase Incubated at Various Conditions

	Control	Incubation with:		
		DEPC 0.5 mM	1mM	NH ₂ OH 30 mM
Asp,Asn	1101	1424	499.3	876.5
Thr	518.3	719.7	236.7	468.5
Ser	886.7	2150	701.3	838
Glu,Gln	1394.6	2509	831.3	1409
Gly	1563.4	3817.7	1386	1380.5
Ala	980.3	1295.3	380.3	918.5
Val	550.3	687	262.6	506.5
Met	137	222.7	138	83.5
Ileu	869.3	743	263.7	668
Leu	1023.7	1166.3	474	857
Tyr	439.7	551.7	219.3	372
Phe	479.3	504	200.7	399
His	399	581.7	236.7	187
Lys	734.3	797	272.6	588
Arg	412.3	715.7	324	385
Cys	(113.3)	()	()	ND
Trp	(97.1)	ND	ND	ND
Pro	(443.6)	ND	ND	ND
Total	12053.2	17884.8	6426.5	9937

Note: All values in picomoles
 ND-not determined
 ()-determined in separate experiments

The above calculation was performed utilizing the MANIP DATA program, described previously. The AA values were entered into a column and multiplied by the appropriate values to produce the NR values.

Analysis of Chemically Modified OPRTase

Other analyses were run on chemically modified OPRTase, so that it could be determined which amino acid residues were affected. Table V.4 lists the number of picomoles of amino acids of these samples (i.e. incubation with 0.5 and 1 mM DEPC and 30 mM NH₂OH in order to compare these with the control, the following calculation was done on the raw data of these three samples (minus dialysates):

$$NR = \frac{AA \times 22,000(1 - 0.0604)}{TA \times 114} \quad (\text{Eq. V.8})$$

with:

0.0604 = fraction of the M. W. of the theoretical control contributed by proline, tryptophan, and cysteine.

and the rest of the values the same as in Equation V.7. Other calculations were performed as above.

Table V.5 lists the distribution of amino acids in OPRTase as calculated by Eq. V.7 and Eq. V.8. Table V.6 lists the distributions of amino acids rounded off to the nearest whole residue.

To determine whether the rounded off values could produce a protein of 21,000 + 1000 M.W. , the following calculation was made. The molecular weight of each amino acid (minus 18 for condensed H₂O) had been previously entered into a column of MANIP DATA. The generated NR values were then multiplied by this column and the total of the generated column provided the molecular weight of the enzyme given that theoretical distribution of amino acid residues. Table V.7 lists the contributions of the various amino acids to the molecular

TABLE V.5
A. A. Analysis of OPRTase Incubated at Various Conditions

	Control	Incubation with:		
		DEPC 0.5 mM	1mM	NH ₂ OH 30 mM
Asp,Asn	16.19	14.44	14.09	15.99
Thr	8.30	7.30	6.68	8.55
Ser	14.20	21.80	19.79	15.29
Glu,Gln	22.33	25.44	23.46	25.71
Gly	25.03	38.71	39.11	25.19
Ala	15.70	13.13	10.73	16.76
Val	8.81	6.97	7.41	9.24
Met	2.19	2.26	3.89	1.52
Ileu	13.92	7.53	7.44	12.19
Leu	16.39	11.82	13.37	15.64
Tyr	7.04	5.59	6.19	6.79
Phe	7.67	5.11	5.66	7.28
His	6.38	5.90	6.67	3.41
Lys	11.76	8.08	7.69	10.73
Arg	6.60	7.26	9.14	7.03
Cys	(1.81)	()	()	ND
Trp	(1.55)	ND	ND	ND
Pro	(7.10)	ND	ND	ND
Total	192.98	181.33	181.33	181.33

Note: All values are in number of residues per subunit and have been rounded off to the nearest 0.01

ND-not determined

()-determined in separate experiments

TABLE V.6
A. A. Analysis of OPRTase Incubated at Various Conditions

	Control	Incubation with:		NH ₂ OH 30 mM
		DEPC 0.5 mM	1mM	
Asp,Asn	16	14	14	16
Thr	8	7	7	9
Ser	14	22	20	15
Glu,Gln	22	25	23	26
Gly	25	39	39	25
Ala	16	13	11	17
Val	9	7	7	9
Met	2	2	4	2
Ileu	14	7	7	12
Leu	16	12	13	16
Tyr	7	6	6	7
Phe	8	5	6	7
His	6	6	7	3
Lys	12	8	8	11
Arg	7	7	9	7
Cys	(2)	(2)	(2)	ND
Trp	(2)	ND	ND	ND
Pro	(7)	ND	ND	ND
Total	193	182	183	184

Note: All values are number of residues per subunit
ND-not determined
()-determined in separate experiments

TABLE V.7
A. A. Analysis of OPRTase Incubated at Various Conditions

	Control	Incubation with:		
		0.5 mM	1mM	NH ₂ OH 30 mM
Asp,Asn	1832	1603	1603	1832
Thr	808	707	707	909
Ser	1218	1740	1914	1305
Glu,Gln	2827	2955.5	3212.5	3341
Gly	1425	2223	2223	1425
Ala	1136	781	923	1207
Val	891	693	693	891
Met	262	524	262	262
Ileu	1582	791	791	1356
Leu	1808	1469	1356	1808
Tyr	1141	978	978	1141
Phe	1176	882	735	1029
His	822	959	822	411
Lys	1536	1024	1024	1408
Arg	1092	1404	1092	1092
Cys	(206)	(206)	(206)	ND
Trp	(372)	ND	ND	ND
Pro	(679)	ND	ND	ND
Total	20813	18733.5	18335.5	19417

ND-not determined

()-determined in separate experiments

weight of the theoretical protein, given the distribution of amino acids in Table V.6.

We had expected initially that if DEPC reacted with histidine, or any other residue, they would appear at a different position in the elution profile. As a control, histidine was reacted with DEPC and then treated by the same acid hydrolysis as the OPRTase. It eluted however, at the same position expected for histidine, suggesting that the DEPC-His bond does not survive hydrolysis. The basic difference between the control and the samples reacted with DEPC seem to be a reduction of longer chain aliphatic amino acids and an increase in glycine and serine. These results will require further investigation. OPRTase reacted with NH_2OH gave an elution profile of amino acids nearly identical to control except for a 50% reduction in the number of histidine residues. This result, along with the inactivation of OPRTase by NH_2OH , suggests, but does not prove, that an essential histidine has been modified.

¹H- and ³²P-NMR STUDIES OF OPRTASE: GENERAL CONSIDERATIONS

Our access to the NMR facilities during the four years over which the NMR experiments were performed, was very limited. At most, 3 days were allowed for each experiment. We could not do any preliminary experiments nor could we return for any additional experiments if our data were lacking in any way. It is hoped that now that a 400 MHz instrument is available at Hunter College, this work can be continued in further detail and performed for other PRTases.

GENERATED ¹H-NMR SPECTRUM FOR OPRTASE IN H₂O

Using the procedure described in detail in "Methods," a spectrum was generated for OPRTase using the amino acid composition determined previously for the native enzyme and the computer program, NMRSPEC (Appendix 5). Table V.8 contains the proton species, spectral positions in ppm, and the height of each triangle contributing to the composite theoretical spectrum for OPRTase. Appendix 8 lists the printout of the entire spectrum produced by NMRSPEC for OPRTase. Fig. V.21 is a graphical representation of these results.

PH DEPENDENCE OF THE ¹H-NMR SPECTRUM OF OPRTASE IN D₂O

The ¹H-NMR spectra of OPRTase at pH 8.0 and pH 7.7 are represented in Fig. V.22 and Fig V.23 respectively. The former is a composite of 780 acquisitions and the latter is that of 682 acquisitions. Fig V.24 and Fig. V.25 represent the ¹H spectra of OPRTase at pH 7.0 as the composite of 936 and 3072 acquisitions respectively. By more than tripling the number of acquisitions, several peaks became more well defined and an additional peak appeared out of the baseline at 8.3 ppm between Fig V.24 and Fig. V.25. This peak also appears in the spectrum acquired at pH 5.0. The ¹H -NMR spectra of OPRTase at pH 6.0

TABLE V.8
Central Positions and Maximum Heights of Composite Triangles

Residue Name	Delta	Total Altitude
LEU CH3	.886	640.
LEU B-CH3+G-CH2	1.636	240.
ILEU CH3	.832	420.
ILEU CH2	1.136	46.2
ILEU CH2	1.409	46.2
ILEU B-CH2	1.932	56.
VAL CH3	.932	316.8
VAL B-CH2	2.250	36.
ALA CH3	1.409	267.2
THR CH3	1.227	149.6
LYS G-CH2	1.432	80.4
LYS D-CH2+B-CH2	1.682	159.6
LYS E-CH2	3.023	109.2
ARG G-CH2	1.659	50.4
ARG B-CH2	1.841	58.8
ARG D-CH2	3.205	100.1
PRO G-CH2	2.023	66.5
PRO B-CH2	2.114	56.
PRO D-CH2	3.295	46.9
GLU B-CH2	1.977	110.
GLU G-CH2	2.273	110.
GLN B-CH2	2.068	110.
GLN G-CH2	2.318	110.
ASP B-CH2	2.682	28.8
ASN B-CH2	2.795	26.4
ASN B-CH2	2.886	25.6
MET CH3	2.068	60.
MET B-CH2	2.068	18.2
MET G-CH2	2.568	25.
CYS B-CH2	3.023	33.2
HIS B-CH2	3.182	42.9
HIS IM-C4	7.068	60.
HIS IM-C2	7.909	60.
TYR CH2	2.977	46.9
TYR O TO OH	6.818	82.6
TYR M TO OH	7.091	82.6
PHE B-CH2	2.955	26.4
PHE B-CH2	3.182	26.4
PHE AROM	7.273	133.6
TRP B-CH2	3.386	14.8
TRP IN C2	7.205	20.
TRP IN C5,C6	7.045,7.114	13.4,13.4
TRP IN C4,C7	7.454,7.545	11.2,11.2

Figure V.21

Predicted ^1H -NMR spectrum (in H_2O) of a random coil protein, having an amino acid distribution as determined for OPRTase.

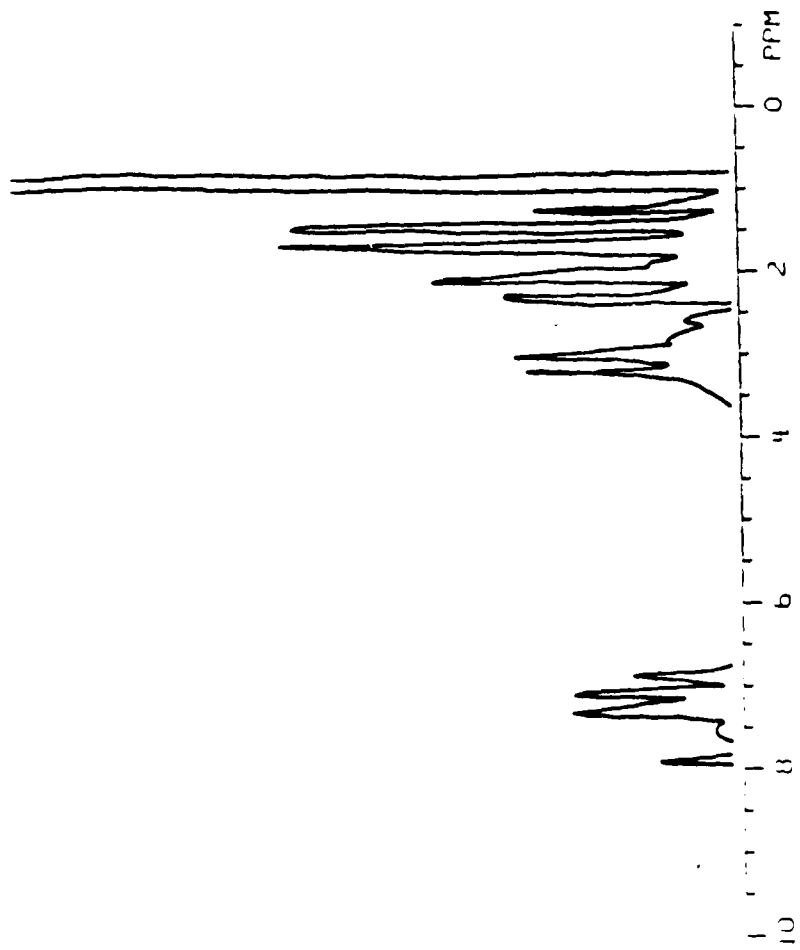


Figure V.22

¹H-NMR spectrum of OPRTase in D₂O at pH 8.0
(780 acquisitions).

Figure V.23

¹H-NMR spectrum of OPRTase in D₂O at pH 7.7
(682 acquisitions).

100 MHz ¹H NMR spectrum of 1,4-dioxane
 in CDCl₃ at 300 K. The spectrum shows
 a multiplet at 4.1 ppm (m, 4H), a multiplet
 at 3.5 ppm (m, 4H), and a multiplet at 1.8 ppm
 (m, 4H).

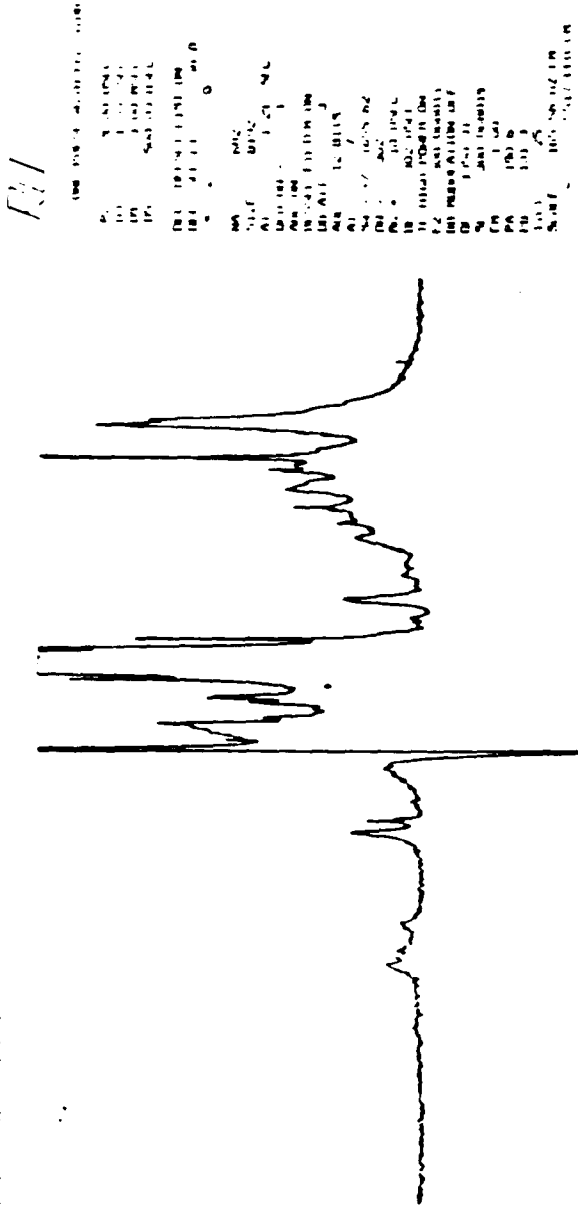
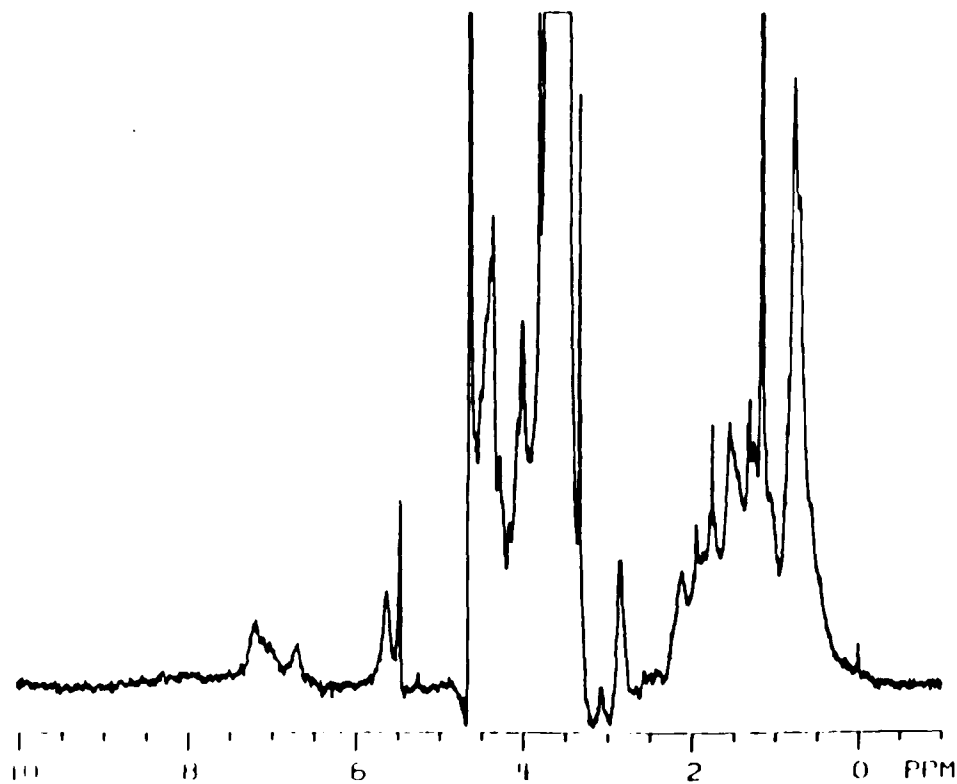


Figure V.24

¹H-NMR spectrum of OPRTase in D₂O at pH 7.0
(936 acquisitions).

SI OAN . 253 F.PICART 25AUG82
OPRIASE PH 7.0 D2O
R10 A20 DB10



RU

ONE PULSE WITH PRESATURAT

P2= 9.00 USEC
DS= 3.00 %C
DN= 3.00 USEC
DS= 500.00 HZ/L

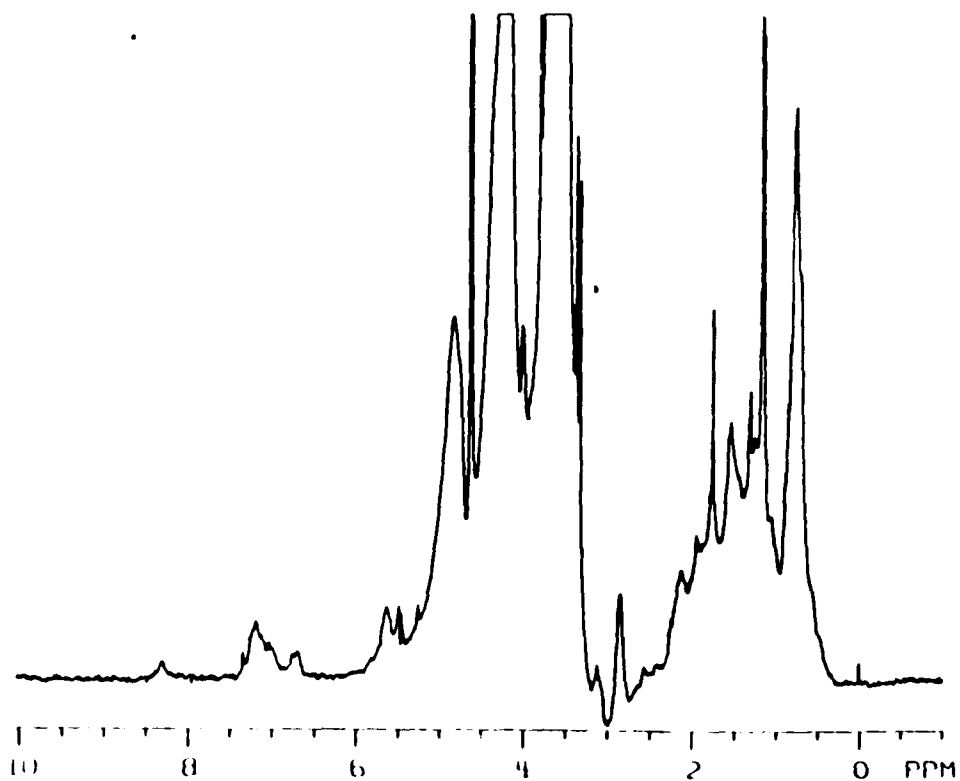
DEC OFFSET 1151 CM
DEL. GAIN 11.0
* 2* .0

NA = 938
LA = 1
SIZE = 8192
AT = 1.25 %C
SPD CM = 1
REL CM
VERS1 FILTER CM
ON ALL = 3
REL = 8 BIT5
AT = 10
SW = 17.1645 62
DN = 302
RL = 10 USEC
DE = 90.0 USEC
TL HIGH POWER CM
F2 = 500 CM/0.15
SD MODULATION OFF
W = 15.0 12
% = 500 CM/0.15
FR = 1.00
PA = 172.5
PB = 125.0
TIC1 = 25
SCALE = 185.55 HZ/LN
* 1516 PPM/LN

Figure V.25

¹H-NMR spectrum of OPRTase in D₂O at pH 7.0
(3072 acquisitions).

SI OAN . BAF F.PICART 30AUG82
OPRIASE PH 7.0 D2O
R10 A50 DB20



RU

ONE PULSE WITH PREPARATION

P2 = 9.00 USEC
D2 = 2.00 SEC
L3 = 3.00 MMFL
D5 = 500.00 MMFL

DEL OFF 11.191 CM
DEL OFF 11.191 CM
• 2 • 0.0000

NA = 3072
LA = 1
SIZE = 0192
A1 = 1.25 SEC
CPD UN = 1
REL UN
SPECT 711174 CM
DB ATT 3
NL = 12.8117
A1 = 10
S1 = 17.16% B2
D4 = 302
RL = 10 USEC
D7 = 302 USEC
T1 HIGH POWER CM
F2 300 UNBOIS
NO PULS ATT CM OF P
CF 1.552 M3
S1 = 300 UNBOIS
FR = 2.00
PA = 221.1
PB = 161.8
TIC1 = 25
SCAN P 165 94 HZ/CM
• 4516 PPM/CM

and pH 5.0, products of 945 and 1536 acquisitions respectively, are found in Fig. V.26 and Fig. V.27 respectively. Fig. V.28 represents the $^1\text{H-NMR}$ spectrum of PRPP in D_2O . Notice that several of these peaks appear on the OPRTase spectra, suggesting that the dialysis was not complete.

We were looking for a spectrum of OPRTase discernible from the baseline noise and wanted to conserve the enzyme and reduce the time it spent unfrozen and at low pH. Therefore, at each pH, the number of acquisitions was different (just enough to discern individual peaks). A comparison of heights of one spectrum versus the other cannot be done. However, we can look at the relative height of peaks at the various positions and these can be compared.

In order to get the clearest picture, the results were expanded and printed out in intervals of 2 ppm each. These expanded spectra are found in reduced form in Appendix 9 and can be compared region by region. The top row is the computed spectrum. This is followed by spectra produced at pH 8.0, 7.7, 7.0 (3072 acquisitions), 6.0, and 5.0 respectively. The spectra from right to left cover the ranges of: 0-2 ppm, 2-4 ppm, 4-6 ppm, 6-8 ppm, and 8-10 ppm.

Only a few minor differences can be seen among the spectra of OPRTase. The first major peak shifts to the left from 0.74 at pH 7.7 ppm to 0.8 ppm at pH 5.0. There is a growth and definition of the peak at 1.8 ppm. At 3.05 ppm, a small wide resonance appears as the pH is decreased. There is also an increase in the height of the peak at 3.8 and a general change in the shape of peaks between 4.2 and 4.5 ppm. The region between 6 and 8 ppm is essentially unchanged. No peak is apparent in the 8-10 region except at 8.3 ppm at pH 7 and two peaks at 8.3 and 8.5 ppm at pH 5. These two spectra are composites of the greatest number of acquisitions. As can be seen in Fig V.24, at pH 7.0 and 936 acquisitions, the 8.3 ppm resonance also does not appear.

Figure V.26

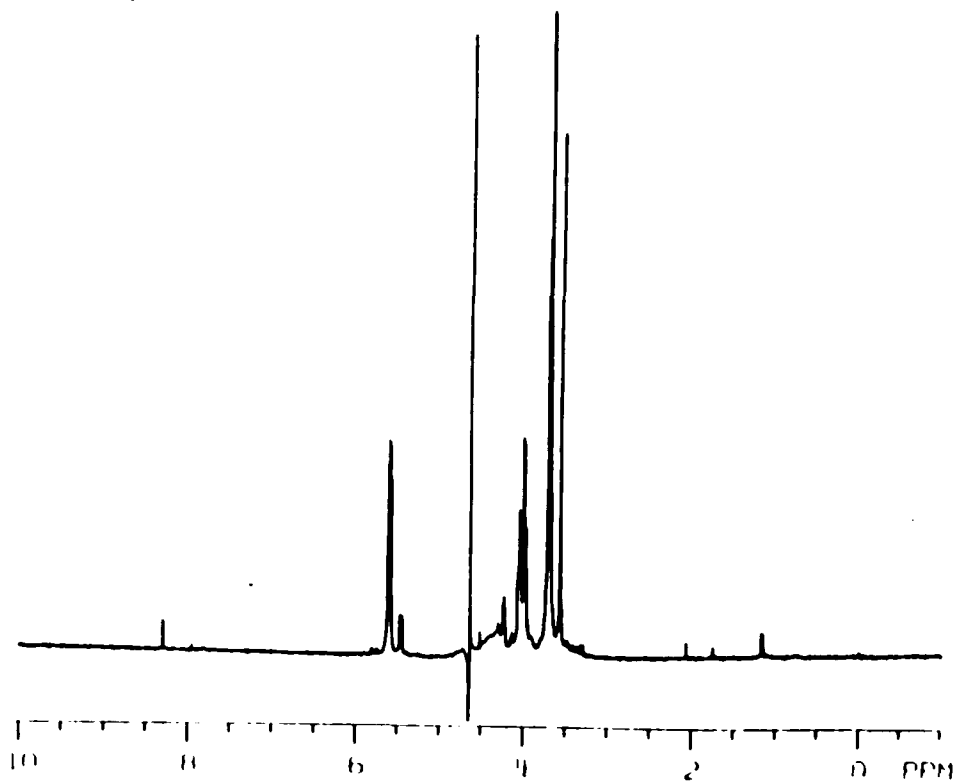
¹H-NMR spectrum of OPRTase in D₂O at pH 6.0
(945 acquisitions).

Figure V.27

¹H-NMR spectrum of OPRTase in D₂O at pH 5.0
(1536 acquisitions).

Figure V.28
¹H-NMR spectrum of PRPP

SIGAN . 261 F.PICART 30AUG82
PRPP D2O
R10 A50 DB10



RU

ONE PULP WITH PREPARATION

P2 = 1.00 MPFC
D3 = 2.00 MPFC
D4 = 3.00 MPFC
D5 = 4.00 MPFC

DEC. OFFSET LIST ON
DEC. OFFSET = 37.0000
* 2 = .00000

NA = 258
DL = 1
SILF = 8192
AI = 1.24 SEC
OPD ON = 1
ADC ON
DEFINT FILTER ON
DB ALL = 5
ADL = 12 B115
AI = 5
SH = 17-1855 62
DM = 302
RL = 10 MPFC
DF = 302 MPFC
TI HIGH POWER ON
F2 = 300 088015
BB PULSE ACTION OFF
DF = 15.2 12
RF = 300 088015
ER = 30
PR = 227.7
PB = 161.6
TIC1 = 161.25
SCAN P = 166.58 1M/CR
* 1517 17M/CR

In general, however, the spectrum seems to be conserved over the pH range studied (5-8). This demonstrates that the enzyme, is probably not undergoing a distinct conformational change within this pH range and therefore the decrease in activity seen with decreasing pH is not due to a change in conformation of the enzyme.

COMPARISON OF GENERATED SPECTRUM OF OPRTASE TO ACTUAL

The resonance positions selected by McDonald, et al.(1969) for computing the $^1\text{H-NMR}$ spectrum of a random coil protein, were found by examination of L-amino acids and short peptides of these amino acids dissolved in D_2O at pD 7. Therefore, for comparison, it's most appropriate to use Fig V.25 (pH 7, 3072 acquisitions) or the expanded pH 7 $^1\text{H-NMR}$ spectrum in Appendix 9. As mentioned in "Methods," the predicted spectrum is for a random-coil protein with its sidechains exposed to solvent and therefore is not expected to completely mimic the $^1\text{H-NMR}$ spectrum of the enzyme in its native state.

Upon superficial examination, the areas of 0.75-3.25 and 6.5-8 ppm are found to contain close to the same number of significant peaks in both the actual and predicted spectra. If the entire spectrum is shifted so that the first major peaks of the predicted (Fig. V.21) and the actual (Fig. V.25) spectra coincide, the following comparisons can be made. Peak number and position are those of the theoretical spectrum.

There are 10 peaks in the 0.75-3.25 ppm region of the theoretical spectrum. Peak #1 (0.89 ppm), representing the methyl protons of leucine, isoleucine, and valine, coincides with the first large resonance of the $^1\text{H-NMR}$ spectrum. Peak #2 (1.23 ppm), representing isoleucine CH_2 and threonine methyl protons, is found at the same position as the shoulder of the next resonance. Peak #3 (1.41 ppm), representing isoleucine CH_2 , alanine methyl,

and lysine gamma-CH₂ protons is shifted downfield from the second major resonance. Peak #4 (1.64 ppm), representing leucine beta-CH₂ and gamma-CH, lysine delta- and beta-CH₂ and arginine gamma-CH₂ protons, coincides with the next wide short peak. Peak #5 (2.07 ppm), representing proline gamma- and beta-CH₂, glutamine and glutamate beta-CH₂ and methionine methyl and beta-CH₂ protons, coincides with the hump following the next tall resonance. Peak #6 (2.23 ppm), representing valine beta-CH, proline beta-CH₂ and glutamate gamma-CH₂, coincides with the small peak following this hump. Hints of peaks #7 and #8 (2.57 and 2.80 ppm respectively), representing two proton species each, aspartate beta-CH₂ and methionine gamma-CH₂ protons and aspartate and asparagine beta-CH₂ protons, respectively, can be found in the next two small bumps. Peak #9 (3.02 ppm), representing lysine epsilon-CH₂, asparagine beta-CH₂, cysteine beta-CH₂, tyrosine CH₂, and phenylalanine beta-CH₂ protons, coincides with a distinct resonance of reasonable size followed by a small resonance coinciding with peak #10 (3.20 ppm), representing arginine and proline delta-CH₂ protons and histidine and phenylalanine beta-CH₂ protons.

The envelope between 3.5-5 ppm contains all alpha-CH protons, the beta hydroxyl protons of serine and threonine, and the glycine alpha-CH₂ protons. Since these resonances are expected to be obscured by H₂O and any PRPP present, they have not been included in the theoretical ¹H-NMR spectrum.

Five peaks are found in the aromatic region of the theoretical ¹H-NMR spectrum. Peak #11 (6.82 ppm), representing tyrosine protons ortho to the hydroxyl, coincides with the first resonance in the aromatic region. Peak #12 (7.07 ppm), representing histidine imidazole-C4 protons, tyrosine protons meta

to the hydroxyl, and tryptophan indole-C5 and -C6 protons, coincides with a shoulder of the next peak. On closer examination, (see Appendix 9), this shoulder contains several small peaks. Note that much of the noise which appears in the spectra generated from under 1000 acquisitions is not observed in this area at pH 7 and the spectra collected at pH 5, the two pH's for which over 1500 transients were made. Peak #13 (7.27 ppm), representing the phenylalanine aromatic protons comes out at the same position as the next resonance. There is some hint of a small hump at the position peak #14 (7.5 ppm), representing the tryptophan indole-C4 and -C7 protons. No resonance is found at the position of peak #15 (7.91 ppm), which would represent histidine imidazole-C2 protons.

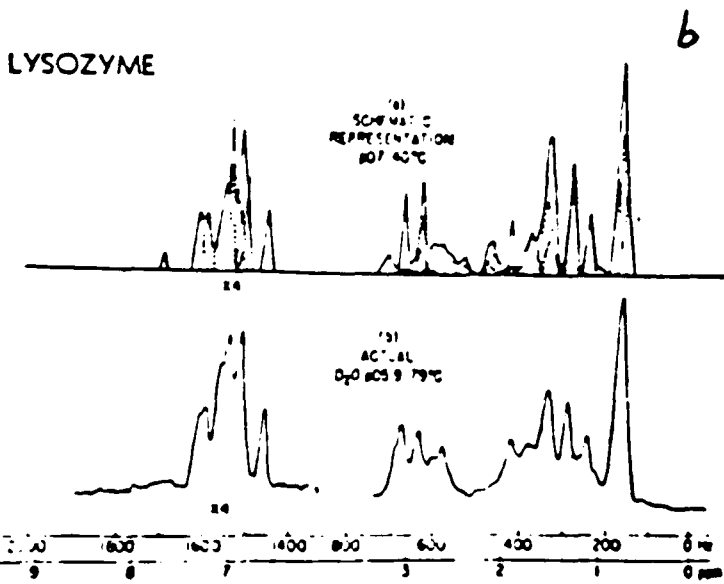
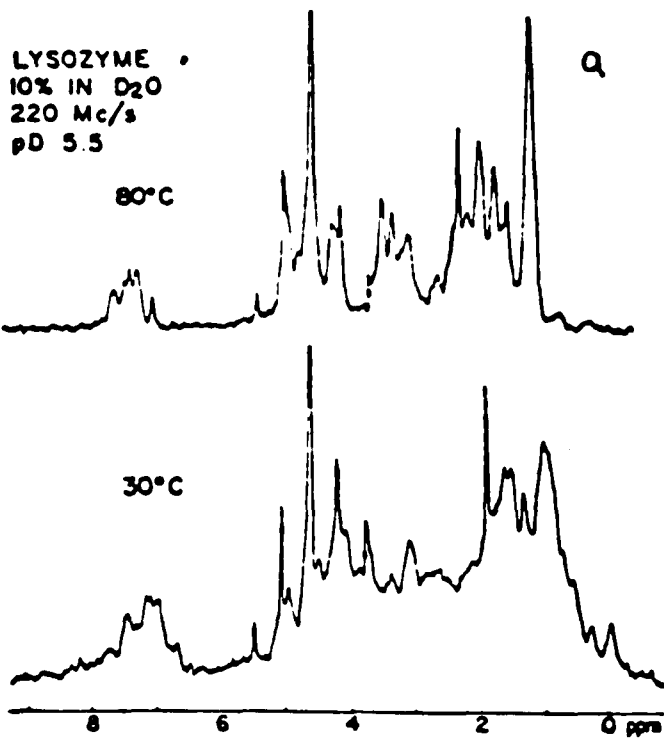
As described in detail above, the number of peaks and their positions relative to the first major peak, closely coincide with those of the theoretical spectrum, though relative heights do not agree as well. Upon thermal or pH denaturation, the $^1\text{H-NMR}$ spectrum should approach that generated by NMRSPEC, with a decrease in the broadness of the peaks. To give a frame of reference for these types of analyses, a comparison of the $^1\text{H-NMR}$ spectra of the native and denatured lysozyme (McDonald & Phillips, 1967A) are given in Fig. V.29A and a comparison of the denatured and theoretical spectra of lysozyme (McDonald & Phillips, 1969) is given Fig. V.29B. Unlike the spectra of native lysozyme which shows several distinct satellite bands upfield from the first major peak and only upon denaturation do they not appear, it was found for native OPRTase that the first major peak has only some very slight bands upfield bands. It was noted by McDonald & Phillips (1967B) that these bands can be attributed to ring-current shift induced in protons of the side chains which loosely approach the faces of the indole groups of the six tryptophan residues in folded

Figure V.29

¹H-NMR spectra of lysozyme

a) comparison of the spectra of the native and the denatured enzyme (McDonald and Phillips, 1967A)

b) comparison of the spectrum of denatured enzyme and the theoretical spectrum based on amino acid composition (McDonald and Phillips, 1969).



Pmr spectra of HEW lysozyme at 220 MHz.

conformation of lysozyme. The absence of these bands in OPRTase can probably be attributed to the fact that there are only between 1-2 tryptophan residues per subunit. The lack of a significant resonance in the spectrum of OPRTase where peak #6 should be seen, has been found in other proteins and may be due to the shifting of valine, glutamate and glutamine resonances or their broadening relative to the computed resonances (McDonald & Phillips, 1969).

The absence of a resonance at 7.91 ppm is probably due to exchange of C-2 protons of histidine imidazoles with D₂O as noted by Meadows & Jardetzky (1968) for lysozyme. Since this region has resonances from only one species of protons would contain useful information if the spectra were performed in H₂O. A small peak appears in the 8-9 ppm region where the amide protons of the backbone should resonate (McDonald & Phillips, 1967A). This demonstrates that while most of the amide protons have exchanged with solvent, a few are difficult to exchange.

From the point of view of studying the active site of the OPRTase, the most interesting region is that from 6-8 ppm (see Appendix 9). In particular, Peak #12, for which half the height is contributed by the histidine imidazole C-4 protons, is broad and contains several small peaks. This suggests that the histidines are in distinctly different environments and that at the concentration of approximately 2mM OPRTase subunits (in a 0.15 ml volume), the spectra is clear enough to discern these different resonances. Note that much of the noise of the spectra collected for under 1000 acquisitions is not observed in the spectra acquired with over 3000 acquisitions at pH 7. The distribution of small peaks in this spectrum around 7 ppm compares quite well to that acquired at pH 5 (and over 1500 acquisitions). Therefore, it seems to indicate that the peaks seen are

real. This opens the way for studying the proximity of substrate to the individual amino acids on the enzyme.

USE OF ^{31}P -NMR SPECTROSCOPY IN SEARCH OF

A P-RIB-OPRTASE INTERMEDIATE

In order to stabilize the OPRTase after the pH dependent NMR study, the enzyme solution was treated as described in "Methods." This solution contained potassium phosphate, MgCl_2 , and PRPP in addition to the enzyme. When it was thawed (nearly two years later), approximately 2 mg of OPRTase remained in solution and was catalytically active. To test whether a phosphoribosylated enzyme (PR-E) had formed, the ^{31}P -NMR spectrum of the starting solution was determined on the JEOL 400 MHz instrument of the CUNY NMR Consortium. As was expected, PRPP, was found intact in the solution as evidenced by peaks at -10 and -4.3 ppm, representing the alpha-phosphate and the beta-phosphate respectively (Fig. V.30 A). The enzyme solution was then extensively dialyzed against Tris to remove as much phosphate as possible and the exogenous PRPP. The ^{31}P -NMR spectra of the dialyzed solution was then determined and is depicted in Fig V.30B. The only significant resonance was that at the position of P_i peak. Excess orotate was then added to knock any phosphoribosyl moiety off the enzyme in the form of OMP. The spectra of this solution (Fig. 30C), however, indicated the reappearance of PRPP. The resonance of particular interest is that at -10 ppm which is where the bridge phosphorous of PRPP should appear. The orotate stock solution was also subjected to ^{31}P -NMR spectroscopy and it revealed no resonances above baseline noise.

The purpose of this experiment was to test for the presence of a tightly bound phosphoribosylated enzyme intermediate formed by the incubation of PRPP with OPRTase in the presence of Mg^{2+} . This could be shown by the

formation of OMP from such incubated enzyme in the absence of exogenous PRPP(i.e. upon dialysis of this incubation mixture). A negative result could be found because of insufficient sensitivity but a positive result would support this theory. Upon dialysis of the OPRTase solution which had been incubating in PRPP and Mg^{2+} , exogenous PP_i and PRPP were removed and some P_i remained. If a PR-E intermediate were present the resonance of the phosphorous moiety would be expected to appear near the P_i peak, probably slightly to the left. However, the concentration could be too low or the resonance could be broad due to its presence on the enzyme. As it turned out, only the P_i peak appeared in the spectrum. It was expected that if a PR-E intermediate had formed (but was obscured by broadening), the addition of Orotate to this solution would cause a burst of production of OMP and the OMP's ^{31}P might appear as a single peak in the vicinity of the P_i peak. If OMP were formed, this is not evident in Fig. 30C, since the spectra shows the resonances of PRPP. It appears that PRPP was tightly bound to the enzyme and was released in response to the addition of orotate in the absence of additional Mg^{2+} . The results of this experiment demonstrate that extra care must be taken in interpreting any results in which PP_i is used to form PRPP from a PR-E enzyme intermediate since a false positive could result if tightly bound PRPP is thereby released.

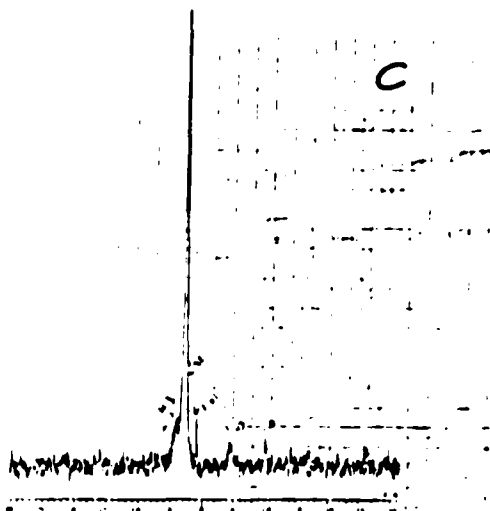
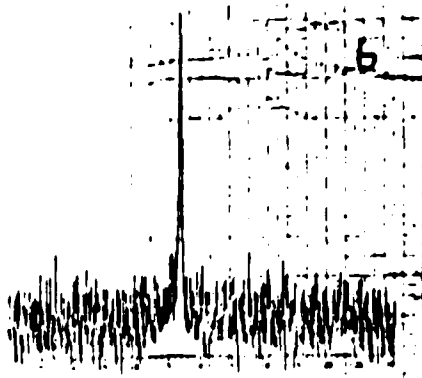
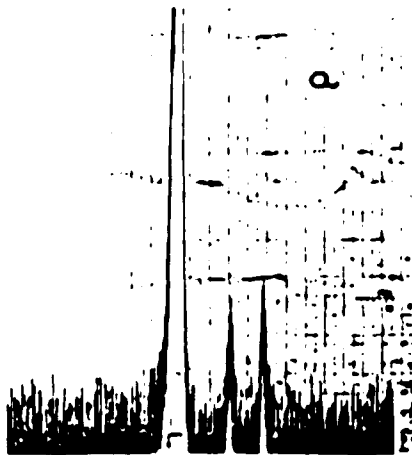
Figure V.30

³²P-NMR spectra of OPRTase

A) with PRPP and Mg²⁺

B) after extensive dialysis of sample in A

C) with the addition of Orotate to sample in B



DETERMINATION OF METAL-PROTON DISTANCES OF THE Mn^{2+} -PRPP
COMPLEX IN THE PRESENCE AND ABSENCE OF OPRTase

Relaxation Measurements

Experiments were performed as described in 'Methods,' on 7 samples:

- A) 100 mM PRPP
- B) 100 mM PRPP + 20 μ M Mn^{2+}
- C) 10 mM PRPP + 1 mM OPRTase
- D) 10 mM PRPP + 5 μ M Mn^{2+} + 2 mM OPRTase
- E) 10 mM PRPP + 10 μ M Mn^{2+} + 2 mM OPRTase
- F) 10 mM PRPP + 10 μ M Mn^{2+} + 1 mM OPRTase
- G) 10 mM PRPP + 10 μ M Mn^{2+} + 0.5 mM OPRTase

To illustrate how the raw data looks, two examples are provided. Fig. V.31 demonstrates the relaxation of the proton NMR spectra of PRPP- Mn^{2+} in the absence of enzyme. From bottom to top the spectra shown represent $T = 0.1, 0.2, 0.3, 0.4,$ and 0.5 sec, respectively. Fig. V.32 demonstrates what happens to the proton spectra of PRPP in the presence of enzyme. From bottom to top, these traces represent $T = 0.05, 0.1, 0.2,$ and 0.3 seconds. Note that when enzyme is present at concentrations near that of PRPP, there is a non-linear baseline which itself relaxes. The enzyme was too fragile to allow for performance of relaxation experiments in the absence of PRPP and the technology provided by the Varian 220 MHz instrument, did not allow for normalization of the baseline. The carbons on PRPP are numbered from C_1 attached to the pyrophosphate moiety through C_5 attached to the phosphate moiety. On both Fig. V.31 and Fig. V.32, arrows indicate positions of resonance

Figure V.31

Relaxation of the ^1H -NMR spectrum of PRPP in the presence of $20\mu\text{M Mn}^{2+}$.

From bottom to top: $\tau = 0.1, 0.2, 0.3, 0.4,$ and 0.5 sec.

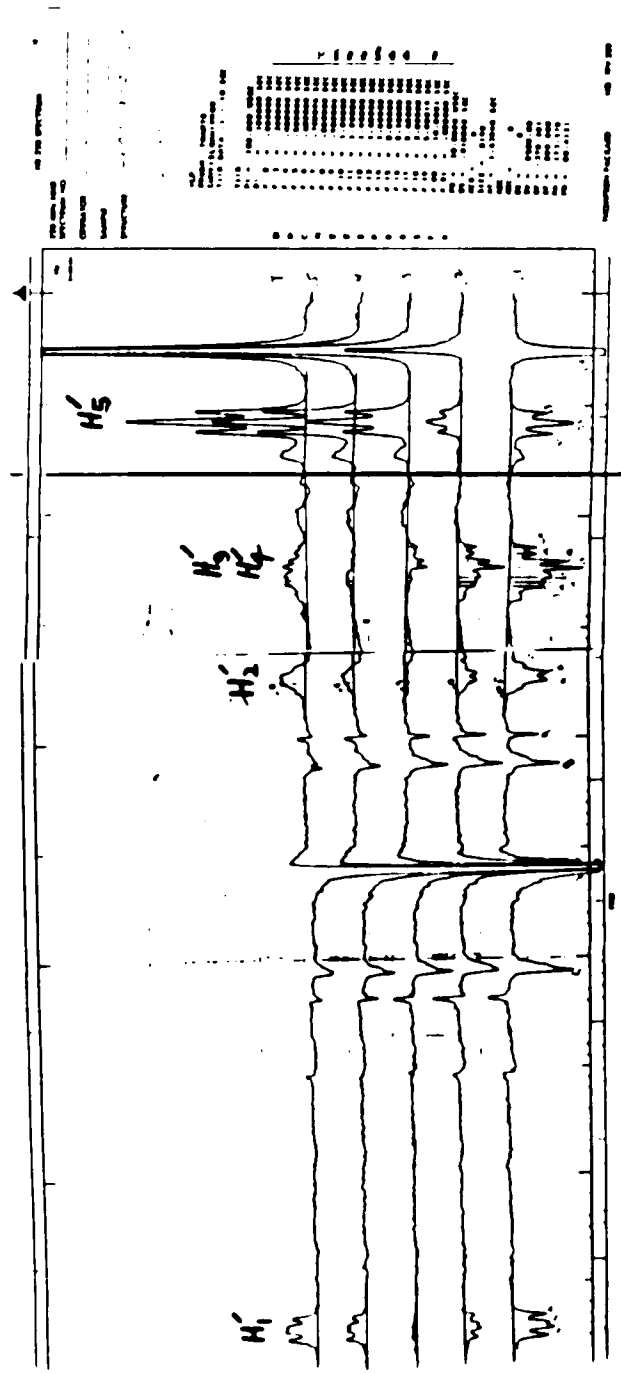
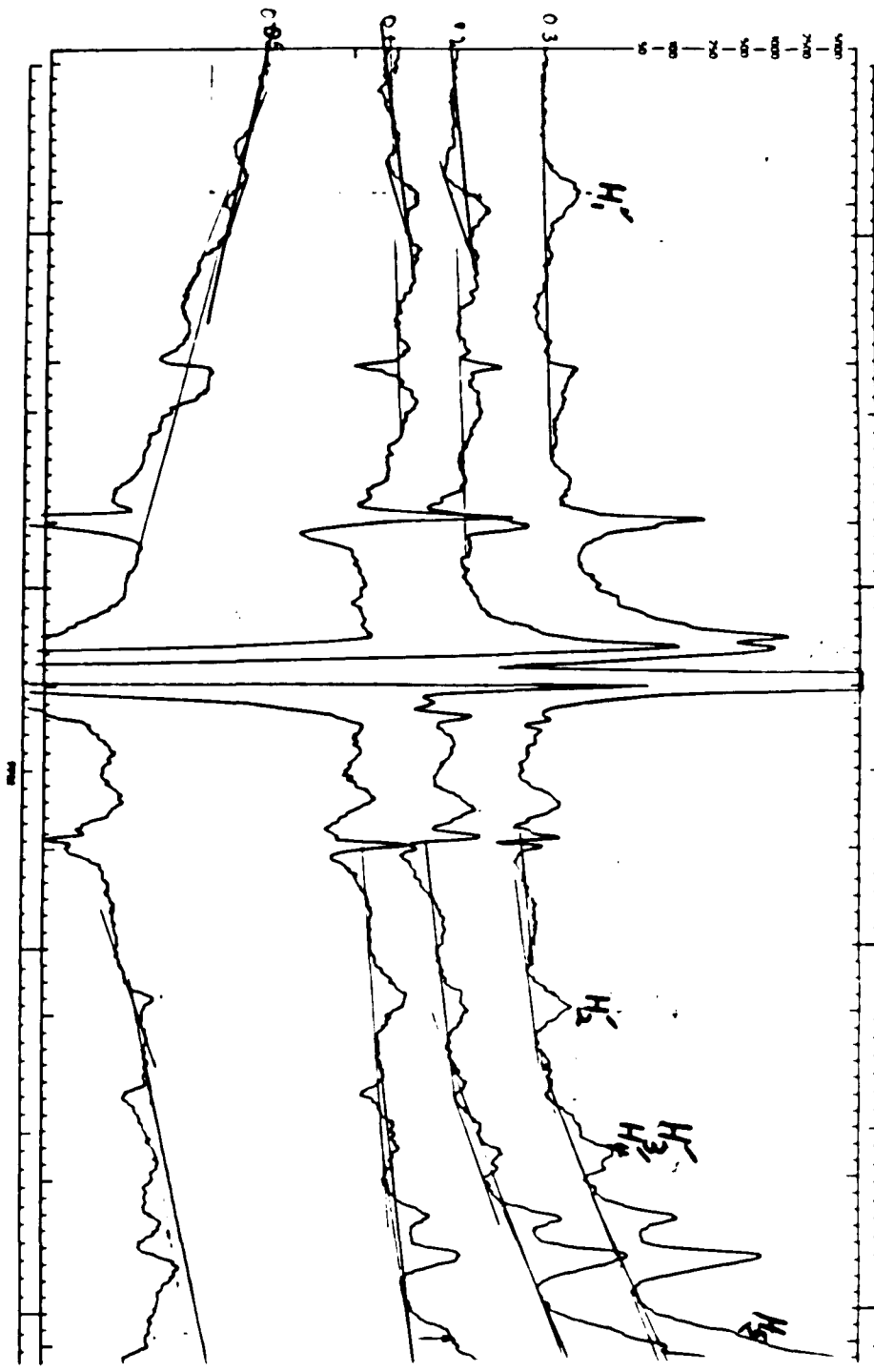


TABLE 1

Peak	Chemical Shift (ppm)	Integration
H_1	~1.0	~1.0
H_2	~2.5	~1.0
H_3	~3.5	~1.0
H_4	~4.5	~1.0
H_5	~7.5	~1.0

Figure V.32

Relaxation of the ^1H -NMR spectrum of PRPP in the presence of $20\mu\text{M Mn}^{2+}$ and 0.25 mM OPRTase .
From bottom to top: $0.05, 0.1, 0.2,$ and 0.3 sec .



of these protons. The spectra of protons on C₃ and C₄ overlap when enzyme is present.

Fig. V.33 is the spectrum of PRPP used for identification of the peaks. Note that the C₁ proton corresponds to a peak near 5.5 ppm, the C₂ proton corresponds to a peak near 4.1 ppm, the C₃ and C₄ protons correspond to peaks near 3.9 ppm and the C₅ proton corresponds to a peak near 3.6 ppm. For spectra taken in the presence of OPRTase, the C₃ and C₄ proton peaks overlap and therefore measurements taken near 3.9 ppm are taken as an average of the two.

In order to determine the distances, (*r*) between protons of the ribose moiety of PRPP and the Mn²⁺ complexed to it, several preliminary calculations must be done on the data to get it to the point where distance calculations can be done.

Generation of (T₁)⁻¹ values

For each condition and proton, the height of the peak at each *T* was determined. This value was then subtracted from the totally relaxed value (*T*_{max}) and the result plotted on semilog paper against *T*.

Table V.9 demonstrates the generation of points for such plots for a sample containing: 10 mM PRPP, 10 μM Mn²⁺, and 0.5 mM OPRTase. Similar calculations were performed on the raw data of each sample. Fig V.34 demonstrates the plotting of these lines. The slopes thus generated = (-T₁)⁻¹.

Generation of (T_{1P})⁻¹ values

(T₁)⁻¹ values of samples not containing Mn ion were then subtracted from the corresponding (T₁)⁻¹ to generate the paramagnetic contribution to (T₁)⁻¹ (or (T_{1P})⁻¹).

Figure V.33

¹H-NMR spectrum of Mg²⁺-PRPP.

Spectrum was taken on a 220 MHz instrument at 20°C
and pH 8.0.

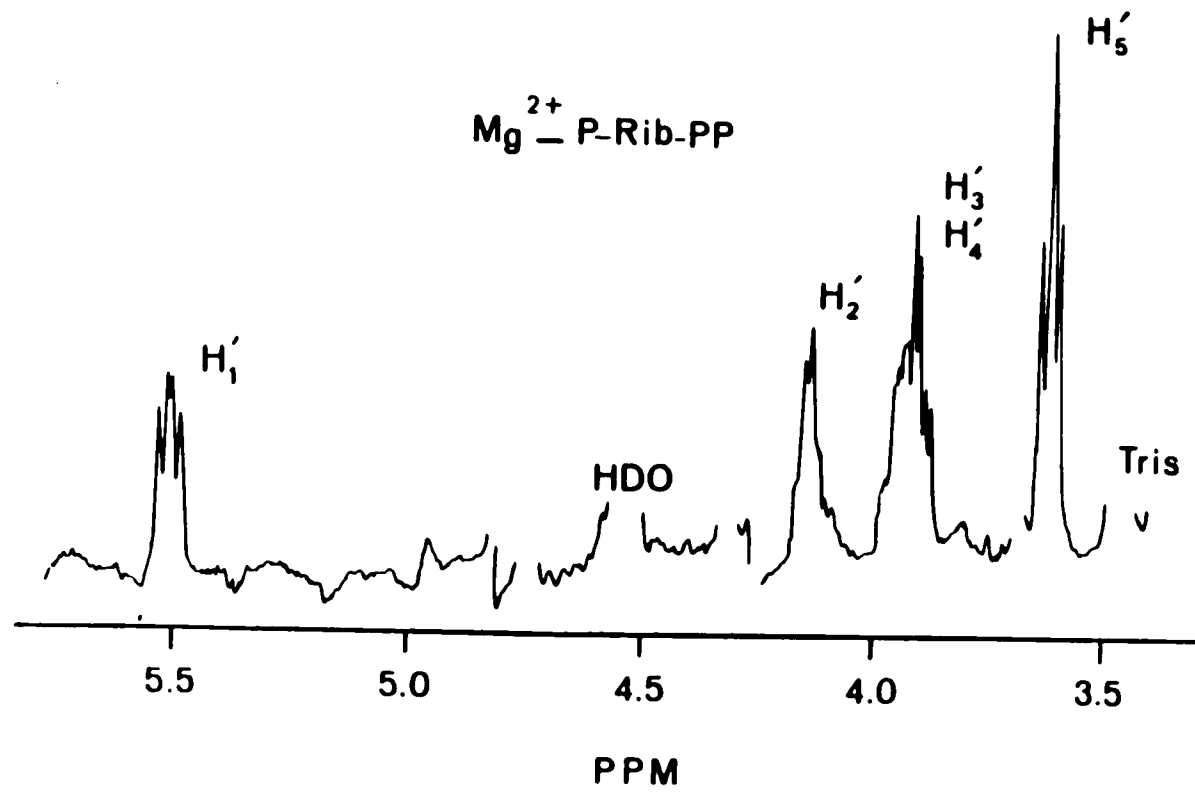
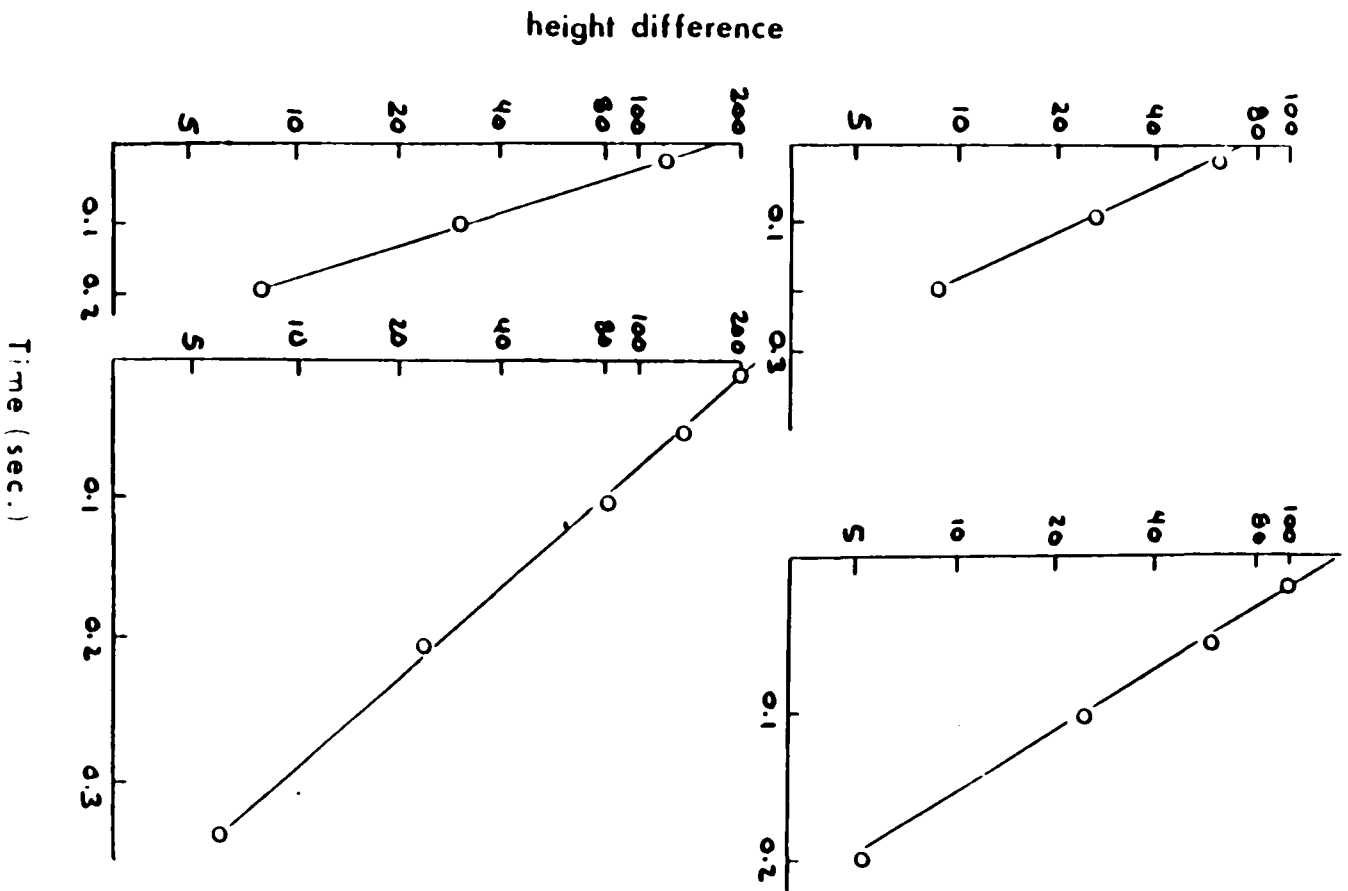


TABLE V.9

I Experimental	II Peak Conditions	III T (sec)	IV Peak Height	V Ht(T_{max}) - IV
10 mM PRPP	C ₁	1	44	0
10 μ M Mn ²⁺		0.2	43	1
		0.05	17	24
0.25 mM OPRTase		0.01	-13	57
	C ₂	1	68	0
		0.2	62	6
		0.1	44.5	23.5
		0.05	-13	55
		0.01	-30	98
	C _{3,4}	1	67	0
		0.2	59	8
		0.1	36.5	30.5
		0.01	-54	121
	C ₅	1	135	0
		0.3	134	1
		0.2	111	24
		0.1	53	82
		0.05	0	135
		0.01	-64	199

Figure V.34

Sample semilog plots for the generation of T_1^{-1} values.
Counterclockwise from upper left are the protons of C1,
C2, C5, and an average of C3 and C4.



Generation of $(T_{1p})^{-1}$ values for each proton species at infinite enzyme

The $(T_{1p})^{-1}$ values were then multiplied by $1/f$ (with f = ratio of $[Mn^{2+}]$ to $[PRPP]$) to give the $(fT_{1p})^{-1}$ values listed in Table V.10. For each proton species, $(fT_{1p})^{-1}$ values of samples E, F, and G were plotted versus $[E]^{-1}$ and the line thus generated extrapolated to infinite enzyme concentration to give the $(fT_{1p})^{-1}$ at infinite enzyme concentration.

Generation of $(T_2)^{-1}$ values

$(T_2)^{-1}$ values for each sample were determined directly by measuring the width at half-height of the totally relaxed spectrum of C_1 and C_2 protons for samples C, E, F, and G.

Generation of $(T_{2p})^{-1}$ values

The paramagnetic contributions to the transverse relaxation time $(T_{2p})^{-1}$ for the C_1 and C_2 protons were generated by subtracting the $(T_2)^{-1}$ values of sample C from the corresponding $(T_2)^{-1}$ of samples E-G.

Extrapolation of (T_{1p}/T_{2p}) to infinite enzyme

$(T_{2p})^{-1}$ values generated above for C_1 and C_2 protons at three $[OPRTase]_s$ were divided by corresponding $(T_{1p})^{-1}$ values to give T_{1p}/T_{2p} for each proton species and enzyme concentration. These values were then plotted against $[OPRTase]^{-1}$ and extrapolated to infinite enzyme. For both C_1 and C_2 protons, a value for T_{1p}/T_{2p} of 7.2 was determined as depicted in Fig. V.35.

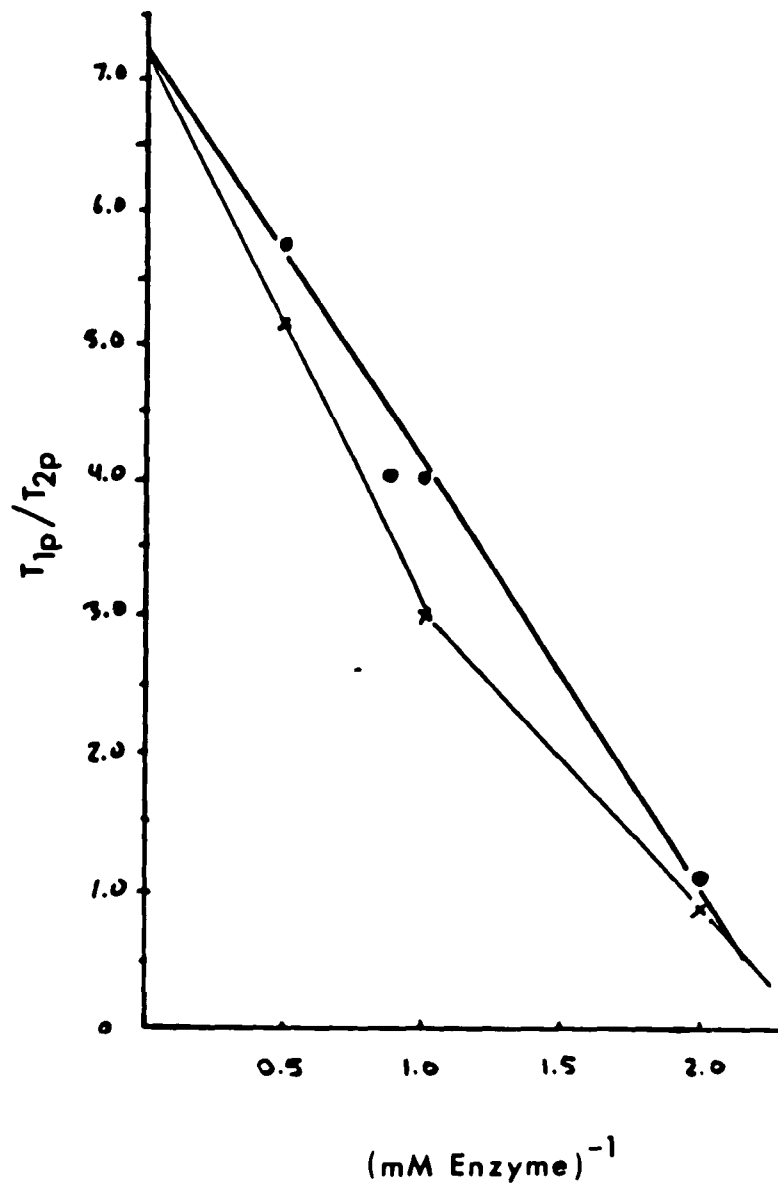
Calculation of T_C for samples containing enzyme

The value of T_C for the samples containing OPRTase was then determined by inserting into the following equation, the value for T_{1p}/T_{2p} extrapolated to infinite enzyme, as determined above:

TABLE V.10
(fT_{1p})⁻¹ values for protons of PRPP in the presence of
OPRTase and Mn²⁺

Experimental Conditions	C-1	C-2	Protons C-3	C-4	C-5
Sample B 100 mM PRPP 10 μ M Mn ²⁺	10800	6400	3200	2400	2600
Sample E 10 mM PRPP 10 μ M Mn ²⁺ 0.25 mM OPRTase	15200	11000	9400	9400	5600
Sample F 10 mM PRPP 10 μ M Mn ²⁺ 0.5 mM OPRTase	5000	3400	4000	4000	3600
Sample G 10 mM PRPP 10 μ M Mn ²⁺ 1 mM OPRTase	3600	2800	1200	1200	1000
Extrapolated to infinite OPRTase	2500	2100	800	800	420
fT_{1p}	0.400×10^{-3}	0.476×10^{-3}	1.25×10^{-3}	1.25×10^{-3}	2.38×10^{-3}

Figure V.35
Extrapolation of T_{1P}/T_{2P} to infinite enzyme.



$$w_i T_C = [3/2(T_{1P}/T_{2P} - 7/6)]^{1/2} \quad (\text{Eq. V.9})$$

with:

$$w_i = 2\pi (220 \times 10^6) = 1.382 \times 10^9$$

for a 220 MHz NMR instrument. The value of T_C thus determined equals 2.176×10^{-9} .

Calculation of $f(T_C)$ for samples containing enzyme

The value of $f(T_C)$ was then determined by substituting T_C into the equation below:

$$f(T_C) = 3T_C / (1 + w_i^2 T_C^2) + 7T_C / (1 + w_s^2 T_C^2) \quad (\text{Eq. V. 10})$$

with:

w_i as above

$$w_s = 2\pi (220 \times 10^6) \times 657 = 0.9082 \times 10^{12}$$

for a 220 MHz instrument and protons as the resonating nuclei. The value of $f(T_C)$ thus determined equals 0.65×10^{-9} sec or 0.65 ns.

Calculation of distances between Mn and H's of PRPP on and off OPRTase

The distances (r) between protons of PRPP and Mn when the complex is either on or off the enzyme were then calculated utilizing the following equation:

$$r = c [q (T_{1P})^x f(T_C)]^{1/6} \quad (\text{Eq. V.11})$$

with:

$q=1$ (coordination number)

$c= 812$ for Mn^{+2}

T_{1P} as determined above for each proton species (see Table V.10)

$f(T_C) = 0.3$ ns for samples without enzyme and 0.65 ns for samples with enzyme

The values for ' r ', thus determined, are in Å and listed in Table V.11.

Model Construction and Graphical representation

Looking at the distances determined above, we can see that on the enzyme, the metal is, in general, further from the protons of PRPP than it is when

TABLE V.11

**Distances (in Å) from Mn²⁺ to protons of PRPP
in the presence and absence of OPRTase**

Experimental Conditions	Protons				
	C-1	C-2	C-3	C-4	C-5
10 mM PRPP ^a 10 μM Mn ²⁺	4.5±0.5	4.9±0.3	5.1±0.3	5.7±0.5	6.0±0.5
10 mM PRPP ^{b,c} 10 μM Mn ²⁺ extrapolated to infinite OPRTase	6.5±0.7	6.7±0.7	7.8±0.8	7.8±0.8	8.7±0.9

a) An $f(T_C)$ value of 0.3 ns for Mn²⁺-complexes in solution (use reference) was employed for these calculations.

b) An $f(T_C)$ value of 0.65 ns was used for these calculations as determined in text.

c) Because of overlap of resonances of protons on C-3 and C-4, only an average distance was calculated.

it is off the enzyme. Also, on the enzyme, it is pulled an even greater distance away from those protons from which it was the furthest to start.

Models were built using the structural formula for PRPP and average bond lengths and angles. It was assumed that the Mn^{2+} is in the vicinity of the 1'-PP_i moiety, but not attached to the 5'-phosphate. Sticks were attached to the H's proportional to their distances to Mn^{2+} and bonds rotated so that they could reach the metal. Fig. V.36 is a graphical representation of the model of PRPP- Mn^{2+} in solution. Fig. V.37 is a graphical representation of the model of PRPP- Mn^{2+} on the OPRTase.

These experiments were performed several years ago when the NMR technology available for use was not as refined as it is today. It has recently been demonstrated, using ³¹P-NMR, that the 5'-phosphate is also near to the Mn^{2+} ion, particularly in absence of enzyme. Models conforming to this new development can be found in Syed (1986).

Figure V.36

Graphical representation of the PRPP-Mn²⁺ complex in solution.

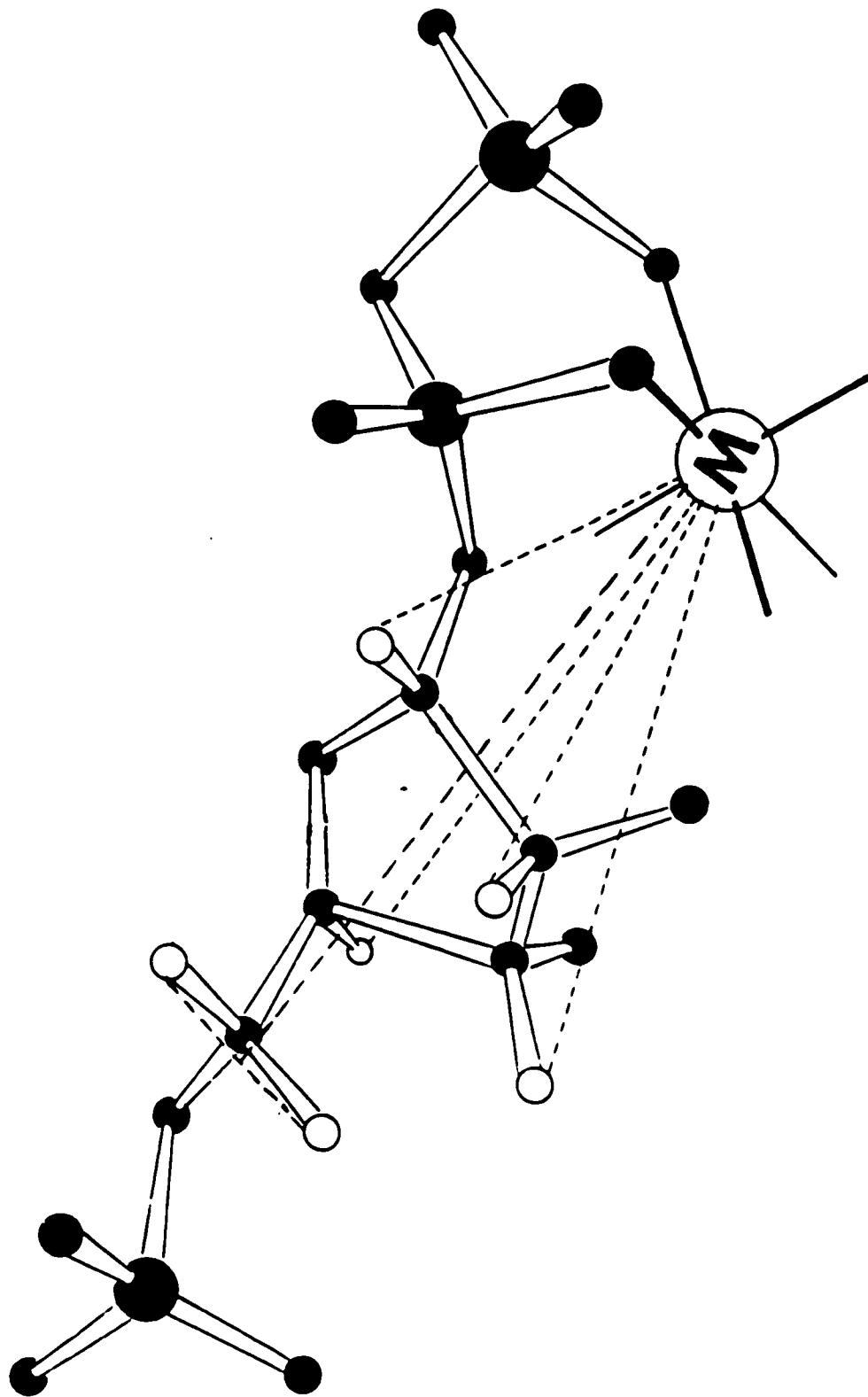
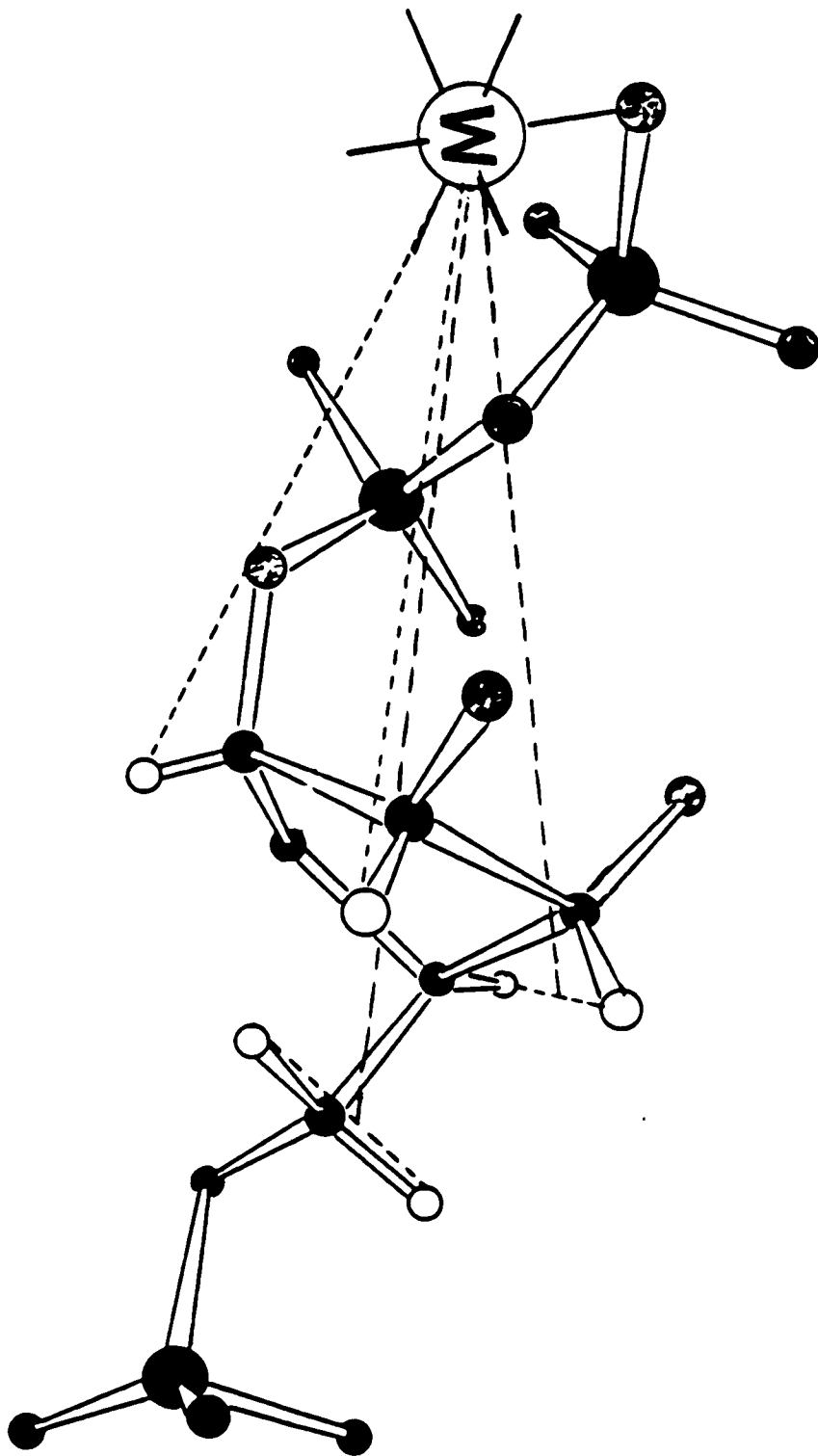


Figure V.37

Graphical representation of the PRPP-Mn²⁺ complex on OPRTase.



Section VI: DISCUSSION

As mentioned in "Rationale," one of the purposes of this thesis research was to explore the amino acid composition and $^1\text{H-NMR}$ spectra of OPRTase. As of this writing, OPRTase is the only PRTase from Baker's yeast that has been studied in this manner in this or any other laboratory. Once other enzymes of this class have been explored, these results can be compared with the findings of this researcher. The amino acid analyses of other PRTases from several other sources, have been completed (Musick, 1981) and their compositions are summarized in Table VI.1 along with that of OPRTase from Baker's yeast. In the first column are the average percent compositions of each amino acid in five PRTases studied, in the second column are the percent compositions of amino acids in proteins in general, and in the third column are the percentages of amino acids in OPRTase as found by this researcher. Compared to other PRTases, most percentages of amino acids of OPRTase are within one standard deviation unit. Exceptions are higher percentages for histidine, serine, and glycine and lower percentages for proline and valine. The serine percentage of OPRTase does agree with that found for proteins in general, however. From the amino acid composition of OPRTase, we were able to generate a theoretical $^1\text{H-NMR}$ spectrum for a random coil protein and when this was compared with the actual $^1\text{H-NMR}$ spectrum of (2 mM) OPRTase, a similar number of major peaks were seen. (Details of this comparison are found in "Results.") The $^1\text{H-NMR}$ spectra of OPRTase taken at various pH values between 8.0 and 5.0 were compared and no significant changes could be observed. In addition, some backbone amide protons which were visible at pH 7.0 were found to have been retained even after several hours at pH 5.0. It was concluded, therefore, that the enzyme is not

undergoing any gross conformational changes in that pH range, as would be evidenced by the appearance of a more random conformation.

In the range of 7.0 to 7.1 ppm (where histidine-imidazole-C4 protons resonate), it was seen that the number of individual peaks are close to that of the number of histidines in OPRTase. Since OPRTase is not a protein that can be purified in large quantities, it is important to know that such an amount of protein can yield spectra in which individual peaks can be discerned. With the new high-field instruments now available, this can be explored even further. By studying the relaxation times of the protons of PRPP in the presence and absence of a high concentration of OPRTase and a very low concentration of Mn^{2+} , the distances between the metal and the carbon protons of PRPP were determined. It was assumed that the 5'-phosphate was not positioned near to the metal ion. Distances consistent with a more closed structure were found for $Mn(II)$ -PRPP off the enzyme whereas a more open conformation was revealed once the $Mn(II)$ -PRPP was in the presence of OPRTase. Since these studies were necessarily carried out with a small concentration of Mn^{2+} relative to the a 10-fold excess utilized in all of the kinetic studies, the conformation may not represent the optimum active complex where more than just a single metal ion site might be occupied.

Chemical modification with two histidine-specific reagents showed irreversible inhibition of the enzyme. These studies were not totally definitive since DEPC can react with the side-chains of lysine and tyrosine residues and pBPB can react with other nucleophilic groups such as the side-chain of methionine. Moreover, the definitive experiment, that of reactivating OPRTase after DEPC incubation with NH_2OH , could not be done since NH_2OH itself inhibits the enzyme. However, in a survey of ten enzymes modified by DEPC, for which

information is known regarding the actual residues modified (Miles, 1977), it was shown that when the incubation buffer used was phosphate (as in our case), only histidines were modified.

The pH profiles of the forward and reverse reactions are consistent with the presence of at least five residues at the active site, that are essential for the combined forward and reverse activities of OPRTase and which undergo protonation or deprotonation between pH 4.5 and pH 9.5. Interestingly, not all are equally essential in each reaction direction.

In Figure VI.1, I speculate on the steps that might be occurring during the reactions catalyzed by OPRTase in the presence of excess Mg^{2+} . In this figure, 'a' represents the active site of the enzymes containing one histidine, two carboxyls and three lysines. Though the actual number of lysines present at the active site is unknown, the presence of at least one such residue has been indicated by the work of Ashton and Sloan(1986). According to the pH profile, one lysine would have a pK value near to 8 and the others over 9. Below pH 8 these lysine residues would mostly be protonated. Though there is no chemical evidence for the presence of a carboxyl group at the OPRTase active site, the pH-Vmax profile indicates the possibility of two such moieties (one with a pK of 4.6 and the other with a pK of 5.2). Evidence for the presence of a histidine at the active site has been shown by a pK of 7.1 for the forward reaction, the inhibition of OPRTase by DEPC and pBPB and the decrease in inhibition in the presence of substrates. Although $Mg(II)$ -PRPP is the best substrate protector, even Mg^{2+} alone protects. In addition, when OPRTase is inactivated by NH_2OH , the only amino acid residue which is significantly affected in the amino acid analysis is histidine.

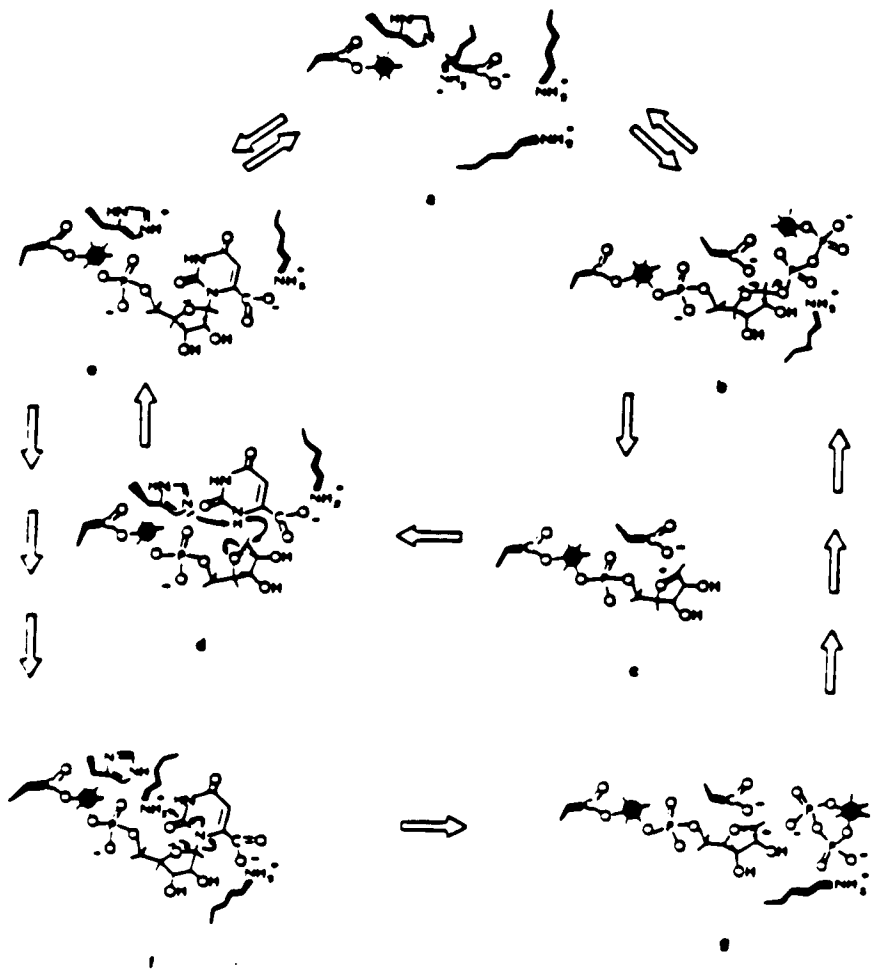
I propose that one carboxyl group acts as a binding site for Mg^{2+} to which the 5'-phosphate moiety of PRPP binds, thereby forming a metal bridge with the

TABLE VI.1
Amino Acid Distributions (%) of PRTases, Proteins, and OPRTase

	PRTase average ±SD	Average protein composition	OPRTase
Glu,Gln	9.8±2.2	9.5	11.4
Asp,Asn	9.4±3.2	9.7	8.2
Lys	4.8±1.7	6.6	6.2
His	1.8±0.5	2.1	3.1
Arg	5.9±1.4	4.5	3.6
Thr	4.5±0.9	5.8	4.1
Ser	5.3±0.9	7.2	7.3
Pro	5.4±1.0	5.6	3.6
Gly	8.7±1.3	8.8	13
Ala	9.6±3.4	8.7	8.3
Cys	2.0±1.0	3.1	1.0
Val	7.7±1.4	6.6	4.7
Met	2.2±1.6	1.7	1.0
Ileu	5.0±2.5	4.6	7.7
Leu	11.8±3.5	7.7	8.3
Tyr	2.7±1.1	3.5	3.6
Phe	3.5±1.3	3.5	4.1
Trp	0.7±.6	1.2	1.0

Figure VI.1

Proposed mechanism of action of OPRTase in the presence of an excess of Mg^{2+} .



enzyme. Alternately, PRPP may bind as $Mg(II)PRPPMg(II)$ with the 5'-P-magnesium portion corner binding to the COO^-Mg^{2+} . In either instance, the result would be that the PRPP would be attached to a carboxyl on the enzyme through a $Mg(II)$ ion. A flexible lysine could then position itself near to the 1'-pyrophosphate side of the PRPP, because of its attraction to the one negative charge of PP_i ; not neutralized by Mg^{2+} . This geometry would place the bond-to-be broken near a second carboxyl group of an aspartate or glutamate, as shown in Figure VI.1b. The bond breaks, possibly driven by the need to relieve the strain of having a phosphate negative charge near to a carboxyl negative charge and by the ability of the newly generated positive and negative charges to be neutralized through tight ion-pair bonds with the carboxyl and lysyl groups respectively (Figure VI.1b). Negatively charged $MgPP_i$ then leaves the enzyme and the site opens up. The charged ribose ring thus formed, is stabilized by the second COO^- on the enzyme. Orotate can now enter. The carboxyl of orotate is stabilized by a protonated lysine on the enzyme and an unprotonated histidine removes a proton from the orotate ring nitrogen, thus leaving the nitrogen in the carbonyl tautomer with electrons free to react with the positively charged ribose ring (Fig. VI.1d) The reaction occurs and OMP (Fig. VI.1e) can then be released, leaving the enzyme with the metal ion still attached at the active site (Fig. VI.1a).

The proposed mechanism of the reverse reaction would also begin with (Fig. VI.a) the active site with a metal ion attached to the carboxyl. Thereafter, OMP would then coordinate to the metal ion on one side, whereas its ring carboxyl substituent would attach to one of the protonated lysine residues. This geometry places the bond-to-be broken in close proximity to the COO^- on the enzyme (not shown). We speculate that the driving force for the breaking of the glycosidic bond of OMP is the protonation of the orotate ring either at the 2-carbonyl group

(to form a hydroxyl group and a new tautomeric form as shown in Figure VI.1f) or at the 1-N position itself (no change in tautomeric form). Orotate dissociates and Mg^{2+} -PP_i is then allowed to bind and positioned so that is in located close to the positively charged ring (Fig. VI.g) to which it reacts to form PRPP.

Some indication for the separate needs of the forward and reverse reactions, can be seen by examining the differences in pH-V_{max} profile (Figure V.9). The reverse reaction is more sensitive to increases in pH. It is possible that the lysine residues have different pK's, and that as one becomes deprotonated, it hampers the reverse reaction which needs it for catalysis. The forward reaction, which utilizes only the other lysines is unaffected by the lysine deprotonation event above pH 8.0. The forward reaction, however, needs an unprotonated histidine residue and therefore its activity is reduced at lower solution pH values.

The scheme of action of OPRTase outlined above contains many facets that are unproven and therefore speculative. It does, however, provide a working model for the development of new avenues of experimentation which may eventually lead to a clearer understanding of the OPRTase mechanism of action.

Section VII: APPENDICES

- Appendix 1: Listing of HYPER**
- Appendix 2: Listing of PHBELL**
- Appendix 3: Listing of HABELL**
- Appendix 4: Listing of MANIP DATA**
- Appendix 5: Listing of NMRSPEC**
- Appendix 6: Data Entry and Interactive Manipulations**
- Appendix 7: Sample Printouts**
- Appendix 8: Printout of NMRSPEC**
- Appendix 9: ¹H-NMR Spectra of OPRTase**

APPENDIX 1: LISTING OF HYPER PROGRAM

```

1  REM HYPER
2  REM PROGRAM TO FIT DATA TO A
   HYPERBOLIC CURVE
3  HOME : PRINT "FIT TO HYPERBOLA
   V=VMSA/(K+A)"
10  DIM V(100),A(100),S(3,4),O(3)
   ,SM(3),SS(3)
20  DIM WE(10),SE(10)
25  PRINT : INPUT "DO YOU WISH TO
   MULTIPLY THE V'S AND/OR A
   'S BY A CONSTANT" :YNS
30  IF YNS = "NO" THEN V(I) = 1/A
   (I) = 1: GOTO 400
35  PRINT : INPUT "ENTER A CONSTA
   NT MULTIPLIER OF V" :V(I)
40  PRINT : INPUT "ENTER A CONSTA
   NT MULTIPLIER OF A" :A(I)
45  PRINT : PRINT "ALL V'S ENTERE
   D WILL BE MULTIPLIED BY",V(I)
50  PRINT : PRINT "ALL A'S ENTERE
   D WILL BE MULTIPLIED BY",A(I)
55  PRINT : INPUT "BEFORE CONTINU
   ING, DO YOU AGREE WITH TH
   ESE VALUES" :YNS
57  IF YNS = "NO" THEN 35
600  REM FOLLOWING IS THE DATA Y
   OU HAVE STORED
1000  HOME : PRINT "FIT TO HYPERB
   OLA V=VMSA/(K+A)"
1003  REM
1004  REM
1010  FOR I = 1 TO 3
1020  PRINT
1030  NEXT I
1040  JJ = 0
1045  REM READ NP,NO
1047  PRINT CHR$(18)
1048  PRINT CHR$(9) + "I"
1050  READ NP,NO
1055  REM
1056  REM
1057  REM
1060  IF NP = 0 THEN 5430
1060  N = 1
1060  II = 0
1065  N = 2
1066  N1 = N + 1
1067  N2 = N + 2
1070  GOTO 5000
2000  REM READ V(I),A(I)
2010  REM
2014  READ V(I),A(I)
2016  V(I) = V(I) * V(I)
2018  A(I) = A(I) * A(I)
2019  IF NO / = 0 THEN 2040
2020  V(I) = 1. / V(I)
2020  J(1) = V(I) ^ 2 / A(I)
2020  J(2) = V(I) ^ 2
2020  J(3) = V(I)
2027  GOTO 5110
2500  CK = S(1,1) / S(2,1)
2510  JJ = JJ + 1
2515  PRINT "LINE NUMBER=",JJ
2520  PRINT "NUMBER OF POINTS=",N
   P
2527  PRINT "CK=",CK
2530  NT = 0
2535  N = 2
2530  GOTO 5000
2540  O = CK * A(I)
2545  O(1) = A(I) / D
3020  O(2) = A(I) / D ^ 2
3030  O(3) = V(I)
3040  GOTO 5110
3500  CK = CK - S(2,1) / S(1,1)
3510  PRINT "CK=",CK
3520  NT = NT + 1
3530  IF NT < 3 THEN 5000
3550  S2 = 0
3570  PRINT
3580  FOR I = 1 TO NP
3590  X2 = 1. / A(I)
3600  X3 = 1. / V(I)
3610  X1 = S(1,1) / (1. + CK / A(I)
   )
3620  DX1 = V(I) - X1
3626  PRINT CHR$(9) + "CONC"
3627  PRINT CHR$(15) : IF I > 1 THEN
   3629
3628  PRINT "CONC"; SPC(16); "1/C
   ONC"; SPC(14); "VELOCITY"; SPC(
   12); "1/VELOCITY"; SPC(10); "
   CALC V"; SPC(14); "DIFF"
3629  XK(1) = A(I);XK(2) = X2;XK(3
   ) = V(I);XK(4) = X3;XK(5) =
   X1;XK(6) = DX1
3630  FOR JK = 0 TO 5:IX = XK(JK +
   1)
3632  SB = 20 - LEN ( STR$(IX))
3633  PRINT IX; SPC( SB);
3634  NEXT JK
3640  S2 = S2 + (V(I) - S(1,1) * A
   (I) / (CK + A(I))) ^ 2
3650  NEXT I
3660  P = NP - 2
3670  LP = P
3680  S2 = S2 / P
3690  S1 = SQR (S2)
3700  SL = CK / S(1,1)
3710  VK = 1. / SL
3720  VN = 1. / S(1,1)
3730  FOR J = 2 TO 3
3740  FOR K = 1 TO 2
3750  S(K,J) = S(K,J) * SM(K) * SM
   (J - 1)
3760  NEXT K
3770  NEXT J
3780  SE(2) = S1 * SQR (S(1,2))
3790  SE(1) = S1 * SQR (S(2,2)) /
   S(1,1)
3800  SE(3) = SE(2) / S(1,1) ^ 2
3810  S(1,2) = S1 * SQR (CK ^ 2 *
   S(1,2) + S(2,3) * 2. * CK *
   S(1,3))
3820  SE(4) = S(1,3) / S(1,1) ^ 2
3825  SE(6) = S(1,3) / CK ^ 2
3830  WE(1) = 1. / SE(1) ^ 2
3840  WE(2) = 1. / SE(2) ^ 2
3850  WE(4) = 1. / SE(4) ^ 2
3850  WE(5) = 1. / SE(5) ^ 2
3870  WE(6) = 1. / SE(6) ^ 2
3880  GF = SL * (1. / ANP) * VN
3890  PRINT : PRINT
3891  PRINT "K=",CK; PRINT "S.E.(
   K)=",SE(1); PRINT "W=",WE(1)
3900  PRINT : PRINT
3911  PRINT "V=",S(1,1); PRINT "S
   E. V)=",SE(2); PRINT "W=",W
   E(2)
3909  PRINT : PRINT
3910  SE(2) = SE(2) / S(1,1)
3920  WE(2) = 1. / SE(2) ^ 2
3930  PRINT "C.V. V)=",SE(2)

```

```

3972 PRINT "WL=1/CV=",WE(2)
3974 PRINT
3976 PRINT : PRINT
3980 PRINT "K/V=",SL: PRINT "S.E
(V/V)=",SE(4): PRINT "W=",W
E(4)
3984 PRINT : PRINT
3986 PRINT "1/V=",VN: PRINT "S.E
(1/V)=",SE(5): PRINT "W=",WE
(5)
3988 PRINT : PRINT
3990 PRINT "V/K=",VK: PRINT "S.E
(V/K)=",SE(6): PRINT "W=",W
E(6)
3992 PRINT : PRINT
3994 SE(7) = SE(6) / VK
3996 WE(7) = 1. / SE(7) ^ 2
3998 PRINT "C.V. (V/K)=",SE(7): PRINT
"WL=1/CV=",WE(7)
3999 PRINT : PRINT
4000 PRINT "1/V AT A=",A(NP)
4002 PRINT " IS ",OF
4004 PRINT : PRINT
4006 PRINT "SIGMA=",S1
4008 PRINT
4010 PRINT "VARIANCE=",S2
4012 PRINT "FOR",LP,"DEGREES OF
FREEDOM"
4014 PRINT
4016 PRINT
4018 IF II / 0 THEN 1047
4020 S1 = 2.6 * S1
4022 FOR I = 1 TO NP
4024 TEST = ABS (V(I) - S(1,1) *
A(I) / (CK + A(I)))
4026 TEST = TEST - S1
4028 IF TEST < 0 THEN 4100
4030 PRINT "POINT DEVIATES MORE
THAN 2.6*SI",V(I),A(I)
4032 GOTO 4120
4034 II = II + 1
4036 V(II) = V(I)
4038 A(II) = A(I)
4040 NEXT I
4042 TEST = NP - II
4044 IF TEST <= 0 THEN GOTO 1
047
4046 NP = II
4048 NT = 0
4050 PRINT "REVISED FIT"
4052 PRINT
4054 PRINT
4056 REM MATRIX SOLUTION SUBROU
TINE
4058 FOR J = 1 TO N2
4060 FOR K = 1 TO N1
4062 S(K,J) = 0
4064 NEXT K
4066 NEXT J
4068 FOR I = 1 TO NP
4070 IF M = 1 GOTO 2000
4072 IF M = 2 GOTO 2000
4074 FOR J = 1 TO N1
4076 FOR P = 1 TO N
4078 S(K,J) = S(K,J) + Q(K) * Q(J)
4080 )
4082 NEXT K
4084 NEXT J
4086 NEXT I
4088 FOR P = 1 TO N
4090 SM(P) = 1. / SQR (S(P,P))
4092 NEXT K
4094 SM(N1) = 1.
4096 FOR J = 1 TO N1
4098 FOR K = 1 TO N
4100 S(K,J) = S(K,J) * SM(K) * SM
(J)
4102 NEXT K
4104 NEXT J
4106 FOR L = 1 TO N
4108 FOR K = 1 TO N
4110 SS(K) = S(K,1) * SM(K)
4112 NEXT K
4114 NEXT L
4116 IF M = 1 GOTO 2500
4118 IF M = 2 GOTO 2500
4120 PRINT : PRINT : PRINT "PROG
RAM COMPLETED TO "JJJ" L
INES."
4122 END

```

APPENDIX 2: LISTING OF PHBELL PROGRAM

```

1  REM PHBELL
5  REM PROGRAM TO FIT DATA TO A
   BELL SHAPED CURVE
10  DIM Y(100),A(100),W(100),S(4,
   S),Q(4),SM(4),SS(4)
20  DIM IK(7),CK(2),SC(2),DX(2),S
   E(4),PK(2)
600  REM FOLLOWING IS THE DATA Y
   OU HAVE STORED
999  DATA 0,0
1000 HOME : PRINT "FIT TO LOG V=
   LOG(C/(1+M/KA + KB/M))": PRINT
   : PRINT : PRINT
1040 JJ = 0
1047 PRINT CHR$(18)
1048 PRINT CHR$(9) + "I"
1050 REM
1055 READ NP
1056 IF NP <= 0 THEN 5430
1057 READ NO
1058 M = INT = 0:IN = 3:NI = 4:IN2
   = 5
1100 FOR J = 1 TO NI: FOR K = 1 TO
   NI
1110 S(K,J) = 0
1120 NEXT K: NEXT J
1130 FOR I = 1 TO NP
1140 IF M = 2 THEN 1200: IF M =
   3 THEN 1200
1150 REM
1152 READ Y(I),A(I),W(I)
1154 REM
1154 REM
1160 Q(1) = 1. / EXP (2.3026 * A
   (I))
1170 Q(2) = Y(I)
1180 Q(3) = A(I) * Q(1)
1190 Q(4) = Q(1) / A(I)
1200 Q(4) = 1.
1210 GOTO 1600
1200 D = 1. + A(I) / CK(1) - CK(2
   ) / A(I)
1210 Q(1) = 1.
1220 Q(2) = A(I) / D
1230 Q(3) = (1. / A(I)) / D
1240 Q(4) = LOG (Y(I) * D)
1250 GOTO 1600
1300 D = 1. + A(I) / CK(1) + CK(
   1) / 4. / A(I)
1310 Q(1) = 1.
1320 Q(2) = (1.25 / A(I) - A(I) /
   CK(1) + 2) / D
1330 Q(3) = LOG (Y(I) * D)
1400 FOR J = 1 TO NI: FOR K = 1 TO
   NI
1410 S(K,J) = S(K,J) + Q(K) * Q(J
   ) * W(I)
1420 NEXT K: NEXT J
1430 NEXT I
1450 FOR K = 1 TO NI
1460 SM(K) = 1. / SCR (S(K,K))
1470 NEXT K
1480 SM(NI) = 1.
1700 FOR J = 1 TO NI: FOR K = 1 TO
   NI
1710 S(K,J) = S(K,J) * SM(K) * SM
   (J)
1720 NEXT K: NEXT J
1730 SS(NI) = - 1.
1740 S(1,NI) = 1.
1800 FOR L = 1 TO NI
1810 FOR K = 1 TO NI
1820 SS(K) = S(K,1)
1830 NEXT K
1840 FOR J = 1 TO NI
1850 FOR K = 1 TO NI
1859 KI = K + 1:JI = J + 1
1860 S(K,J) = S(KI,JI) - SS(KI) *
   S(1,JI) / SS(1)
1870 NEXT KI: NEXT JI: NEXT L
1900 FOR K = 1 TO NI
1910 S(K,1) = S(K,1) * SM(K)
1920 NEXT K
1925 IF M = 2 THEN 2100: IF M =
   3 THEN 2200
1930 CK(2) = S(3,1) / S(1,1)
1940 CK(1) = S(1,1) / S(2,1)
1950 JJ = JJ + 1
1960 PRINT "LINE NUMBER= "JJ
1970 PRINT "NUMBER OF POINTS= "
   NP
1980 PRINT : PRINT "CKA=";CK(1)
1990 PRINT : PRINT "CKB=";CK(2)
2000 SC(1) = CK(1)
2010 SC(2) = CK(2)
2020 M = 2
2030 GOTO 1100
2100 CK(1) = CK(1) + S(2,1) * CK
   (1)
2110 CK(2) = CK(2) - S(3,1)
2120 PRINT "CKA=";CK(1)
2130 PRINT "CKB=";CK(2)
2135 IF CK(1) > 0 THEN 2150
2140 CK(1) = SC(1)
2150 IF CK(1) > 0 THEN 2170
2160 CK(2) = SC(2)
2170 CV = EXP (S(1,1))
2180 NT = NT + 1
2190 IF INT = 5) THEN 1100
2195 IF (NT > 5) THEN 2300
2200 CK(1) = CK(1) - S(2,1)
2210 PRINT "CKA=";CK(1)
2220 NT = NT + 1
2230 IF (NT = 5) THEN 1100
2240 CV = EXP (S(1,1))
2250 CK(2) = CK(1) / 4.
2300 FOR J = 2 TO NI: FOR K = 1 TO
   NI
2310 S(K,J) = S(K,J) * SM(K) * SM
   (J - 1)
2320 NEXT K: NEXT J
2340 S2 = 0
2400 FOR I = 1 TO NP
2410 X = CV / (1. + A(I) / CK(1) +
   CK(2) / A(I))
2420 PH = - .43429 * LOG (A(I))
2430 X2 = LOG (Y(I)) / LOG (10)
2440 X3 = LOG (X) / LOG (10)
2450 DX(1) = X2 - X3
2460 DX(2) = Y(I) - X
2465 PRINT CHR$(9) + "I:DN"
2467 PRINT CHR$(15): IF I = 1 THEN
   3629
2469 PRINT "PH": SPC(16): EXPTL
   "V": SPC(11): "CALC V": SPC(
   12): "DIFF": SPC(14): EXPTL
   LOG V": SPC(7): "CALC LOG V"
   : SPC(3): "DIFF"
2469 X(1) = PH: X(2) = Y(I): X(3)
   = X: X(4) = DX(2): X(5) =
   X2: X(6) = X3: X(7) = DX(1)

```

```

3530 FOR J# = 0 TO 6:IX = X(J) -
    1
3531 SA = LEN ( STR# (IX))
3532 SB = 10 - SA
3533 PRINT IX; SPC( SB);
3534 NEXT J#
3540 S2 = S2 + W(1) * (DX(1) + 2)

3550 NEXT I
3560 P = NP - N
3580 S2 = S2 / P
3590 S1 = SOR (S2)
3700 SE(1) = S1 * SOR (S(1,2)) *
    CV
3710 CB = 1. / CV
3720 SE(2) = SE(1) / (CV + 2)
3730 PRINT ; PRINT ; PRINT "C=";
    CV; PRINT "S.E. (C)="; SE(1)
3740 PRINT ; PRINT ; PRINT "1/C="
    1./CV; PRINT "S.E. (1/C)="; SE(
    2)
3750 IF P = 3 THEN 3770
3800 IF CK(1) > 0 THEN 3840
3820 PRINT "KA NEGATIVE"
3830 GOTO 3870
3840 PK(1) = -.43429 * LOG (CK
    (1))
3850 SE(3) = S1 * .43429 * SOR (
    S(2,3)) * CK(1)
3860 PRINT ; PRINT ; PRINT "PKA="
    PK(1); PRINT "S.E. (PKA)=";
    SE(3)
3870 IF CK(2) > 0 THEN 3910
3880 PRINT ; PRINT ; PRINT "KB N
    EGATIVE"
3900 GOTO 3940
3910 PK(2) = -.43429 * LOG (CK
    (2))
3920 SE(4) = S1 * .43429 * SOR (
    S(3,4)) / CK(2)
3930 PRINT ; PRINT ; PRINT "PKB="
    PK(2); PRINT "S.E. (PKB)=";
    SE(4)
3940 PRINT ; PRINT ; PRINT "SIGN
    A="; S1
3950 PRINT ; PRINT ; PRINT "VARI
    ANCE="; S2
3960 IF M = 3 THEN 1047
3970 X = (CK(1) + 2) * 4. * CK(1)
    * CK(2)
3980 IF X <= 0 THEN 4500
3990 X = SOR (X)
4000 CK(2) = (CK(1) - X) / 2
4010 CK(1) = (CK(1) + X) / 2
4020 PK(1) = -.43429 * LOG (CK
    (1))
4025 IF CK(2) < 0 THEN PRINT "S
    HIPPING 4030"; GOTO 4045
4030 PK(2) = -.43429 * LOG (CK
    (2))
4040 PRINT ; PRINT ; PRINT "IF T
    WO GACUFS ARE INVOLVED, TRUE
    P'S ARE:"
4045 PRINT ; PRINT "PKA="; PK(1);
    GOTO 4070
4050 PRINT ; PRINT "PKB="; PK(1);
    PRINT "PKC="; PK(2)
4070 GOTO 1047
4500 PRINT ; PRINT ; PRINT "P'S
    TOO CLOSE. ASSU
    ME MIN SEPAR ATIO

```

```

N (0.6 PH UNITS) 401740
S IF 2 GACUFS INVOLV
ED, TRUE P'S ARE
NTICAL
4510 M = 3
4520 N = 2
4530 N1 = 3
4540 N2 = 4
4550 NT = 0
4560 GOTO 1100
5000 PK(1) = -.43429 * LOG (CK
    (1))
5010 PK(2) = PK(1) * .6625
5020 SE(2) = S1 * .43429 * SOR (
    S(2,3)) / CK(1)
5030 SE(4) = SE(2)
5040 PRINT ; PRINT ; PRINT "PKA="
    PK(1); PRINT "S.E. (PKA)=";
    SE(3)
5050 PRINT ; PRINT ; PRINT "PKB="
    PK(2); PRINT "S.E. (PKB)=";
    PK(4)
5060 GOTO 3940
5430 PRINT ; PRINT ; PRINT "PROG
    RAM COMPLETED FOR "0000"
    LINES
5500 END

```

APPENDIX 3: LISTING OF HABELL PROGRAM

```

1  REM HABELL
5  REM PROGRAM TO FIT DATA TO
   LEFT SIDE OF BELL-SHAPED
   CURVE
10  DIM Y(100),A(100),W(100),S(2,
    4),Q(3),SM(2),SS(3)
20  DIM IK(7),CK(2),SC(2),DX(2),S
    E(4),PM(2)
600  REM FOLLOWING IS THE DATA Y
    YOU HAVE STORED
999  DATA 0,0
1000 HOME : PRINT "FIT TO LOG V=
    LOG(C/(1+M/KA))": PRINT : PRINT
    : PRINT
1040 JJ = 0
1047 PRINT CHR$(18)
1049 PRINT CHR$(9) + "I"
1050 REM
1055 READ NP,NO
1056 IF NP <= 0 THEN 5430
1058 M = 1:NT = 0
1100 FOR J = 1 TO 4: FOR K = 1 TO
    2
1110 S(K,J) = 0
1120 NEXT K: NEXT J
1120 FOR I = 1 TO NP
1140 IF M = 2 THEN 1300
1150 REM
1152 READ Y(I),A(I),W(I)
1154 REM
1156 REM
1160 A(I) = 1. / EXP (.23026 * A
    (I))
1170 Q(1) = Y(I)
1180 Q(2) = A(I) * Q(1)
1190 Q(3) = 1.
1210 GOTO 1600
1200 D = 1. + A(I) / CK(1)
1210 Q(1) = 1.
1220 Q(2) = A(I) / D
1240 Q(3) = LOG (Y(I) * D)
1600 FOR J = 1 TO 3: FOR K = 1 TO
    2
1610 S(K,J) = S(K,J) + Q(K) * Q(J)
    * W(I)
1620 NEXT K: NEXT J
1670 NEXT I
1650 FOR P = 1 TO 2
1660 SM(P) = 1. / SQR (S(K,K))
1670 NEXT K
1680 SM(3) = 1.
1700 FOR J = 1 TO 3: FOR K = 1 TO
    2
1710 S(K,J) = S(K,J) * SM(K) * SM
    (J)
1720 NEXT K: NEXT J
1770 SE(3) = - 1.
1740 S(1,4) = 1.
1810 FOR L = 1 TO 2
1810 FOR P = 1 TO 2
1820 SE(P) = S(K,L)
1870 NEXT P
1840 FOR J = 1 TO 3
1850 FOR K = 1 TO 2
1859 PI = P + 1:JI = J + 1
1859 S(K,JI) = S + 1.0:JI) - SS(K) *
    S(K,JI) / SS(1)
1870 NEXT K: NEXT J
1870 FOR P = 1 TO 2
1870 SE(P) = S(K,1) * SM(K)
1870 NEXT P
1915 IF M = 2 THEN 2100
1940 CK(1) = S(1,1) / S(2,1)
1950 PRINT "CHA = ",CK(1)
1960 CK(2) = CK(1)
2100 CK(1) = CK(1) + S(2,1) * CK(
    1) ^ 2
2120 PRINT "CPA = ",CK(1)
2125 IF CK(1) > 0 THEN 2170
2140 CK(1) = SC(1)
2170 CV = EXP (S(1,1))
2180 NT = NT + 1
2190 IF (NT <= 5) THEN 1100
2300 FOR J = 2 TO 3: FOR K = 1 TO
    2
2310 S(K,J) = S(K,J) * SM(K) * SM
    (J - 1)
2320 NEXT K: NEXT J
2330 JJ = JJ + 1
2335 PRINT "LINE NUMBER = ",JJ
2340 S2 = 0
2600 FOR I = 1 TO NP
2610 X = CV / (1. + A(I) / CK(1))
2620 PM = - (LOG (A(I)) / LOG
    (10))
2630 X2 = LOG (Y(I)) / LOG (10)
2640 X3 = LOG (X) / LOG (10)
2650 DX(1) = X2 - X3
2660 DX(2) = Y(I) - X
2626 PRINT CHR$(9) + "132N"
2627 PRINT CHR$(15) IF I > 1 THEN
    2629
2628 PRINT "PM": SPC(16): "EXPTL
    V": SPC(11): "CALC V": SPC(
    12): "DIFF": SPC(14): "EXPTL
    LOG V": SPC(7): "CALC LOG V"
    : SPC(8): "DIFF"
2629 IK(1) = PM:IK(2) = Y(I):IK(3)
    = X:IK(4) = DX(2):IK(5) =
    X2:IK(6) = X3:IK(7) = DX(1)
2630 FOR JK = 0 TO 6:IX = IK(JK +
    1)
2631 SA = LEN (STR$(IX))
2632 SB = 18 - SA
2633 PRINT IX: SPC(SB)
2634 NEXT JK
2640 S2 = S2 + W(I) * (DX(1) ^ 2)
2650 NEXT I
2660 P = NP - 2
2680 S2 = S2 / P
2690 S1 = SCR (S2)
2700 SE(1) = S1 * SQR (S(1,2)) *
    CV
2710 CB = 1. / CV
2720 SE(2) = SE(1) / (CV ^ 2)
2730 PRINT : PRINT : PRINT "C = ",
    CV: PRINT "S.E.(C) = ",SE(1)
2740 PRINT : PRINT : PRINT "1/C =
    ",CB: PRINT "S.E.(1/C) = ",SE
    (2)
2800 IF CK(1) > 0 THEN 2840
2820 PRINT "A NEGAT: E"
2830 GOTO 3940
2840 PM(1) = - .43429 * LOG (C)
    (1)
2850 SE(3) = S1 * .43429 * SQR
    (S(2,2)) * CK(1)
2860 PRINT : PRINT : PRINT "PM =
    ",PM(1): PRINT "S.E. PM = ",
    SE(3)
2940 PRINT : PRINT : PRINT "SICP
    A = ",S1
2950 PRINT : PRINT : PRINT "VARI
    ANCE = ",S2
3420 GOTO 1047
3430 PRINT : PRINT : PRINT "PROG
    RAM COMPLETED FOR ",JJJ:
    PRINT
    LINES
55 0 END

```

```

4220 IF R = 2 THEN D(I,NU) = D(I
,01) - D(I,02)
4230 IF R = 3 THEN D(I,NU) = D(I
,01) * D(I,02)
4235 IF ((R = 4) AND (D(I,02) =
0)) THEN GOSUB 4575
4237 IF (R = 0) THEN 990
4240 IF R = 4 THEN D(I,NU) = D(I
,01) / D(I,02)
4245 IF R = 5 THEN D(I,NU) = (D(
I,01) - D(I,02)) / 2
4250 NEXT K
4255 REM
4260 RETURN
4265 REM ERRATA SUBROUTINE
4305 IF (R = 1) OR (R = 4) THEN
RETURN
4307 IF ((R = 2) AND (X = 0)) OR
((R = 3) AND (X = 0)) THEN RETURN
4310 IF (R = 3) THEN PRINT "CAN
NOT COMPUTE THE LN OF A NUMB
ER = 0"
4320 IF (R = 2) AND (X = 0) THEN
PRINT "CANNOT COMPUTE THE I
NVERSE OF ZERO"
4330 IF (R = 5) AND (X < 0) THEN
PRINT "CANNOT COMPUTE THE S
QUARE ROOT OF A NEGATIVE NUM
BER"
4332 GOTO 4540
4335 PRINT "CANNOT DIVIDE BY ZER
O"
4340 IF NK > NF THEN 4700
4380 PRINT : PRINT : PRINT "YOU
MUST NOW REGENERATE COL # " :
NU
4700 PRINT : PRINT : INPUT "READ
COMMENTS, ENTER YOUR INITIA
LS TO CONTINUE";YNS
4705 NF = NF
4710 K = - R : RETURN
4800 REM SPECIAL FUNCTION
4801 HOME : PRINT "PRODUCE A NEW
COLUMN WHICH FITS THE F
OLLOWING FUNCTION"; PRINT
4807 PRINT "BIPHASIC PH CURVE"; PRINT

4808 PRINT : PRINT "ENTER THE FO
LLOWING:" : PRINT
4810 INPUT "COL # " : I01
4831 PRINT
4840 INPUT "NEW COL # " : NU
4841 PRINT
4850 INPUT "YL=" : YL(I)
4860 INPUT "YH=" : YH(I)
4870 INPUT "K=" : CK(I)
4880 CK(I) = EXP (( LOG (10)) *
(- CK(I)))
4892 PRINT : PRINT "LOOK OVER TH
E ABOVE VALUES."
4893 INPUT "DO YOU AGREE WITH TH
EM? " : YNS
4895 IF YNS = "NO" THEN PRINT "
HERE'S YOUR CHANCE TO REENTE
R THE PROPER VALUES." : PRINT
: GOTO 4800
4900 FOR Y = 1 TO RW
4910 D(Y,NU) = (CK(I) + CK(I) * C
K(I) / D(Y,01)) / (1 + CK(I)
/ D(Y,01))
4920 NEXT K
4925 IF NU > NK THEN NK = NU
4930 RETURN

```

```

5000 FOR I
5100 PRINT CHR$(19) + "1234"
5110 PRINT CHR$(15)
5120 SC = 0 : IF NF = 0 THEN SC =
INT (100 / NF)
5125 SC = SC - 6
5130 FOR L = 1 TO NF
5132 PRINT "COL #": SPC( SC) :
5134 NEXT L
5136 PRINT
5140 FOR K = 1 TO RW : FOR J = 1 TO
NK
5142 S1 = LEN ( STR$( D(I,J)))
5146 S2 = S2 + S1
5147 PRINT D(I,J) : SPC( S2) :
5148 NEXT J : PRINT : NEXT K
5150 PRINT
5151 FOR J = 1 TO NF : SUM(J) = 0
5152 FOR K = 1 TO RW : SUM(J) = SU
M(J) + D(I,J) : NEXT K : NEXT
J
5155 FOR J = 1 TO NK
5154 S1 = LEN ( STR$( SUM(J)))
5155 S2 = S2 + S1
5156 PRINT SUM(J) : SPC( S2) :
5157 NEXT J
5160 PRINT
5170 PRINT CHR$(19)
5180 PRINT CHR$(9) + "1"
5185 FOR 0
5190 NF = NK
6000 GOTO 900
6300 HOME
7000 PRINT "YOUR GENERATED VALUE
S ARE NOW ERASED FROM MEMORY
.YOUR ORIGINAL DATA REMAINS.
IF YOU WOULD LIKE TO TRY AG
AIN, PRINT RUN"
7200 PRINT "FOLLOWED BY CARRIAGE
RETURN."
7500 END

```

APPENDIX 4: LISTING OF MANIP DATA PROGRAM

```

10  REM      MANIP DATA
20  DIM D(100,10)
30  HOME
100 READ RW
105 IF (RW < 1) OR (RW > 100) THEN
    PRINT "YOU GOOFED!"; PRINT
    GOTO 100
110 PRINT
200 READ NK
205 IF (NK < 1) OR (NK > 8) THEN
    PRINT "YOU GOOFED!"; PRINT
    GOTO 200
210 NF = NK
290 PRINT ; PRINT
300 FOR J = 1 TO NK
320 REM
323 FOR K = 1 TO RW
325 READ D(K,J)
330 NEXT K; PRINT ; NEXT J
400 REM THE FOLLOWING IS THE DATA YOU HAVE STORED
900 HOME ; PRINT "THE FOLLOWING OPTIONS ARE AVAILABLE!"; PRINT

901 PRINT " 1.PERFORM A FUNCTION ON ONE COLUMN"
902 PRINT " 2.PERFORM A FUNCTION ON TWO COLUMNS"
903 PRINT " 3.PRINT"
904 PRINT " 4.CHANGE A VALUE"
905 PRINT " 5.STOP"
906 PRINT " 6.SPECIAL FUNCTION"

907 PRINT ; PRINT ; INPUT "ENTER OPTION # "; NC
910 IF NC = 1 THEN GOSUB 1500
911 IF NC = 2 THEN GOSUB 4000
913 IF NC = 6 THEN GOSUB 4800
914 IF NC = 4 THEN GOSUB 3000
915 IF NC = 5 THEN GOTO 920
916 IF NC = 3 THEN GOTO 920
917 PRINT ; PRINT ; INPUT "WOULD YOU LIKE A PRINTOUT? "; YNS
918 IF YNS = "NO" THEN GOTO 920
920 GOTO 5000
1500 REM SUBROUTINE FOR ONE COLUMN
1505 INPUT "ENTER OLD COLUMN # "; OLD
1510 INPUT "ENTER NEW COLUMN # (MAX=8) "; NU
1512 IF (NU < 1) OR (NU > 8) THEN
    PRINT "YOU GOOFED!"; PRINT
    GOTO 1510
1515 IF NU = NK THEN NK = NU
1530 PRINT "FUNCTION TO PERFORM:"
1560 PRINT " 1.X"
1570 PRINT " 2.1/X"
1580 PRINT " 3.LN(X)"
1590 PRINT " 4.EXP(X)"
1592 PRINT " 5.SQR(X)"
1594 PRINT " 6.ABS(X)"
1600 PRINT " 7.C * X"
1610 PRINT " 8.C + X"
1620 PRINT " 9.X ^ C"
1630 PRINT " 10.C/(1 + X/KA + KB/X)"
1640 PRINT " 11.CONC H="
1800 PRINT ; INPUT "ENTER FUNCTION # "; R
2500 IF R = 1 THEN DEF FN A(X) = X
2520 IF R = 2 THEN DEF FN A(X) = 1 / X
2530 IF R = 3 THEN DEF FN A(X) = LOG (X)
2540 IF R = 4 THEN DEF FN A(X) = EXP (X)
2550 IF R = 5 THEN DEF FN A(X) = SQR (X)
2560 IF R = 6 THEN DEF FN A(X) = ABS (X)
2570 IF R = 7 THEN DEF FN A(X) = C * X
2580 IF R = 8 THEN DEF FN A(X) = C + X
2590 IF R = 9 THEN DEF FN A(X) = X ^ C
2595 IF R = 11 THEN DEF FN A(X) = EXP (( LOG (10) * ( - X))) GOTO 2700
2600 IF R > 6 THEN INPUT "ENTER C (INTEGER OR REAL-NO FRACTIONS) "; C
2610 IF R = 10 THEN INPUT "ENTER KA "; KA; INPUT "ENTER KB "; KB
2700 FOR K = 1 TO RW
2710 X = D(K,OLD)
2715 IF (X <= 0) AND (R <= 5) THEN GOSUB 4500
2717 IF (R < 0) THEN 900
2718 IF R = 10 THEN D(K,NU) = C / (1 + X / KA + KB / X); GOTO 2730
2720 D(K,NU) = FN A(X)
2730 NEXT K
2800 RETURN
3000 REM CHANGES SUBROUTINE
3010 HOME ; PRINT "TO CHANGE ONE VALUE:"
3020 PRINT ; INPUT "ENTER COLUMN # "; J
3030 PRINT ; INPUT "ENTER ROW # "; I
3040 PRINT ; INPUT "ENTER NEW VALUE "; D(I,J)
3060 RETURN
4000 REM SUBROUTINE FOR TWO COLUMNS
4010 PRINT "FUNCTION TO PERFORM:"
4020 PRINT " 1.COL#X + COL#Y"
4030 PRINT " 2.COL#X - COL#Y"
4040 PRINT " 3.COL#X * COL#Y"
4050 PRINT " 4.COL#X / COL#Y"
4060 PRINT " 5.(COL#X-COL#Y)^2"
4100 PRINT ; INPUT "ENTER FUNCTION # "; R
4110 PRINT ; INPUT "ENTER X "; O1
4120 PRINT ; INPUT "ENTER Y "; O2
4130 PRINT ; INPUT "ENTER NEW COL # (MAX=8) "; NU
4135 IF (NU < 1) OR (NU > 8) THEN
    PRINT "YOU GOOFED!"; PRINT
    GOTO 4130
4200 IF NU > NK THEN NK = NU
4205 FOR K = 1 TO RW
4210 IF R = 1 THEN D(K,NU) = D(K,O1) + D(K,O2)

```

APPENDIX 5: LISTING OF NMRSPEC PROGRAM

```

1  REM  NMRSPEC
10  REM  PROGRAM TO DETERMINE
    NMR SPECTRA FROM AMINO
    ACID DISTRIBUTION
100  DIM P(50),B(50),A(50),NR(50)
    ,AL(50),DL(50)
105  DIM RESIDUE(50)
110  DIM SP(360),HS(360),RRES(360)
200  READ N
210  FOR I = 1 TO N
220  READ RESIDUE(I),P(I),B(I),A
    (I)
225  DL(I) = P(I) / 220
230  NEXT
240  FOR I = 1 TO N
250  READ NR(I)
260  AL(I) = A(I) * NR(I)
270  NEXT
280  PRINT "RESIDUE", "POSITION"
282  FOR I = 1 TO N
284  PRINT RESIDUE(I),P(I)
285  NEXT
286  PRINT "DELTA", "BASE"
287  FOR I = 1 TO N: PRINT DL(I),
    B(I): NEXT
288  PRINT "ALTITUDE", "NO. OF RES
    IDUES"
289  FOR I = 1 TO N: PRINT A(I),N
    R(I): NEXT
290  PRINT "TOTAL ALTITUDE"
291  FOR I = 1 TO N: PRINT AL(I):
    NEXT
300  FOR I = 1 TO N
400  DX = B(I) / 10
405  SN = P(I) / 5
410  FOR J = - DX TO DX
415  SJ = SN + J
420  K = ABS (J)
440  RA = 10 * AL(I) / B(I)
450  HS(SJ) = HS(SJ) + AL(I) - K *
    RA
455  RRES(SJ) = RRES(SJ) + RESID
    UE(I)
460  NEXT J
470  NEXT I
500  PRINT "SPECTRAL POSITION", "H
    EIGHT"
510  FOR J = 1 TO 360
520  IF HS(J) = 0 THEN GOTO 532
530  PRINT 5 * J,HS(J)
531  PRINT
532  NEXT J
540  PRINT : PRINT "DELTA", "HEIGH
    T"
542  FOR J = 1 TO 360
544  IF HS(J) = 0 THEN GOTO 550
545  PRINT RRES(J)
546  PRINT 5 * J / 220,HS(J)
550  NEXT

```

APPENDIX 6: DATA ENTRY and INTERACTIVE MANIPULATIONS

Introduction

The data for the programs listed in Appendices 1 thru 5 are entered as lines of the programs. For HABELL, PHBELL, and NMRSPEC this is the only interaction the user has with the program. For HYPER, the user can also enter constants to multiply velocity or concentration in response to an inquiry from the screen. MANIP DATA is totally interactive except for the actual entry of data. HYPER, PHBELL, HABELL, and MANIP DATA also exist in forms which allow for the interactive entry of data, but the data is not saved from one run to the next. These variations, which need very little instruction to run, are not listed in the Appendix but are available from me upon request.

HYPER

The data for HYPER are listed as lines 601-998 in the following format:

]600 REM FOLLOWING IS THE DATA YOU HAVE STORED

]linenum REM description of first set of data

]linenum DATA $n_1.c_1$

]linenum DATA $v_{11}.a_{11}.v_{12}.a_{12}.....v_{1j}.a_{1j}.....v_{1n_1}.a_{1n_1}$

]linenum REM description of last set of data

]linenum DATA $n_L.c_L$

]linenum DATA $v_{L1}.a_{L1}.v_{L2}.a_{L2}.....v_{Lj}.a_{Lj}.....v_{Ln_L}.a_{Ln_L}$

]999 DATA 0.0

with:

n_i = number of data points in the i th curve to be analyzed

c = 0, unless velocity data is to be entered as $1/v$

v = velocity of enzyme catalyzed reaction under given conditions

a = concentration of substrate used to generate previous v

The data can be broken up into any number of entry lines as long as the sequence is retained. It is advisable, however, not to enter too many points per entry line so as to be able to correct mistakes or easily remove points. As soon as one curve is analyzed, the next is read. If 0 is encountered as the number of points per line then the entire run is ended. This is the reason for line 999.

A sample entry is given below:

]600 REM FOLLOWING IS THE DATA YOU HAVE STORED

]601 REM MULT. CONC. BY 0.125

]602 REM LINE 1 REVERSE

]605 DATA 9,0

]606 DATA .0145, 60, .0145, 60, .0147, 60

]608 DATA .0102, 30, .0108, 30, .0115, 30

]610 DATA .0178, 100, .0177, 100, .0172, 100

]620 REM LINE 2

]622 DATA 12, 0

]624 DATA .0135,60, .0147,60, .0123, 60, .0131,60, .0125, 60, .0127, 60

]626 DATA .0097, 30, .0089, 30, .0087, 30

]628 DATA .0141, 100, .0157, 100, .0155, 100

]999 DATA 0.0

When HYPER is run, there is an inquiry on the screen as to whether 'v' and/or 'a' should be multiplied by constants. These constants can then be entered for that particular run. The generated values are then used for the analysis and printed in the output, but only the data entered as lines of the program are saved for future runs.

HABELL PHBELL

The data for HABELL and PHBELL are entered as lines 601-998 in the following format:

```
]600 REM FOLLOWING IS THE DATA YOU HAVE STORED
]linenum REM description of data
]linenum DATA n, c
]linenum DATA Vm1, pH1, w1, ... Vmi, pHi, wi, ... Vmn, pHn, wn
]999 DATA 0,0
```

with:

- n = number of points in the pH profile
- c = 0, unless Vm is to be entered as 1/Vm
- Vm_i = Velocity extrapolated to infinite substrate concentration
- pH_i = assay pH at which corresponding Vm was determined
- w_i = weighting of ith point; if no weighting wanted put 1

Data for more than one curve can be entered at one time, but this is not usually the case and is therefore not spelled out above. As in HYPER, if 0 is encountered as the number of points in a particular line, then the entire run is ended.

A sample entry is given below:

```
]600 REM FOLLOWING IS THE DATA YOU HAVE STORED
]602 REM REVERSE REACTION DATA
```

```

]605 DATA 14, 0
]610 DATA .00533, 4.65, 1
]615 DATA .00953, 5.2,1, .01472, 5.45, 1, .019545, 5.9, 1
]620 DATA .01928, 6.2,1, .02155, 6.2, 1, .02494, 6.5,1, .02435, 6.7, 1,
.02375, 6.9, 1
]625 DATA .02451, 7.3,1, .0205, 7.7, 1, .01773, 7.9, 1
]630 .01665, 8, 1, .01485, 8.2, 1
]999 DATA 0, 0

```

As with HYPER, the data can be broken into any number of entry lines as long as the sequence is retained.

MANIP DATA

The data for MANIP DATA are entered as lines 601-899 according to the following format:

```
]600 REM FOLLOWING IS THE DATA YOU HAVE STORED
```

```
]linenum DATA nr,nc
```

```
]linenum REM description of data in first column
```

```
]linenum DATA d11.d12.....d1i.....d1nr
```

.

.

.

```
]linenum REM description of data in last column
```

```
]linenum DATA dnc1.dnc2.....dnci.....dnc nr
```

with:

nc = number of columns

nr = number of rows (or points per column)

d = data points

A sample entry is given below:

```
J600 REM FOLLOWING IS THE DATA YOU HAVE STORED
J601 REM REVERSE DATA
J605 DATA 14,2
J610 REM PH'S
J615 DATA 4.65, 5.2, 5.45, 5.9, 6.2, 6.2, 6.5, 6.7, 6.9, 7.3, 7.7, 7.9, 8, 8.2
J617 REM VMAX'S
J618 DATA .00533, .00953, .01472, .01945, .01928, .02155, .02494, .02435,
.02375, .02451, .0205, .01773, .01665, .01485
```

Up to 8 columns and 150 points per column may be entered. The data can be broken up into any number of entry lines as long as its sequence is retained. This data and any generated in the course of a run can be subjected to several functions by response to inquiries from the screen (with X and Y representing the columns and C representing a constant). The generated values can be put into any column designated by the user. Printouts can be produced repeatedly at any point during the run. (This does not terminate the run.) If one of several common errors is encountered (e.g. division by zero, or taking the log of a negative number) the user is notified so the error can be corrected without aborting the run.

The functions below are those available on the version of MANIP DATA printed in Appendix 4. In addition, the program can be easily modified to include any other function on any number of columns with the restriction that the printout is limited to 8 columns.

i. Functions on one column

1. X
2. 1/X

3. LN(X)
4. EXP(X)
5. SQR(X)
6. ABS(X)
7. C * X
8. C + X
9. X^C
10. C/(1 + X/Ka + Kb/X)
11. Conc. H⁺ (if the column entered contains pH values)

II. Functions on two columns:

1. Col X + Col Y
2. Col X - Col Y
3. Col X * Col Y
4. Col X / Col Y
5. (Col X - Col Y)²

III. Print

Prints out all columns stored or generated with the column number and column total at the top and bottom respectively.

IV. Change a value

Inquiry from the screen for column number, row number, and new value.

V. Stop

Ends the run.

VI. Special function

Space for any function: in the case of Appendix 4, the equation for a Biphasic pH curve.

NMRSPEC

The data for NMRSPEC are entered as lines 1000 and on, according to the following format:

```
]1000 REM
]linenum DATA n
]linenum DATA NAME1, SP1, B1, H1
.
.
.
]linenum DATA NAMEn, SPn, Bn, Hn
]linenum DATA NRES1,NRES2,...
]linenum DATA NRESi,...
]linenum DATA ...,NRESn
```

with:

n = number of proton species to be represented

NAME = The name of the particular species of proton (e.g. LEU CH3)

SP = spectral position in Hz (based on a 220 MHz instrument)

B = width of base in Hz (based on a 220 MHz instrument)

H = height of triangle representing that proton species

NRES = number of residues in OPRTase (from amino acid analysis)

NRES values are listed separately since it is this set of values which is varied with different amino acid analyses while NAME, SP, B, and H are based on literature values.

The data used for NMRSPEC are listed in Table IV.1. Columns 1 thru 5 contain the values entered for NAME, SP, B, H, and NRES respectively.

APPENDIX 7: SAMPLE PRINTOUTS

Below are descriptions of the sample printouts of HYPER, PHBELL, and MANIP DATA followed by the printouts themselves. The actual printouts were not clear enough for reproduction in this thesis. Therefore, abridged facsimilies with the pertinent information contained in the printouts are provided instead. Values have been truncated to fit the page.

A. HYPER

The sample printout of HYPER was produced using the data listed in Appendix 6, if the user had indicated to multiply the concentrations by 0.125. Notice that the values for concentration (Column 1) have thereby been changed from those entered. Column 3 contains the inputted velocity values. Columns 2 and 4 list the inverses of the concentrations and velocities, respectively. Column 5 lists the theoretical velocity based on the concentrations given and the V_{max} and K_m derived. Column 6 lists the differences between the experimental and the theoretical velocity values.

The rest of the printout is a listing of various constants and values of interest and their standard errors.

B. PHBELL. HABELL

The data used to produce the sample printout for PHBELL are listed in Appendix 6. Column 1 contains the pH values. Column 2 contains the experimental V_{max} 's found at the corresponding assay pH's. Column 3 contains the calculated V_{max} 's given the pH values in Column 1 and the C , pK_a , and pK_b generated by the program. Column 4 lists the difference between the experimental and calculated V_{max} values. Columns 5 and 6 are the logarithmic equivalents of Columns 2 and 3 respectively and Column 7 is the difference

between Columns 5 and 6. These columns of data are followed by calculated values of C, pKa, and pKb, and their standard errors. The printout of HABELL is similar to that of PHBELL except that no pKb is generated.

C.MANIP DATA

MANIP DATA can be used for many functions. The sample described below is that for generating theoretical curves and comparing them with the experimental data. The first printout is that of data itself. One may notice that the column number is printed on top and the column total is separated from the rest by a blank line. In this case, the first column contains pH values and the second column contains experimental Vmax values for the corresponding pH's.

The second printout contains the entered data and in Column 3, the $[H^+]$ values generated by using the Conc H^+ from Column 1.

The third printout contains generated values in addition to that in the second printout. Columns 4 thru 8 were generated by performing the following function on column 3:(i.e. Option 10 of 'Functions of one Column', Appendix 6)

$$V_{max} = C / (1 + [H^+]/K_a + K_b/[H^+])$$

with:

$$C = 0.0260$$

$$K_b = 5.0119 \text{ E-}09 \text{ (i.e. pKb} = 8.3 \text{)}$$

$K_a = 5.01187 \text{ E}^{-06}, 3.98107 \text{ E}^{-06}, 3.16228 \text{ E}^{-06}, 2.51189 \text{ E}^{-06}, 1.99526 \text{ E}^{-06}$ (i.e. pKa = 5.3, 5.4, 5.5, 5.6, 5.7) for columns 4 thru 8 respectively.

For the third printout, Option 5 of 'Functions of 2 Columns' (Appendix 6) was used and this was performed between Column 2 and Columns 4-8 respectively to produce the new columns 4 thru 8. The sums of these columns are the RSS.

Appendix 7A: PRINTOUT OF HYPER

IRUN

FIT TO HYPERBOLA $V=VM*A/(K+A)$

DO YOU WISH TO MULTIPLY THE V'S AND /OR A'S BY A CONSTANT? YES

ENTER A CONSTANT MULTIPLIER OF V 1

ENTER A CONSTANT MULTIPLIER OF A .125

ALL V'S ENTERED WILL BE MULTIPLIED BY 1

ALL A'S WILL BE MULTIPLIED BY .125

BEFORE CONTINUING, DO YOU AGREE WITH THESE VALUES? YES

LINE NUMBER= 1
NUMBER OF POINTS= 9

CONC	1/CONC	VELOCITY	1/VELOCITY	CALC V	DIFF
7.5	.133	0145	68.96	01479	-2.910E-04
7.5	.133	0145	68.96	01479	-2.910E-04
7.5	.133	0147	68.02	01479	-9.161E-05
3.75	.266	0102	98.03	01071	-5.107E-04
3.75	.266	0108	92.59	01071	8.924E-05
3.75	.266	0115	86.95	01071	7.892E-04
12.5	.08	0178	56.17	01745	3.487E-04
12.5	.08	0177	56.49	01745	2.487E-04
12.5	.08	0172	58.13	01745	-2.512E-04

K= 4.6164
S.E.(K)= .4433

V= 0239
S.E.(V)= 8.564E-04

C.V.(V)= 0358

K/V= 193.188
S.E.(K/V)= 12.054

1/V= 41.8478
S.E.(1/V)= 1.4997

V/K= 5.178E-03
S.E.(V/K)= 3.2298E-04

C.V.(V/K)= .0823
SIGMA= 4.3373E-04

VARIANCE= 1.8812E-07
FOR 7 DEGREES OF FREEDOM

LINE NUMBER= 2
NUMBER OF POINTS= 12

CONC	1/CONC	VELOCITY	1/VELOCITY	CALC V	DIFF
7.5	.133	0135	74.97	0129	5.6E-04
7.5	.133	0147	68.02	0129	1.78E-03
7.5	.133	0123	81.30	0129	-6.32E-04
7.5	.133	0131	76.33	0129	1.87E-04
7.5	.133	0125	80	0129	-4.32E-04
7.5	.133	0127	78.74	0129	-2.32E-04
3.75	.266	9.7E-03	103.09	9.32E-03	3.79E-04
3.75	.266	8.9E-03	112.35	9.32E-03	-4.20E-04
3.75	.266	8.7E-03	114.94	9.32E-03	-6.20E-04
12.5	.08	0141	70.92	0153	-1.20E-03
12.5	.08	0157	63.69	0153	3.95E-04
12.5	.08	0155	64.51	0153	1.95E-04

K= 4.744
S.E.(K)= .957

V= 0211

SE (V)= 1.621E-03
C.V. (V)= 0.788
K/V= 224.71
SE (K/V)= 29.843
1/V= 47.361
SE (1/V)= 3.83
V/K= 4.450E-03
SE (V/K)= 5.711E-04
C.V. (V/K)= 1.2835
SIGMA= 8.0419E-04
VARIANCE= 6.4672E-07
FOR 10 DEGREES OF FREEDOM

PROGRAM COMPLETED FOR 2 LINES.

Appendix 7B: PRINTOUT OF PHBELL

IRUN
 FIT TO LOG V=LOG(C/(1+H/KA + KB/H))

LINE NUMBER= 1
 NUMBER OF POINTS= 14

PH	EXPTL V	CALC V	DIFF	EXPTL LOG V	CALC LOG V	DIFF
4.64998	5.33E-03	4.7059E-03	6.240E-04	-2.2732	-2.3273	0.540
5.19998	9.53E-03	0.1123	-1.701E-03	-2.0209	-1.9495	-0.713
5.44997	0.1472	0.1473	-1.815E-05	-1.8720	-1.8315	-5.251
5.89997	0.1955	0.1965	-3.121E-04	-1.7089	-1.7020	-6.881
6.19997	0.1928	0.2189	2.613E-03	-1.7148	-1.6598	-0.552
6.19997	0.2155	0.2189	-3.434E-04	-1.6685	-1.6598	-8.887
6.49997	0.2484	0.2298	1.870E-03	-1.6031	-1.6388	0.357
6.89997	0.2435	0.2327	1.075E-03	-1.6135	-1.6331	0.198
6.89997	0.2375	0.2330	4.477E-04	-1.6243	-1.6326	8.265E-03
7.29997	0.2451	0.2250	2.009E-03	-1.6106	-1.6478	.0371
7.69997	0.205	0.2019	3.035E-04	-1.6882	-1.6947	6.497E-03
7.89998	0.1773	0.1831	-5.187E-04	-1.7512	-1.7372	-0.140
7.99998	0.1685	0.1718	-5.307E-04	-1.7785	-1.7649	-0.136
8.19998	0.1485	0.1460	2.422E-04	-1.8282	-1.8354	7.143E-03

C= 0.2488
 S.E.(C)= 4.058E-04

1/C= 40.551
 S.E.(1/C)= .8673

PKA= 5.277
 S.E.(PKA)= .0201

PKB= 8.363
 S.E.(PKB)= .0367

SIGMA= 0.368

VARIANCE= 1.340E-03

IF TWO GROUPS ARE INVOLVED, TRUE PKs ARE:

PKA= 5.277
 PKB= 8.363

APPENDIX 8: PRINTOUT OF NMRSPEC

On the following pages are the individual points of the curve generated by using NMRSPEC and Table IV. 1 (which contains the amino acid analysis values found in Table V.6, Column 1). The values are listed in the format of one line containing the proton species contributing to the point followed on the next line by the spectral position based on a 220 MHz instrument, the position in ppm, and the height of the curve at that point. This is not the actual format of the printout generated by NMRSPEC but a paste-up thereof.

	ILEU CH2	
	.75	4.5
	ILEU CH2	
170	.7307307307	210
	ILEU CH2	
175	.7257257257	215
	ILEU CH2ILEU CH2	
180	.7197197197	400
	ILEU CH2ILEU CH2	
185	.7147147147	500.733374
	ILEU CH2ILEU CHEVAL CH2	
190	.7087087087	675.257256
	ILEU CH2ILEU CHEVAL CH2	
195	.7027027027	875.447052
	ILEU CH2ILEU CHEVAL CH2	
200	.6966966967	650.290196
	ILEU CHEVAL CH2	
205	.6916916917	530.133334
	ILEU CHEVAL CH2	
210	.6856856857	225.62552
	VAL CH2	
215	.6806806807	130.447052
	ILEU CHEVAL CH2	
220	1	37.2705887
	ILEU CH2	
225	1.0000000001	7.70000001
	ILEU CH2	
230	1.04010401	15.4
	ILEU CH2	
235	1.08010801	27.1
	ILEU CH2	
240	1.09090909	30.9
	ILEU CH2	
245	1.11676767	38.5
	ILEU CH2	
250	1.13636364	46.2
	ILEU CH2TR CH2	
255	1.15202021	47.25
	ILEU CH2TR CH2	
260	1.18181818	86.2
	ILEU CH2TR CH2	
265	1.20454545	125.95
	ILEU CH2TR CH2	
270	1.22222222	165
	ILEU CH2TR CH2	
275	1.25	110.55
	ILEU CH2ILEU CH2TR CH2	
280	1.27272727	50.1
	ILEU CH2TR CH2	
285	1.29545455	17.25

270	ILEU CHDIAA CHDLYS G-CHD	1.7115771	191.1
275	ILEU CHDIAA CHDLYS G-CHD	1.7115771	191.1
280	ILEU CHDIAA CHDLYS G-CHD	1.7115771	191.1
285	ILEU CHDIAA CHDLYS G-CHD	1.7115771	191.1
290	ILEU CHDIAA CHDLYS G-CHD	1.7115771	191.1
295	ILEU CHDIAA CHDLYS G-CHD	1.7115771	191.1
300	ILEU CHDIAA CHDLYS G-CHD	1.7115771	191.1
305	ILEU CHDIAA CHDLYS G-CHD	1.7115771	191.1
310	ILEU CHDIAA CHDLYS G-CHD	1.7115771	191.1
315	ILEU CHDIAA CHDLYS G-CHD	1.7115771	191.1
320	ILEU CHDIAA CHDLYS G-CHD	1.7115771	191.1
325	ILEU CHDIAA CHDLYS G-CHD	1.7115771	191.1
330	ILEU CHDIAA CHDLYS G-CHD	1.7115771	191.1
335	ILEU CHDIAA CHDLYS G-CHD	1.7115771	191.1
340	ILEU CHDIAA CHDLYS G-CHD	1.7115771	191.1
345	ILEU CHDIAA CHDLYS G-CHD	1.7115771	191.1
350	ILEU CHDIAA CHDLYS G-CHD	1.7115771	191.1
355	ILEU CHDIAA CHDLYS G-CHD	1.7115771	191.1
360	ILEU CHDIAA CHDLYS G-CHD	1.7115771	191.1
365	ILEU CHDIAA CHDLYS G-CHD	1.7115771	191.1
370	ILEU CHDIAA CHDLYS G-CHD	1.7115771	191.1
375	ILEU CHDIAA CHDLYS G-CHD	1.7115771	191.1
380	ILEU CHDIAA CHDLYS G-CHD	1.7115771	191.1
385	ILEU CHDIAA CHDLYS G-CHD	1.7115771	191.1
390	ILEU CHDIAA CHDLYS G-CHD	1.7115771	191.1
395	ILEU CHDIAA CHDLYS G-CHD	1.7115771	191.1
400	ILEU CHDIAA CHDLYS G-CHD	1.7115771	191.1
405	ILEU CHDIAA CHDLYS G-CHD	1.7115771	191.1
410	ILEU CHDIAA CHDLYS G-CHD	1.7115771	191.1

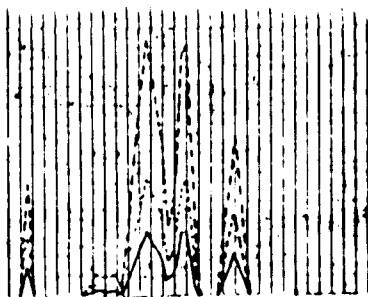
415	VAL B-CHPRO G-CH2GLU B-CH2	1.00000000	100.000000
420	VAL B-CHPRO B-CH2GLU G-CH2	1.00000000	100.000000
425	VAL B-CHPRO G-CH2GLU G-CH2	1.00000000	100.000000
430	VAL B-CHPRO G-CH2GLU B-CH2	1.00000000	100.000000
435	VAL B-CHPRO G-CH2GLU B-CH2GLN B-CH2MET B-CH2	1.00000000	100.000000
440	VAL B-CHPRO G-CH2GLU B-CH2GLU B-CH2GLN B-CH2	1.00000000	100.000000
445	VAL B-CHPRO G-CH2GLU B-CH2GLU B-CH2GLN B-CH2MET B-CH2	1.00000000	100.000000
450	VAL B-CHPRO G-CH2GLU B-CH2GLU B-CH2GLN B-CH2MET B-CH2	1.00000000	100.000000
455	VAL B-CHPRO B-CH2GLU B-CH2GLN B-CH2MET B-CH2	1.00000000	100.000000
460	VAL B-CHPRO B-CH2GLN B-CH2MET B-CH2	1.00000000	100.000000
465	VAL B-CHPRO B-CH2GLN B-CH2MET B-CH2	1.00000000	100.000000
470	VAL B-CHPRO B-CH2GLN B-CH2MET B-CH2	1.00000000	100.000000
475	VAL B-CHPRO B-CH2GLN B-CH2MET B-CH2	1.00000000	100.000000
480	VAL B-CHPRO B-CH2GLU G-CH2	1.00000000	100.000000
485	VAL B-CHPRO B-CH2GLU G-CH2	1.00000000	100.000000
490	VAL B-CHPRO B-CH2GLU G-CH2GLN G-CH2	1.00000000	100.000000
495	VAL B-CHGLU G-CH2GLN G-CH2	1.00000000	100.000000
500	VAL B-CHGLU G-CH2GLN G-CH2	1.00000000	100.000000
505	VAL B-CHGLU G-CH2GLN G-CH2	1.00000000	100.000000
510	VAL B-CHGLU G-CH2GLU G-CH2	1.00000000	100.000000
515	VAL B-CHGLU G-CH2GLU G-CH2	1.00000000	100.000000
520	VAL B-CHGLU G-CH2GLN G-CH2	1.00000000	100.000000
525	VAL B-CH2	1.00000000	100.000000
540	VAL B-CH2	1.00000000	100.000000
545	VAL B-CH2	1.00000000	100.000000

550	ASP B-CH2MET G-CH2	31.704545
	0.5	
555	ASP B-CH2MET G-CH2	13.8177073
	0.5007073	
560	ASP B-CH2MET G-CH2	11.2791031
	0.5007073	
565	ASP B-CH2NET G-CH2	40.7090909
	0.55818182	
570	ASP B-CH2MET G-CH2	35.5141708
	0.5907073	
575	ASP B-CH2MET G-CH2	30.2204546
	0.41757577	
580	ASP B-CH2MET G-CH2	25.1261364
	0.4754364	
585	ASP B-CH2ASN B-CH2	26.1818182
	0.65909091	
590	ASP B-CH2ASN B-CH2	33.2
	0.68181818	
595	ASP B-CH2ASN B-CH2	34.9018182
	0.70181818	
600	ASP B-CH2ASN B-CH2	36.7656364
	0.72727273	
605	ASP B-CH2ASN B-CH2ASN B-CH2	38.5454545
	0.75	
610	ASP B-CH2ASN B-CH2ASN B-CH2	44.5939394
	0.77072727	
615	ASP B-CH2ASN B-CH2ASN B-CH2	50.6424243
	0.79545455	
620	ASP B-CH2ASN B-CH2ASN B-CH2PHE B-CH2	47.8909091
	0.91818182	
625	ASP B-CH2ASN B-CH2ASN B-CH2TYR CH2PHE B-CH2	47.5727273
	0.91890909	
630	ASP B-CH2ASN B-CH2ASN B-CH2TYR CH2PHE B-CH2	59.0454545
	0.93636364	
635	ASP B-CH2ASN B-CH2ASN B-CH2TYR CH2PHE B-CH2	60.469697
	0.9476364	
640	ASP B-CH2ASN B-CH2ASN B-CH2TYR CH2PHE B-CH2	69.1015152
	0.90909091	
645	LYS B-CH2ASP B-CH2ASN B-CH2ASN B-CH2TYR CH2	90.260061
	0.93181818	
650	LYS B-CH2ASN B-CH2TYR CH2PHE B-CH2	113.028738
	0.95151515	
655	LYS B-CH2ASN B-CH2CYS B-CH2TYR CH2PHE B-CH2	132.570707
	0.97070707	
660	LYS B-CH2ASN B-CH2CYS B-CH2TYR CH2PHE B-CH2	161.690405
	-	
665	LYS B-CH2ASN B-CH2CYS B-CH2TYR CH2PHE B-CH2	186.866667
	0.90000000	
670	LYS B-CH2CYS B-CH2TYR CH2PHE B-CH2PHE B-CH2	175.998485
	0.94545455	

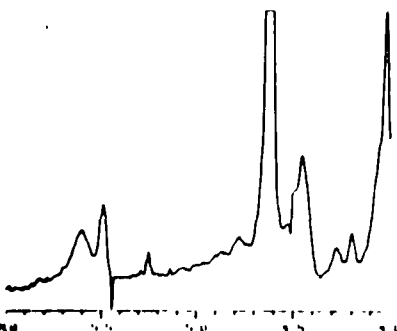
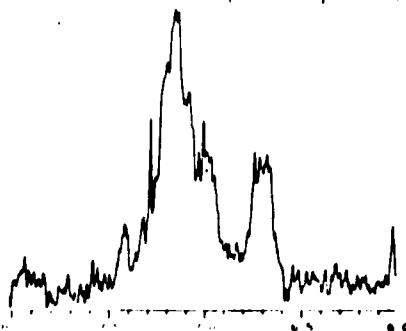
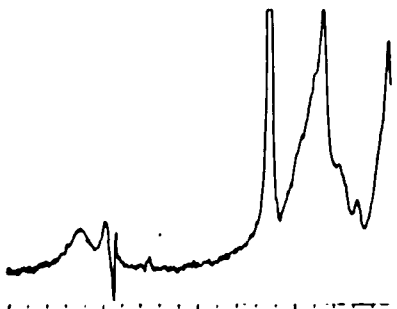
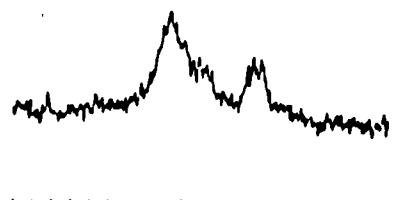
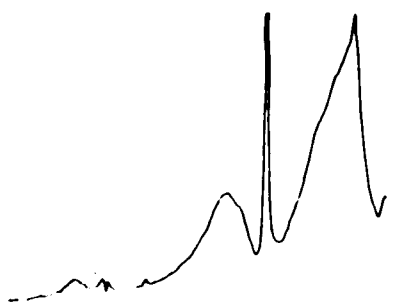
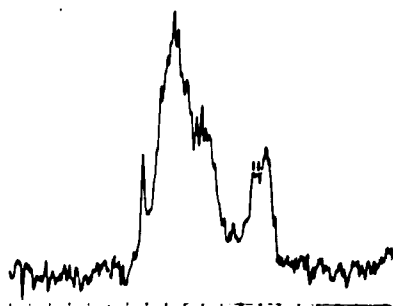
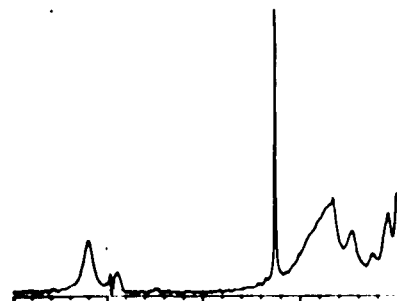
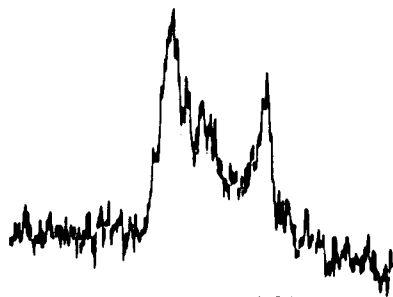
675	LYS E-CH2PHE B-CH2	3.07200000	82.6192641
680	LYS E-CH2PHE B-CH2	3.07200000	82.6192641
685	LYS E-CH2HIS B-CH2TYR CH2PHE B-CH2	3.11765535	43.0451299
690	HIS B-CH2PHE B-CH2	3.17777777	37.1755715
695	HIS B-CH2PHE B-CH2	3.17777777	37.1755715
700	ASP D-CH2HIS B-CH2PHE B-CH2	3.24100000	111.4416507
705	ASP D-CH2HIS B-CH2PHE B-CH2	3.24100000	111.4416507
710	ASP D-CH2HIS B-CH2PHE B-CH2	3.24100000	111.4416507
715	ASP D-CH2HIS B-CH2PHE B-CH2	3.24100000	111.4416507
720	PRO D-CH2HIS B-CH2PHE B-CH2TYR B-CH2	3.27100000	61.2367725
725	PRO D-CH2HIS B-CH2PHE B-CH2TYR B-CH2	3.27100000	61.2367725
730	PRO D-CH2HIS B-CH2PHE B-CH2TYR B-CH2	3.27100000	61.2367725
735	PRO D-CH2HIS B-CH2PHE B-CH2TYR B-CH2	3.27100000	61.2367725
740	PRO D-CH2HIS B-CH2PHE B-CH2TYR B-CH2	3.27100000	61.2367725
745	PRO D-CH2HIS B-CH2PHE B-CH2TYR B-CH2	3.27100000	61.2367725
750	PRO D-CH2HIS B-CH2PHE B-CH2TYR B-CH2	3.27100000	61.2367725
755	PRO D-CH2HIS B-CH2PHE B-CH2TYR B-CH2	3.27100000	61.2367725
760	TYR B-CH2	3.10100000	6.57777778
765	TYR B-CH2	3.10100000	6.57777778
770	TYR B-CH2	3.10100000	6.57777778
1495	TYR D TO OH	6.75	9.21761705
1490	TYR D TO OH	6.75	9.21761705
1495	TYR D TO OH	6.75	9.21761705
1500	TYR D TO OH	6.75	9.21761705
1505	TYR D TO OH	6.75	9.21761705

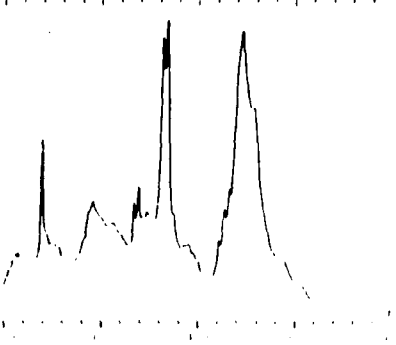
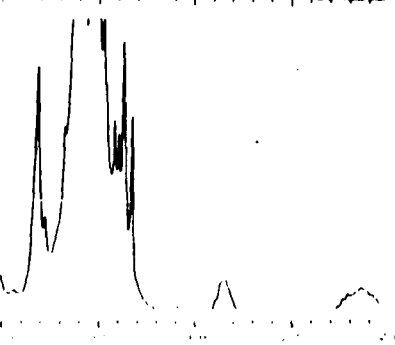
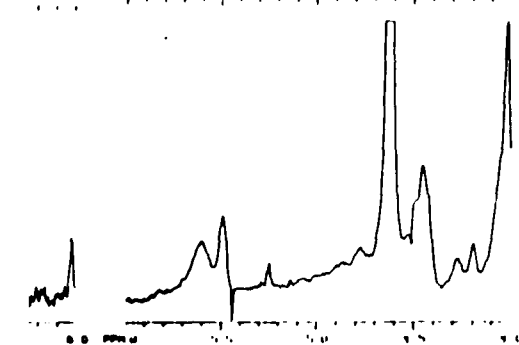
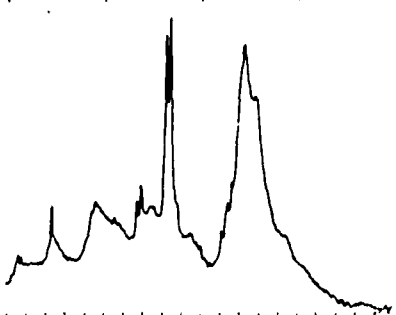
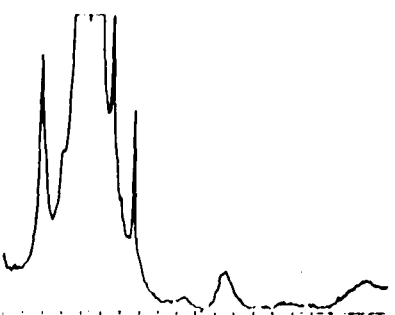
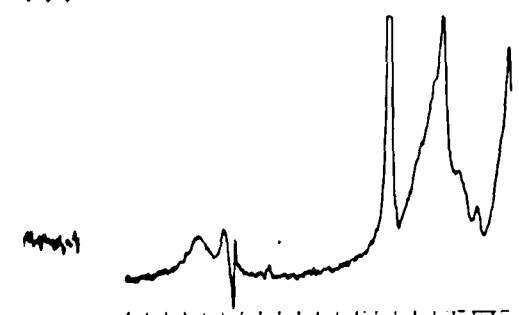
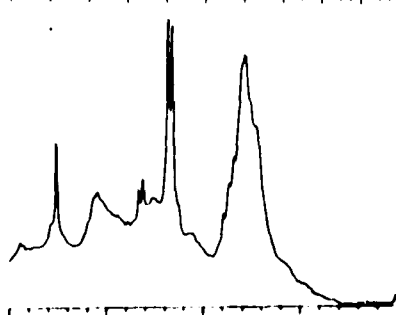
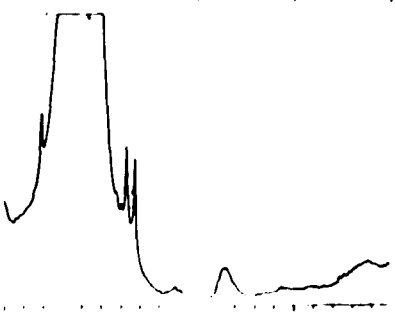
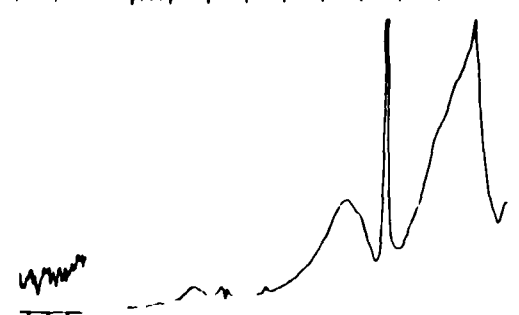
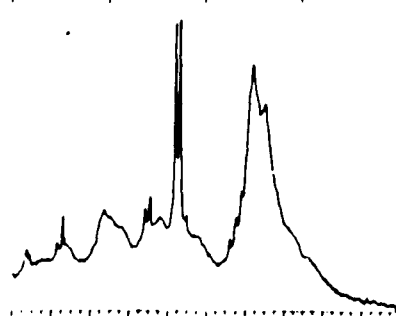
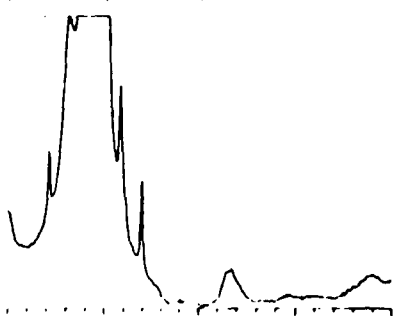
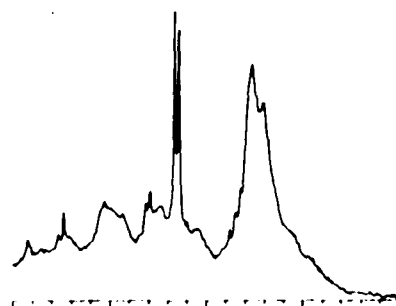
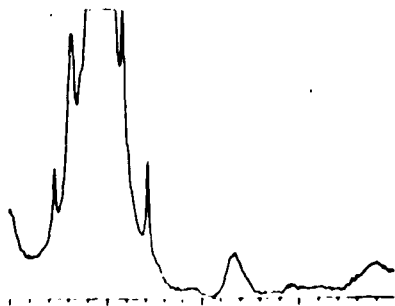
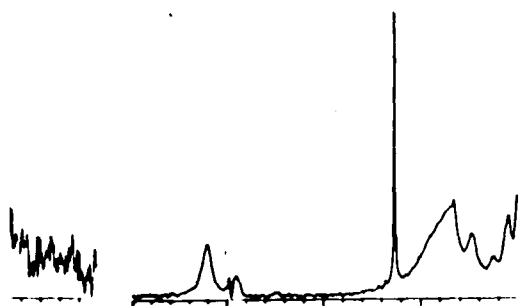
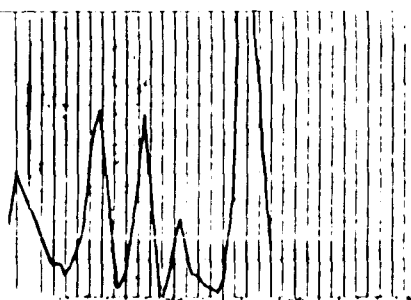
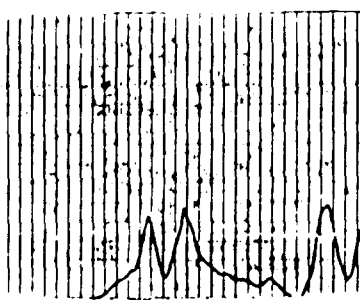
1510	TYPE O TO OH	6.91747134	71.4117447
1515	TYPE O TO OH	6.93674011	9.71751706
1540	TRF IN C5	7	4.16666667
1545	HIS IN C1TRF M TO OHTRF IN C5	7.02070707	18.5508904
1550	HIS IN C1TRF M TO OHTRF IN C5TRF IN C5	7.04545455	77.4117647
1555	HIS IN C1TRF M TO OHTRF IN C5TRF IN C5	7.06810102	131.705382
1560	HIS IN C1TRF M TO OHTRF IN C5TRF IN C5	7.09200709	125
1565	HIS IN C1TRF M TO OHTRF IN C5TRF IN C5	7.11301301	11.1058307
1570	TYPE M TO OHFHE AROMTRF IN C6	7.12603761	42.745099
1575	TYPE M TO OHFHE AROMTRF IN C2TRF IN C6	7.14704714	36.4500901
1580	FHE AROMTRF IN C2TRF IN C6	7.18181818	54.5000000
1585	FHE AROMTRF IN C2	7.20454545	85.8
1590	FHE AROMTRF IN C2	7.22727273	99.0666667
1595	FHE AROMTRF IN C2	7.25	111.000000
1600	FHE AROM	7.27000000	133.5
1605	FHE AROM	7.29000000	111.000000
1610	FHE AROM	7.31000000	89.0666667
1615	FHE AROM	7.34000000	66.8
1620	FHE AROM	7.36000000	44.5000004
1625	FHE AROMTRF IN C4	7.38000000	24.1000000
1630	FHE AROMTRF IN C4	7.40000000	4.97777778
1635	TRF IN C4	7.43000000	3.09088889
1640	TRF IN C4	7.45000000	11.0
1645	TRF IN C4TRF IN C7	7.47000000	9.70000000
1650	TRF IN C4TRF IN C7	7.5	9.85555556

1655	TRF IM-02 7.90191818	7.90191818
1660	TRF IM-02 7.90191818	7.90191818
1665	TRF IM-02 7.90191818	7.90191818
1670	TRF IM-02 7.90191818	7.90191818
1675	TRF IM-02 7.90191818	7.90191818
1735	HIS IM-02 7.90191818	7.90191818
1740	HIS IM-02 7.90191818	7.90191818
1745	HIS IM-02 7.90191818	7.90191818



APPENDIX 9





Section VIII: BIBLIOGRAPHY

- Altona, C. and Sundaralingam, M. (1973) *J. Am. Chem. Soc.* **95**, 2333.
- Appel, S. H. (1968) *J. Biol. Chem.* **243**, 3924.
- Ardalan, B., Villacorte, D., Heck, A., and Corbett, T. (1982) *Biochem. Pharmacol.* **31**, 1989.
- Ashton, R. W. and Sloan, D. L. (1986) *Federation Proc.* **45**, 1503.
- Brown, G.K. and O'Sullivan, W. J. (1977) *Biochemistry* **16**, 3235.
- Chen, R.F., Smith, P.P. and Maly, M. (1978) *Arch. Biochem. Biophys.* **189**, 24.
- Cleland, W. W., and Mildvan, A. S. (1979) in Adv. in Inorganic Biochemistry Vol. I (Eichhorn and Manzilli, eds) Elsevier/North Holland, N. Y., p. 180.
- Davies, D.B. and Danyluk, S.S. (1974) *Biochemistry* **13**, 4417.
- Foster, D. M., Lee, C. S., and O'Sullivan, W. J. (1973) *Biochem. Med.* **7**, 61.
- Goitein, R. K., Chelsky, D., and Parsons, S. M. (1978) *J. Biol. Chem.* **253**, 2963.
- Gabrielle, M. et al. (1986) *Anal. Biochem.* (in press)
- Hanna, L., Hess, S., and Sloan, D. L. (1983) *J. Biol. Chem.* **258**, 9745.
- Jencks, W. P. (1975) Adv. in Enzymology **43**, 419-410
- Jones, M. E. (1971) *Adv. in Enzyme Reg.* **9**, 19.
- Jones, M. E. (1972) in Current Topics in Cellular Regulation (Horecker, B. L. and Stadtman, E. R., eds.) Vol. **6**, pp. 227-265, Academic Press.
- Kasbekar, D. K., Nagabhushanam, A., and Greenberg, D. M. (1964) *J. Biol. Chem.* **239**, 4245.

- Kavipurapu, P. R. and Jones, M. E. (1976) *J. Biol. Chem.* **251**, 5589.
- McDonald, C. C., and Phillips, W. D. (1967A) in Proceedings of the Second International Conference on Magnetic Resonance in Biology, Pergammon Press, Inc., New York, N. Y.
- McDonald, C. C. and Phillips, W. D. (1967B) *J. Am. Chem. Soc.* **89**,6332.
- McDonald, C. C. and Phillips, W. D. (1969) *J. Am. Chem. Soc.* **91**,1513.
- McClard, R. W., Black, M. J., Livingstone, L. R., and Jones, M. E. (1980) *Biochemistry* **19**, 4699.
- Meadows, P. H. and Jardetzky, O. (1968) *Proc. Natl. Acad. Sci. U. S.* **60**,92.
- Miles, G. W. (1977) in Methods in Enzymology Vol. 47, 431.
- Musick, W. D. L. (1981) *CRC Crit. Rev. Biochem.* **11**, 1-34.
- Plagemann, G. W., Marz, R., Wohlheutter, J. C., Graff, J. C., and Zylka, J. M. (1981) *Biochim. Biophys. Acta* **126**, 275.
- Rathod, P. K. and Reyes, P. (1983) *J. Biol. Chem.* **258**, 2852.
- Reyes, P. (1977) *Anal. Biochem.* **77**, 363.
- Reyes, P. and Inress, C. (1978) *Life Sci.* **22**, 577-582.
- Schwartz, P. M., Dunigan, J. M., Marsh, J. C., and Handschumacher, R. E. (1980) *Canc. Res.* **40**, 1885.
- Smith, L. H., Huguley, C. M., and Bain, J. A. (1972) in The Metabolic Basis for Inherited Disease, 3rd Ed. (Stanbury, J. B., Wyngaarden, J. B., Fedrickson, D. S., eds.) p.1003, McGraw-Hill, New York.
- Sperling, O., Brosh, S., Boer, P., Kupfer, B., Benjamin, D., Weinberger, A., and Pinkhas, J. (1979) *Biomedicine* **31**, 20.
- Stein, S., Bohlem, P., Stone, J., Dairman and W., Udenfriend, S. (1973) *Arch. Biochem. Biophys.* **155**,202.

- Stein, S. and Brink, L. (1981) in Methods in Enzymology Vol. 79 Academic Press, New York.
- Sweeney, M. J., Parton, J. W., and Hoffman, D. H. (1974) *Adv. in Enzyme Reg.* **12**, 385.
- Syed, D. (1986) Doctoral Dissertation, C.U.N.Y., Dept. of Bioch.
- Tax, W. J. M. , Veerkamp, J. H., and Trijbels, J. M. F. (1976) *Comp. Biochem. Phys. B* **54**, 209.
- Traut, T. W.(1980)*Arch. Biochem. Biophys.* **200**,590.
- Victor, J., Greenberg, L., and Sloan, D. L. (1979a) *J. Biol. Chem.* **254**, 2647.
- Victor, J., Leo-Mensah, A., and Sloan, D. L. (1979b) *Biochemistry* **18**,3597.
- Walther, R., Wald, K., Glund, K., and Tewes, A. (1984) *J. Plant Physiol.* **116**, 301.
- Weber, G., Hager, J. C., Lui, M. S., Prajda, N., Tzeng, D. Y., Jackson, R. C., Takeda, E., and Eble, J. N.(1981) *Canc. Res.* **41**, 854.
- Worthy, T. E., Grobner, W., and Kelley, W. N. (1974) *Proc. Natl. Acad. Sci. U. S.* **71**, 3031.
- Yoshimoto, A., Amaya, T., Kobayashi, K., and Tomita, K. (1978) in Methods in Enzymology Vol. 51, pp.69-79, Academic Press, New York.

CURRICULUM VITAE

ROSALYN S. STRAUSS

Dept. of Chemistry
City College of New York
138th Street & Convent Avenue
New York, N.Y. 10031
(212) 690-8169

Home:
24 Bennett Avenue
New York, N.Y. 10033
(212) 795-5693
Birthdate: Feb. 5, 1955

Education

B.S., January 1978, City College of New York

M.A., June 1982, City University of New York

Ph.D., June 1986, City University of New York

Awards and Fellowships

CUNY Graduate Fellowship (1979)
Sigma Xi (1982)
Graduate Research Assistantship (1978, 1980-1984)
Phi Beta Kappa (1977)
Honors research (9 credits) 1976-1977
Benjamin Harrow Memorial Award for Excellence in
Undergraduate Research (1977)
Merck Index Award (1977)
Magna Cum Laude (1978)
Regents' Scholarship (1973-1977)
Freshman Honors Program (Honors core curriculum)

Publications

Sloan, D.L., and Strauss, R.S. (1982) Determination of a Histidine Residue at the Yeast Orotate Phosphoribosyl-transferase Active-Site. *J. Clin. Chem. Clin. Biochem.* 20, 419 (Abstract).

Sloan, D.L., and Strauss, R.S. (1984) Determination of a Histidine Residue at the Yeast Orotate Phosphoribosyl-transferase Active Site, in *Purine Metabolism in Man*, *Adv. Exp. Med. Biol.* 165 B, (C.deBruyn et al., Eds.) Plenum Press, N.Y., p. 89-9

Syed, D.B., Strauss, R., Mayer, L., and Sloan, D.L., (1984) NMR Studies of Phosphoribosylpyrophosphate-Yeast Orotate Phosphoribosyltransferase Complexations, *Biochemistry* 23, 3356. (Abstract).

Syed, D.B., Strauss, R.S., Ashton, R.W., and Sloan, D.L. , (1985)
Magnetic Relaxation Studies of the Conformation of
Phosphoribosyl Pyrophosphate Bound to Orotate
Phosphoribosyltransferase from Yeast, Fed. Proc. 44, 672. (Abstract).

Syed, D.B., Strauss, R.S., and Sloan, D.L. , (1986) Orotate
Phosphoribosyl Transferase and Hypoxanthine/Guanine
Phosphoribosyltransferase from Yeast: Magnetic Relaxation Studies of
the Confirmation of Enzyme-bound Phosphoribosyl 1-Pyrophosphate
(manuscript submitted to Biochemistry)

Computer Skills

Languages: Fortran , PL-1, and Basic

Coursework:

Introductory Programming
Advanced Algorithms
Biometry with Lab utilizing the statistical software
package-Statpak

Experience:

- Design of programs for data analysis for minicomputer
- Translation Fortran programs to Basic for use on the Apple II
- Conversion of aforementioned programs to an interactive form for use by others
- Specific development of enzyme kinetics programs from original data to graphic and publication level display

Teaching Experience

City College of New York, Dept. of Chemistry:

Chem 8: Introductory Qualitative and Quantitative
Analysis (Lab and Lecture), 1977-1978
Chem 4: Freshman Chemistry (Recitation), 1978
Chem 126: General and Organic Chemistry for Nursing
Students (Lecture and Course Coordinator),
Spring 1986

Laboratory Techniques

All phases of enzyme purification including:

- Protein fractionation utilizing ethanol and ammonium sulfate
- Column chromatography: molecular seive, hydroxy-apatite, ion exchange, and affinity
- Disc gel electrophoresis(columns and slabs) and protein determination

Kinetic analysis of enzyme mechanisms using spectroscopic assays

Chemical modification of enzymes

NMR Spectroscopy of protein

Studies of enzyme-substrate interactions with magnetic relaxation techniques

References

- Dr. D. L. Sloan, Dept. of Chemistry, City College of New York, 138th Street and Convent Ave., New York, N. Y. 10033. (212) 690-8306,8169
- Dr. C. S. Russell, Dept. of Chemistry, City College of New York, 138th Street and Convent Ave., New York, N. Y. 10033. (212) 690-6681